The Institute of Paper Chemistry

Appleton, Wisconsin

Doctor's Dissertation

An Investigation of the Compression Response of Ideal Unbonded Fibrous Structures by Direct Observation

Thomas Carlton Elias

June, 1965

AN INVESTIGATION OF THE COMPRESSION RESPONSE OF IDEAL UNBONDED FIBROUS STRUCTURES BY DIRECT OBSERVATION

A thesis submitted by

Thomas Carlton Elias

B.S. 1960, Western Michigan University
M.S. 1961, Lawrence College

in partial fulfillment of the requirements
of The Institute of Paper Chemistry
for the degree of Doctor of Philosophy
from Lawrence University
Appleton, Wisconsin

June, 1965

TABLE OF CONTENTS

SUMMARY

Equipment and techniques were developed which allowed individual fibers in the interior of thick glass fiber mats to be observed while the mat was subjected to compression. This was accomplished by saturating the mats with a liquid having the same index of refraction as the glass, which made the mats essentially transparent. The fibers which were studied were made visible by coating them with a thin layer of silver. It was demonstrated that the silvered fibers have essentially the same stiffness as the unsilvered fibers and that they may be considered representative of all fibers in the bed.

By studying visually the arrangement and configuration of fibers within filtration-formed mats, progress has been made in understanding how the initial structures are influenced by fiber dimensions and how these structures respond to compression. It was found that the internal geometry of newly formed beds was influenced considerably by the dimensions of the fibers. As the length-to-diameter ratio decreased, the average z-orientation increased. This effect became very pronounced for length-to-diameter ratios below 250. However, even for a length-to-diameter ratio of 313, 5.9% of the fibers were oriented at angles greater than 10 degrees with the horizontal in the newly formed beds. Compaction of the beds reduced the z-orientation of the fibers by an amount which could be predicted reasonably well for most fibers. It was demonstrated that to explain the compression response of fibrous mats they must be treated as three-dimensional networks, because the amount of z-orientation largely determines their behavior. In general, the segment length at a given solid fraction decreases as the mean z-orientation of the fibers increases. At low applied stresses, the segment length decreases with decreasing fiber length. As the beds are compressed, the segment length tends to become independent of fiber length. Consequently, the longer fibers experience a greater change in

segment length with increasing compaction than do the shorter fibers of the same diameter. This result is reflected in the increased compressibility of the beds of longer fibers. The effect of fiber diameter was not studied in detail, but it was learned that for a given change in the solid fraction of the bed, large diameter fibers bend less than do smaller diameter fibers.

By utilizing a number of different saturants, it was found that frictional forces between the fibers had an appreciable effect upon the compression response of unbonded fibrous structures, especially those composed of long fibers. Low friction favored increased compressibility.

Beds of fibers with a length-to-diameter ratio of 313 were studied extensively for evidences of fiber repositioning during compression. The method employed was to photograph fibers within the beds before, during, and after compression and to compare photographs. During a single compression, fiber slippage was important only insofar as it influenced bending of the fibers. The hysteresis in the compression response of glass fiber beds resulted from a small amount of axial slippage of the fibers. Translational or rotational repositioning of the fibers was found to be insignificant. If any appreciable slippage occurred, it was due to a fiber having high z-orientation, and the direction of motion was colinear to the axis of the fiber. The evidence indicated that fiber repositioning during compression is not a universal property of unbonded fibrous structures. When possible, explanations other than fiber repositioning should be sought to explain particular characteristics of the compression response of fibrous mats.

Little if any evidence of nonrecoverable deformation could be detected. This was attributed primarily to a lubrication of the fibers by the saturants employed. When nonrecoverable deformation of beds of elastic fibers occurs,

it is probably due to nonrecoverable bending, especially if the fibers have a high length-to-diameter ratio.

None of the mathematical theories to predict the compression response of unbonded fibrous structures is entirely satisfactory, although Wilder's shows considerable promise. A better description is needed of what constitutes a layer of the structures and of how the stiffness of a segment increases during compression. It appears that the theory of Onogi and Sasaguri (31) is reasonably satisfactory for calculating the segment length as a function of solid fraction if the z-orientation distribution of the newly formed bed is known, and the change in z-orientation with compaction is accounted for.

PRESENTATION OF THE PROBLEM

One of the characteristic differences between fibrous structures and other representative porous media, such as soils and beds of gravel or sintered metals, is that fibrous structures are readily deformed by compressive stresses. For reasons not clearly understood at present, mats prepared under identical conditions from similar fibers often exhibit distinctly different responses to compression stresses. When the properties of the fibers are markedly different, the compression response of mats formed from them may be considerably different, although most fibrous structures exhibit certain common characteristics. Because of its importance to the papermaker in the areas of stock preparation and sheet formation, a clearer understanding is needed of the variables affecting the compression response of fibrous structures.

In many papermaking operations, fibrous mats are subjected to compressive stresses caused by the drag force of water flowing through the fiber structures. In these instances, the rate of flow through the structure is itself a strong function of the compression characteristics of the structure. Often it is desirable to be able to predict the rate of water flow through or out of a fibrous mat. For these calculations it is necessary to know the porosity of the structure as a function of the compacting pressure. This function is usually determined by measuring the change in porosity of the bed as it is subjected to mechanical loading. Attempts to predict the compression behavior of fibrous structures from known mechanical properties of the fibers have been only partially satisfactory. Theoretical expressions relating the compressibility of fibrous structures and the mechanical properties of their fibers have been limited by a scarcity of information concerning the relative importance of the mechanisms thought to cause compaction. Moreover, it has been

demonstrated that the compression response of fibrous structures is affected by the dimensions of the fibers in addition to their other characteristics. It is suspected that the internal geometry of fibrous structures as well as the manner in which the compressive stresses are distributed throughout the structure are influenced by the fiber dimensions.

The objectives of this thesis are to clarify the effect of fiber dimensions on the structure of filtration-formed mats and to determine the relative importance of the mechanisms responsible for the compaction of fibrous mats under mechanical compression.

INTRODUCTION AND HISTORICAL REVIEW

COMPRESSIVE BEHAVIOR OF FIBROUS STRUCTURES

The manner in which saturated, unbonded fibrous mats behave during compression applied perpendicularly to the plane of the mat has been studied by a rather small number of investigators. This work has been reviewed recently by Jones (1). Not all of the reported experiments were based upon mats which were formed under controlled laboratory conditions. Moreover, all of these prior studies, except those of Jones (1) and Wilder (2), were complicated by surface tension forces within the mats caused by the entry of air during recovery from compression. Consequently, these two studies are the most pertinent to the present investigation and have been considered in some detail. As this present study was prompted by the work of Jones (1), frequent reference will be made to this work throughout this dissertation, and only a brief summary of his results will be given in this section.

Wilder (2) studied the compression creep properties of saturated loblolly pine summerwood mats, whereas Jones (1) studied the compression behavior of saturated fibrous mats composed of several synthetic fibers. In these studies, fibrous mats composed of nylon, dacron, or glass fibers exhibited compression-recovery behavior basically similar to that of wood pulp mats. Double logarithmic plots of mat density vs. applied stress gave curves of nearly identical shape for all beds, though differing in position and slope. This finding suggests that the fundamental characteristics of most fibrous mats are the same.

When a mat with no previous history of loading is subjected to a compressive stress, it shows an immediate response. If the fibers of the mat are viscoelastic, the mat also exhibits a time dependent response. The first few compression-recovery cycles produce nonrecoverable deformation, after which the cycles are

essentially reproducible and the bed is said to be mechanically conditioned. However, even the mechanically conditioned beds show hysteresis, i.e., their density at any given pressure is greater during recovery than during compression. The possible mechanisms which can cause compaction of the mats were identified by Wilder (2) as fiber bending, fiber repositioning, and deformation of the fibers at their points of contact.

One of the most significant contributions of Jones' work (1) is the elucidation of the effect of fiber dimensions on the compression response of filtration-formed fiber mats. He found that, for fibers of a given diameter, beds composed of shorter fibers possessed a higher initial density but showed a smaller change in density with increasing compressive stress than did beds composed of longer fibers. The effect of fiber diameter is not quite as clear. In general, beds composed of thicker fibers have a higher density than those formed from thinner fibers of equal length, and this difference is greater for short than for long fibers. The effect of fiber diameter is usually less than that of fiber length.

Jones (1) concluded that fiber repositioning in the bed is probably the most important mechanism in the first compression of the bed, particularly at low loads. He found that the relationship between nonrecoverable deformation and length-to-diameter ratio showed a maximum at what was termed the "critical length-to-diameter ratio." In his work with glass fibers, nonrecoverable deformation was attributed entirely to slippage. However, as noted by Jones, experimental difficulties during the first compression of the glass fiber beds made determinations of nonrecoverable deformation somewhat questionable. The observed hysteresis in the compression-recovery response of mechanically conditioned glass fiber beds was also attributed to recoverable fiber slippage. The

curvature, for low stresses, of logarithmic plots of mat density vs. applied stress has indicated that the controlling mechanism in this region may not be fiber bending, but fiber slippage.

Several empirical expressions have been proposed to correlate the results of compression studies. The most commonly used expression,

$$C = MP^N \qquad (1),$$

where C is mat solid concentration or weight of fiber per unit volume of the bed, P is the apparent stress applied to the bed, and M and N are empirical constants, was first applied to pulp mats by Qviller (3). Because Equation (1) implies that an unloaded bed will have a concentration of zero, Ingmanson and Whitney (4) have suggested the following modification:

$$C - C_o = MP^N \qquad (2),$$

where C_o is the concentration of the mat before it has been subjected to any compacting stress. For mats which exhibit time dependent deformation, Wilder (2) has found that an expression of the form

$$C - C_o = (A + B \log t)P^N \qquad (3)$$

could be employed, where A and B are constants to be determined experimentally, and t is duration of stress. Under most conditions, Equation (1) applies well except at low values of P, where Equation (2) fits the data somewhat better.

When comparing data from beds having fibers of different density, it is convenient to express the results as a dimensionless quantity, rather than in terms of mat solids concentration, C. Solid fraction, σ, and porosity, ϵ, are commonly used. These quantities are defined by:

$$\sigma = 1 - \epsilon = C/\rho$$

where ρ is the density of the fiber. It can be seen that the solid fraction, σ, represents the volume of fiber per unit volume of the bed.

REVIEW OF MICROSCOPIC METHODS

The desire to inspect the interior of a sheet of paper to learn more about its structure and how it responds to stresses has prompted several investigations reported in the literature. Page and Tydeman (5), using polarized light, were able to observe the optically bonded areas between fibers near the surface of paper. A number of workers used a saturant to improve the transparency of their specimens. Van den Akker, et al. (6) utilized mineral oil to improve visibility when studying the breaking of individual dyed fibers during rupture of paper in tension. Later, in a similar investigation, Helle (7) used xylene as the saturant. Corte (8) used castor oil as a saturant to estimate the amount of interweaving of fibers in thin sheets of paper. Manby (9) employed a technique of partially embedding semitransparent fibers in a medium having the same index of refraction as the fibers to study their surface characteristics.

Hillend (10) suggested that a technique essentially identical with the one employed in this present investigation might be useful for observing fiber collapse during the compression of fibrous mats. A somewhat similar technique has been employed, but for a different type of study, by Morrell and Hildebrand (11), who used a suspension of transparent and colored balls in an index-matching fluid as a model for the structure of liquids. As far as ascertainable from a search of the literature, however, nobody has reportedly refined the technique of matching the index of refraction of fibers with that of a saturant, to the extent achieved in the present study.

PROPERTIES OF GLASS

To assess which properties of the glass fiber mats are characteristic of fibrous structures in general and which depend upon the nature of glass, certain properties of glass will be reviewed briefly. Being a class of materials rather than a single substance, glass may vary greatly in composition and properties from sample to sample. Thus, although the generic term glass is used in the following discussion, it should be noted that the characteristics which are described do not apply equally to all specimens. By definition though, except for its surface, which may have a composition distinctly different from its interior, glass is amorphous and completely isotropic (12).

Dry glass fibers are perfectly elastic and are Hookean up to levels of stress causing breakage (13). Samuelsson (14), however, reported that the stiffness of wet glass fibers, mounted as cantilever beams, dropped 5% during repeated bending in which the maximum deflection amounted to only 15% of the suspended length. Plastic flow of glass ensues at high pressure (15), and the surface of the glass flows under conditions of mechanical polishing (16). It has been shown that the moduli of elasticity of glass fiber in tension and in compression are identical (17). Glass is unaffected by organic solvents and is resistant to most acids and alkalies. However, the surface of glass is considerably altered by a number of materials (16). Water combines chemically with the surface of glass, producing hydroxyl groups. Glass in contact with water is considered to be covered with a film of silica gel having a thickness of about 50 A. (18). Even moist air reduces the refractive index of the surface of fire polished glass, presumably by leaching away some alkali. Depending upon the composition of the glass and the treatment, exposure to acids causes considerable change in the refractive index of the surface of glass. The refractive index of the surface

of a crown and of a flint glass was lowered by 0.02 and 0.1, respectively, by treatment with 1.0N sulfuric acid at 20° for 4 hours. For less resistant glass, the effect of acids is considerably greater. Exposure of a lead content glass for one minute to 0.1N hydrochloric acid lowered the refractive index of a 10^{-4} cm. thick layer of the surface by 0.29 (18).

Moisture also affects the mechanical properties of glass fibers. Wet glass fibers under a continued tensile stress have demonstrated creep (19), while dry fibers or those wetted by a nonpolar hydrocarbon did not creep. The pressure at which the fibers begin to break within a glass-fiber cloth, during compression, is about twice as great for cloth exposed to dry air as for cloth exposed to high humidity (20). This loss in resistance to compression is recoverable upon drying the cloth. However, Jones (1) found no significant difference between wet and dry glass fibers in the modulus of elasticity in bending.

Part of the characteristic behavior of glass fiber mats has been attributed to the high coefficient of friction of glass. For very clean glass on glass the coefficient of friction, u, is almost exactly 1.0 (21, 13). However, for naturally contaminated glass, u is about 0.3. Various cleaning procedures can give any value of u from 1.0 to 0.3. Exposure of cleaned glass to the atmosphere causes a pronounced lowering of u. The value of u also depends upon the relative humidity of the air surrounding the sample. For clean glass at 100% R.H., u equals 1.0, which is the same value obtained when the surfaces are wet with ultra-pure liquid water. When the air is very dry u may drop to 0.7.

APPROACH TO THE PROBLEM

One of the goals of studies of the compression response of fibrous structures is the ability to predict their compression behavior from certain known properties of the fibers. Conversely, it is desirable to estimate certain fiber properties, such as flexibility, from the compression response of fibrous mats. Attempts to relate the compression response of fibrous structures to the characteristics of their fibers have been hampered by the introduction of several simplifying assumptions in the mathematical treatments. Most of these assumptions were necessitated by a lack of knowledge about the initial structure of fibrous beds and how it changes with compression.

The task of overcoming these obstacles was resolved into two separate, but related, problems: (I) to describe the orientations and configurations of the fibers in freshly formed beds, particularly the extent to which these factors are influenced by the fiber dimensions; and (II) to determine and explain in detail how the individual fibers behave during compression and especially to clarify the manner and amount of fiber repositioning, which has been a matter of conjecture. Since the number of contacts between fibers is probably the most important quantity which must be known before the behavior of a fibrous structure can be adequately described, special attention was devoted to learning the relationship between fiber dimensions and the frequency of fiber contacts as a function of the density of the structure.

The method of study chosen for this investigation was to observe visually the interior of fibrous mats as they were subjected to mechanical compression. Fibrous beds were formed by filtration, dried, and saturated with a liquid having the same index of refraction as the fibers. The fiber beds thus became

invisible except for a few labeled fibers which could be observed by employing equipment especially designed for this purpose.

Glass fibers of known and uniform dimensions were used throughout this investigation. Since Jones (1) had shown that beds of glass fibers behave similarly to beds of other synthetic fibers and to beds composed of wood pulp fibers, the results obtained were expected to be representative of fibrous structures in general. Once the behavior of the individual fibers had been determined, it became possible to assign certain characteristics of the compression response of the beds to specific fiber properties. Quantitative results were used to test a number of pertinent theories.

EXPERIMENTAL APPARATUS AND PROCEDURES

PREPARATION OF FIBERS

The choice of fibers suitable for this investigation was limited. Because of the technique being employed, birefringent fibers could not be used. Of the common fibers, only Vinyon HH and glass fibers are not birefringent (22). Glass fibers were chosen because they are perfectly elastic, their high modulus of elasticity minimized deformation of the fibers at their points of contact, and because they were readily available.

The fibers used in this study were prepared from continuous Type E (13) glass filament obtained from Owens-Corning Fiberglas Corp. Although the Type E glass reportedly has exceptional moisture resistance (22), perhaps somewhat better transparency of the beds could have been obtained if the more chemically resistant Type C filament had been used. Almost all of the continuous filament Fiberglas is, however, Type E. Fibers with a narrow length distribution were prepared, using razor blade cutters, according to the method described by Estridge (24), Myers (25), and Jones (1). The dimensions of the four groups of fibers used are given in Table I. The fact that the weight and number average fiber lengths were almost identical showed that the fibers of each group had a nearly uniform length. The pertinent physical characteristics of Type E Fiberglas are given in Table II.

Because of its importance to the success of this investigation, special mention will be made of the method used in cleaning the fibers. Cleaning was required since, as obtained from the manufacturer, the fibers were covered with a sizing material. After cutting, the fibers were extracted in a Soxhlet extractor, first by acetone and then by petroleum ether. The acetone removed any

Duco Cement which may have been spilled on them during the cutting procedure, and the petroleum ether removed the waxy fraction of the sizing material.

TABLE I

DIMENSIONS OF FIBERS STUDIED

Mean Diameter, μ	Fiber Length	
	Arithmetic Average, mm.	Weighted Average, mm.
7.22[a]	1.09	1.10
7.22	2.26	2.26
7.22	4.55	4.56
12.86[b]	2.30	2.31

[a]Determined by electron microscopy. Standard deviation equaled 0.55.

[b]Determined by Jones (1) using optical microscope. Limits of error estimated as ± 0.94 μ.

TABLE II

SELECTED PHYSICAL PROPERTIES OF TYPE E GLASS FIBERS (13)

Specific gravity	2.54
Modulus of elasticity in tension, g./sq.cm.	73.9×10^7
Poisson's ratio	0.22
Hysteresis	None
Creep	None
Index of refraction at 550 mμ and 32°C.	1.549

After drying, the fibers were thoroughly washed in distilled water by decantation, using a minimum of five exchanges of water. Decantation was necessary to avoid the formation of nondispersible clumps. Dilute acid and also 30%

hydrogen peroxide were used in unsuccessful attempts to improve the cleaning procedure. After the hydrogen peroxide treatment, the fibers formed clumps which could not be dispersed without breaking the fibers. Dilute acid markedly improved the dispersibility of the fibers but made them unsatisfactory for this study by changing the refractive index of the glass surface. This was especially true of hydrochloric acid.

PREPARATION OF SILVERED FIBERS

It was not possible to obtain fibers of the desired diameters made from colored glass. Although a sample of dark blue glass fibers was obtained, the intensity of their color was too low to allow them to be readily distinguished from the colorless fibers. The problem of obtaining fibers which could be observed in the saturant and which had the same size and stiffness as the colorless fibers was solved by silvering the colorless fibers.

A modified Brashear (26) process was used to silver the fibers. After precleaning, the fibers were washed successively with concentrated nitric acid, with a dilute solution of stannous chloride, and with distilled water, and then added to the silvering solution. Stannous chloride promotes adhesion of silver to glass. The silvering solution was prepared by adding 30 ml. of silver nitrate (10 g./l.) to 500 ml. of potassium hydroxide (200 g./l.) and then adding just sufficient ammonium hydroxide to dissolve the silver oxide. The resulting volume of solution was made up to four liters, using a suspension containing 0.5 g. of fibers. Distilled water was used exclusively. The exact amount of ammonium hydroxide required is very important and varies with several factors, including the rate of agitation of the solution. If an excess of ammonia is used, no silver layer will be deposited, whereas a deficiency of ammonia will cause the silver to contain particles of silver oxide. To improve the adherence

of the silver layer, the fibers were stirred for a minimum of thirty minutes in the silvering solution before addition of the reducing solution. The reducing solution consisted of 90 g. glucose per liter, and 5 ml. of this solution were used per gram of silver nitrate.

Successful silvering of the fibers required maintaining their cleanliness, eliminating any chloride ion before adding the fibers to the silvering solution, and obtaining an optimum ammonium hydroxide concentration. It should also be noted that ammoniacal silver nitrate solutions will, and did occasionally, explode spontaneously, so that proper safety precautions were necessary. The procedure outlined for producing silvered fibers is similar to that described by (27), which was disclosed after the above method had been developed. When properly prepared, the silvered fibers were essentially opaque; they had a fairly smooth and highly reflective surface, and the silver adhered to the glass well enough to allow their suspensions to be agitated by laboratory mixers without the silver peeling off.

For a portion of this study, it was desirable to know the stiffness, EI, of the fibers being studied. This value could be ascertained only if all silvered fibers in the bed had the same stiffness. This condition was met by isolating single filaments from the thread, silvering them, determining their stiffness, then cutting them into fibers of the desired length, and keeping the fibers from each filament separate. With this method, the filaments were wound on glass frames and silvered in vacuo. Except as otherwise noted, the silvered fibers used in this work were silvered from solution.

It was necessary to ascertain what effect the layer of silver on the fibers had upon their stiffness, EI. Because the coated fibers were nonhomogeneous in cross section, the proper determination of their stiffness was by means of a

bending technique. Also, because the fibers were cut before silvering, it was necessary to determine the stiffness of comparatively short fibers. The common static bending test was rejected as a possibility, because the fibers deflected negligibly under their own weight. The resonance frequency test (28) was rejected, for two reasons. This technique becomes less precise for fibers with small diameters and high moduli of elasticity. Moreover, it was not deemed feasible for this investigation to assemble and calibrate the equipment required to perform the resonance frequency test.

Instead, the small device shown (minus its cover) in Fig. 1 was designed and constructed. It allows the stiffness of a test fiber to be determined relative to a reference fiber. The fibers to be tested were fastened to small stainless steel pins with an epoxy resin and were held at right angles to each other by the stationary Clamp B and the movable Clamp A so that their ends overlapped. Moving Clamp A by means of the micrometer screw, beyond the point where the fibers just touched, caused both fibers to deflect. The lengths of both fibers, from their points of support to their intersection, and their deflections were measured using the eyepiece scale of the microscope (to be described). Slippage of one fiber over the other at their point of intersection was minimized by design of the device and by using small deflections. No slippage could be observed during the tests.

Values of relative stiffness, S_r, were calculated from the equations for the deflection of a cantilever beam as follows:

$$S_r = \frac{EI}{E'I'} = \frac{\Delta' L^3}{\Delta L'^3} \qquad (4).$$

In Equation (4), L was the length of fiber from its glue line to its point of intersection with the other fiber, Δ was the deflection of the fibers, and the

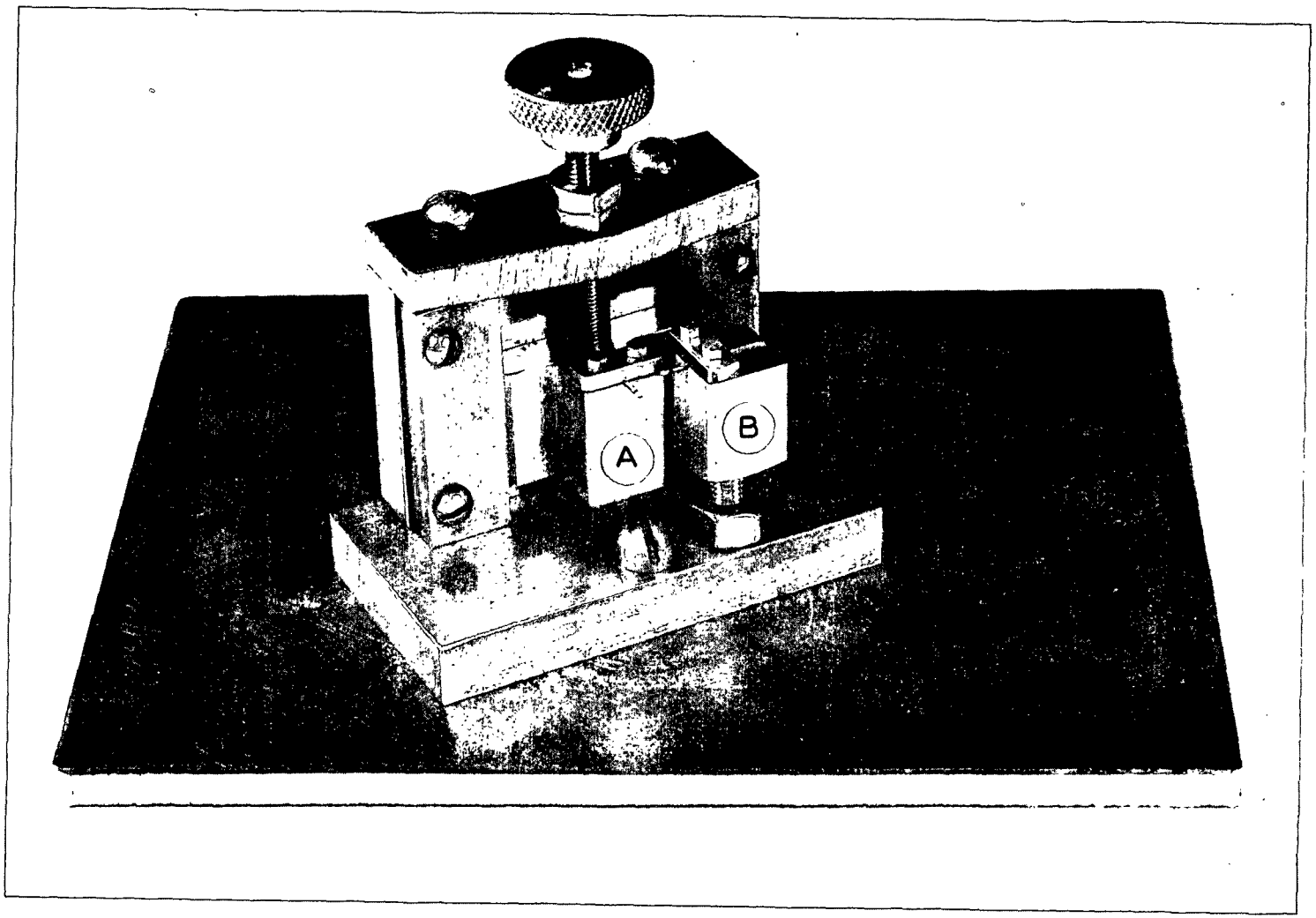

Figure 1. Device for Determining Relative Stiffness of Silvered Fibers

primes referred to the reference fiber on the movable support. Table III gives representative data for the stiffness of the 2.26 mm. by 7.22 μ fibers before and after removal of the silver with nitric acid. Nitric acid was shown to have no measurable effect on the stiffness of the unsilvered fibers. All values in Table III were determined relative to the same reference fiber. The variability between duplicate determinations of the stiffness of an individual fiber is about as great as would be obtained using the resonance frequency test on fibers of this length. Although the coating of silver upon the fibers was found to increase their stiffness, this increase was small compared to the difference in stiffness between unsilvered fibers caused by small differences in their diameters. Other data showed that the stiffness of each fiber along its length was essentially constant, as indicated by the fact that fibers cut from widely separated areas along a single filament had nearly identical stiffness values.

An electron microscope was used to determine accurately the diameter of the reference fiber and approximately the distribution of diameters of the other filaments in the thread. It then became possible to calculate the absolute stiffness of the fibers from their relative stiffness as determined by the bending technique. In order to measure their diameters, the fibers were mounted on electron microscope grids containing styrene latex particles of known size. Simultaneously, the images of the fibers and particles were recorded on 35 mm. film (Adox KB 14) at a nominal magnification of 1,200 diameters. The dimensions of these images were then measured by using the eyepiece scale of the microscope shown in Fig. 3, p. 27. It can be seen from Table IV that, even for the small number of fibers measured, the variability of the fibers as indicated by relative stiffness values obtained in the bending test, agreed well with the calculated values obtained by electron microscopy. In Table IV all results were expressed in terms of relative stiffness rather

TABLE III

EFFECT OF SILVERING ON RELATIVE STIFFNESS
OF 2.26 MM. BY 7.22 μ FIBERS

Fiber No.	Relative Stiffness Silvered Trials	Mean	Unsilvered Trials	Mean
1	1. 2.69		2.21	
	2. 2.50		2.24	
	3. 2.71		2.28	
	4. 2.74		2.31	
	5. 2.94		2.28	
		2.71		2.26
2	1. 1.44		1.18	
	2. 1.49		1.25	
	3. 1.44		1.20	
	4. 1.44		1.24	
	5. 1.45		1.27	
		1.45		1.23
3	1. 0.972		0.813	
	2. 1.00		0.855	
	3. 0.945		0.826	
	4. 0.995		0.846	
	5. 1.03		0.840	
		0.988		0.836
4	1. 1.25		0.836	
	2. 1.31		0.900	
	3. 1.23		0.871	
	4. 1.29		0.811	
	5. 1.29		0.911	
		1.27		0.866

than fiber diameters. Relative stiffness varies as the fourth power of fiber diameter and illustrates more clearly the variability of the fibers.

Electron micrographs of fibers silvered from solution showed that their surface was not as smooth as that of unsilvered fibers. The silvered fibers gave the appearance of being covered with a layer of fine granular dust, which was probably a mixture of metallic silver and silver oxide. Etching of the glass substrate by the alkaline silvering solution did not appear to be important.

TABLE IV

COMPARISON OF BENDING TECHNIQUE AND ELECTRON MICROSCOPY FOR DETERMINING FIBER DIAMETER DISTRIBUTIONS

Sample	Method: Bending Technique	Method: Electron Microscopy
	Mean Relative Stiffness	
All fibers	1.48	1.55
Reference fiber	1.00	1.00
	Standard Deviation of Sample	
All fibers	0.606	0.528[a]
Reference fiber	0.048	0.055
	Number in Sample	
All fibers	11	32
Reference fiber	7	4

[a]Calculated from fiber diameters.

Although it seems possible that the silvered fibers, being rougher, might slip considerably less than the unsilvered ones, it is believed that the layer of silver did not appreciably restrict any tendency of the fibers to slip, for at least three reasons. In the first place, the height of the asperities, which was of the order of 0.06 μ, was small compared to the diameter of the fibers. Secondly, the layer of silver did not adhere tightly to the glass and flaked off rather easily. In addition, some axial slippage of the fibers during compression was noted, which would have been more seriously restricted by their roughness than would lateral slippage. Even if the silvered fibers could not slide upon the unsilvered ones, it is highly unlikely that the unsilvered fibers could rearrange their position while keeping the relative positions of the silvered fibers constant. For these reasons, it was concluded that the behavior of the silvered fibers during compression gave an accurate indication of what was happening to the unsilvered fibers.

FORMATION OF FIBER BEDS

The fiber beds were formed by filtration from very dilute suspensions (0.0008 to 0.0002%), using the equipment diagrammed in Fig. 2. The initial flow rate was about 2.9 cm./sec. and this was reduced as the bed was formed, to maintain the pressure drop across the bed at less than 1.0 cm. of water. The septum consisted of a drilled brass plate (0.1563 inch countersunk holes on 0.200 inch centers) covered with a 16-mesh stainless steel screen and this in turn with a 150-mesh screen. The Lucite formation tube was 3 inches in diameter and 20 inches tall from inlet to septum. Four turbulence-reducing vanes extended downward 17.5 cm. from the inlet of the formation tube. Except for a few minor changes to the forming tube and the addition of manometers, this equipment was identical to that assembled and constructed by Arnold (29).

Control of the flow rate was obtained by manipulation of the bypass valve and was measured by an orifice plate and two manometers. The pressure drop across the bed and septum was measured by a chlorobenzene-filled manometer.

Considerable care was taken to prevent aggregation of the fibers during formation of the beds. As the fibers approached the septum they could be observed. Each fiber was separate from the others and slowly rotating. Flocculation of the fibers did not occur. Fibers near the center of the tube did not move noticeably faster than those near the edge, which indicated that the velocity profile was reasonably uniform. No preferential orientation of the fibers approaching the septum could be noted either in the x-y plane normal to the direction of flow or in the z-direction parallel to the flow.

Difficulty was encountered in obtaining and maintaining satisfactorily clean water. Even the distilled water used contained small amounts of suspended

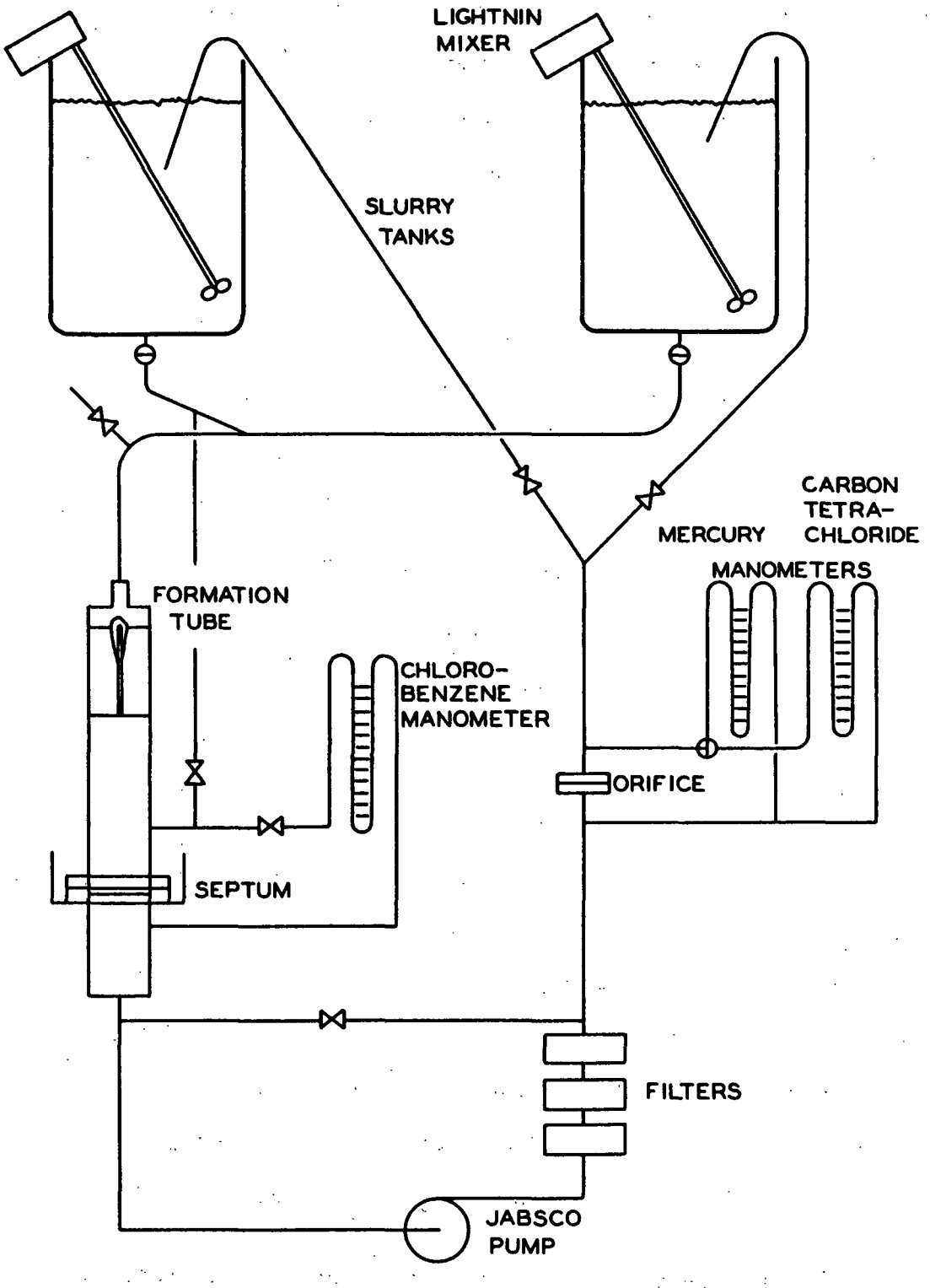

Figure 2. Schematic Diagram of Apparatus Used to Form Fiber Beds

matter, probably of bacterial origin, which was only partially removed by the cellulose filters. The suspended material tended to concentrate in the fiber mats and caused poor visibility when the beds were saturated with the refractive index-matching liquid. Slimicides were used to help control the growth of micro-organisms. Formaldehyde, phenylmercuric acetate, copper sulfate, and Dowicide B were employed. None of these was entirely satisfactory. The completely formed mats were washed, while still in the forming tube, with 6 liters of fresh filtered distilled water containing no slimicides.

After formation and while still on the septum, the beds were transferred to aluminum dishes. Deaerated distilled water was added to bring the water level up even with the top of the bed after which they were quick frozen. When solidly frozen, the septum was removed and the diameter of the bed was reduced to 5.8 cm. by cutting off the edge of the bed with a small jig saw. This was necessary because Jones (1) had reported that the edge of the beds exhibited anomalous compression-recovery behavior. This behavior was attributed to a wall effect during formation which resulted in the fibers near the edge of the bed being oriented nearly vertically.

As it was desirable to obtain the dried beds in as nearly an uncompressed state as possible, the beds were freeze dried. This prevented compression of the bed by the surface tension of the water and minimized "bonding" of the glass fibers. It will be demonstrated later that air drying produced some "bonding" of the fibers. After drying, the beds were stored until they were needed. At that time, the dried beds were weighed, their diameters were measured, and they were carefully transferred to the glass plate of the observation cell (Fig. 5). The weights of the beds ranged from 0.7 to 1.6 g. They were then saturated by slightly tilting the observation cell and slowly filling it with the desired

saturant. Tilting the cell caused the meniscus of the saturant to advance into the bed from one side only, preventing entrapment of air within the bed. When this operation was performed properly, no air remained in the bed. Any bubbles could have been easily detected. After saturation was completed, the observation cell was clamped into its support, and the glass plate, which supported the bed, was firmly seated into the gear holding it.

The saturant used during most of this investigation was Cargille Immersion Liquid (Refractive Index – 1.548), obtained from R. P. Cargille Laboratories, Inc., Cedar Grove, New Jersey. This oily liquid was clear, colorless, nonvolatile, and stable. It was learned (30) that it contained mineral oil in addition to certain halogenated hydrocarbons. For simplicity, throughout this dissertation the Cargille Immersion Liquid will be referred to as the oil.

MICROSCOPE AND ASSOCIATED EQUIPMENT

To study visually the saturated fiber beds, special equipment was constructed and assembled. This equipment allowed the fiber beds to be observed alternately vertically (Fig. 3) and horizontally (Fig. 4) while the bed was being compressed by a piston. For the purpose of discussion, it is convenient to divide this equipment into three parts. These are: the microscope and its support, the glass-walled chamber which contained the fiber bed and its saturant, and the loading mechanism used to compress the bed.

A Bausch & Lomb Stereomicroscope was the heart of this experiment. It was one of the K series stereoscopic microscopes with a "Stereo-Zoom Power Pod." It was equipped with twenty-power widefield eyepieces to give a total magnification ranging from 14 to 60 diameters. Regardless of the magnification, a working distance of 10 cm. was obtained.

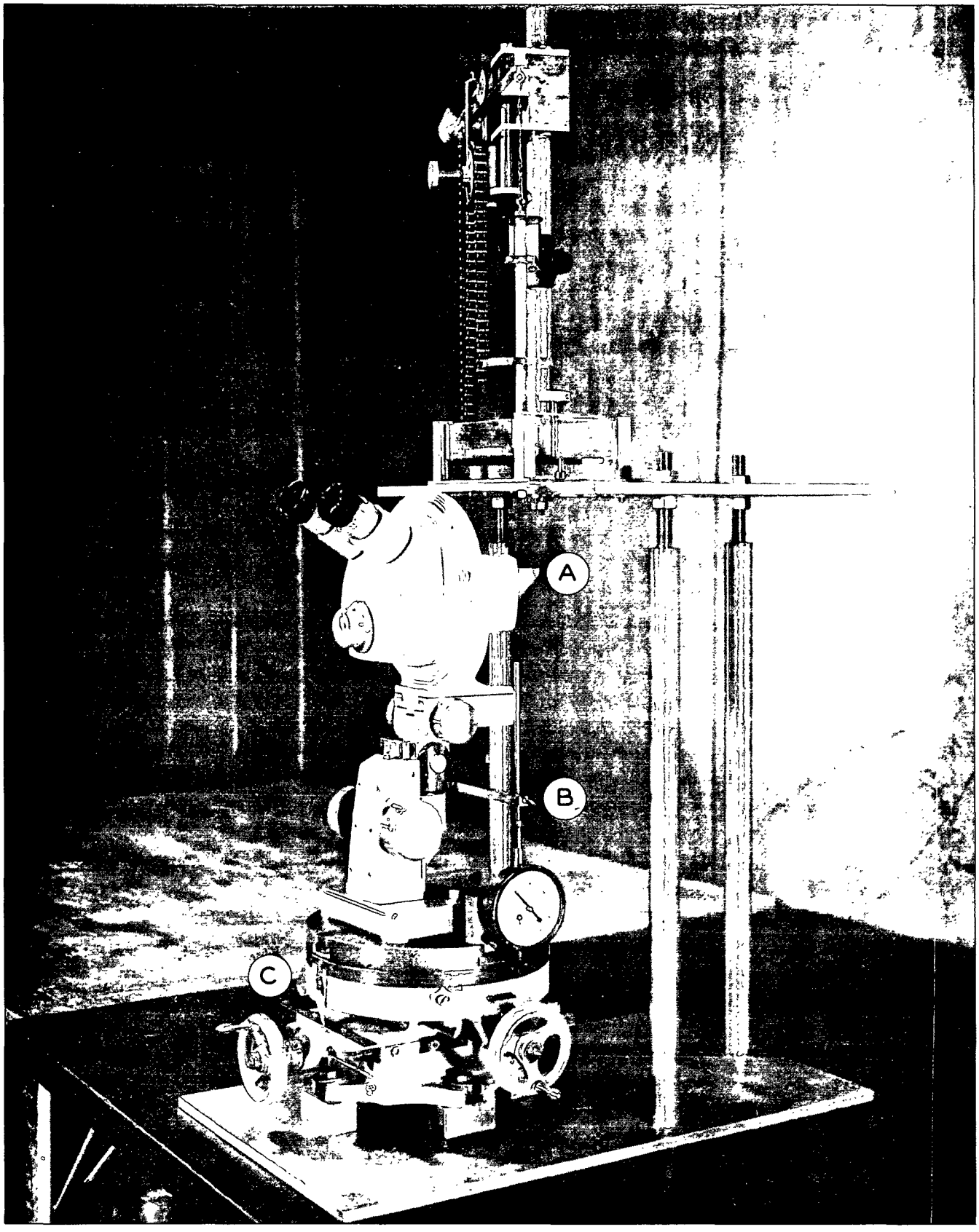

Figure 3. Microscope in Position for Viewing Vertically Through Bed

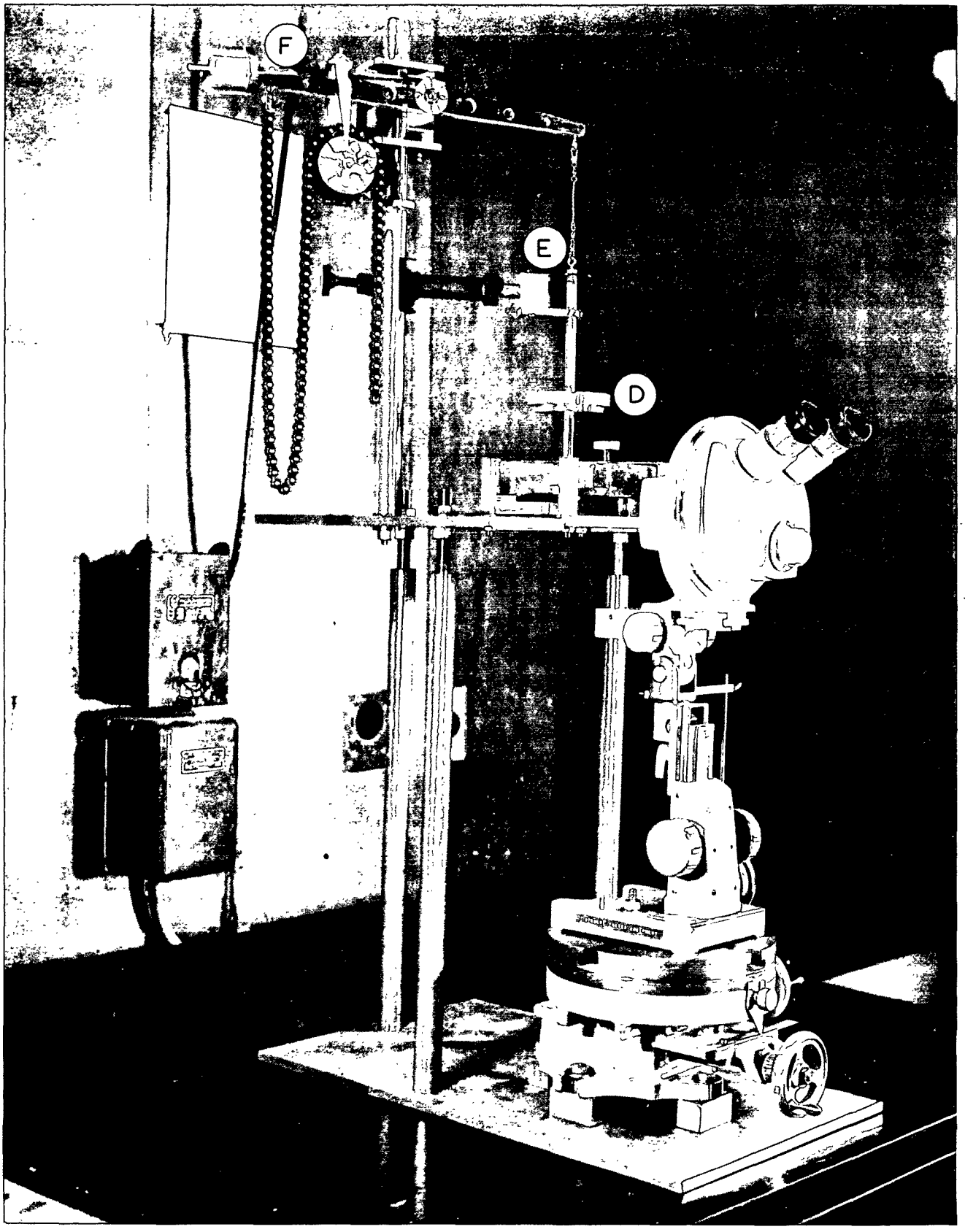

Figure 4. Microscope in Position for Viewing Horizontally into Bed

It would not have been possible to compress the bed, view it vertically from above, and simultaneously to rotate the bed in the x-y plane. Consequently, it was necessary to view the bed from below. This was accomplished by using a prism as shown at A in Fig. 3. The corners on one face of a right angle prism were ground off so that it could be cemented into the ring which had held the clear glass shield supplied with the instrument. The objective end of the Power Pod is threaded so that the ring holding the prism could be screwed into it. For horizontal viewing (Fig. 4), the prism was removed. Because of the special stand of the K series microscopes, a total vertical displacement of 15 cm. could be obtained. If needed, the Power Pod could also be rotated 360° about its optic axis.

As it was not possible to move the bed while compressing it, it was necessary to provide means of moving the microscope. This was achieved by mounting the microscope on a Palmgren No. 82 dual cross slide milling table. Maximum travel in both directions was 4-1/4 in. The dials were graduated in thousandths of an inch. Steel rules graduated in tenths of an inch (see C, Fig. 3) were added. A dial micrometer graduated in thousandths of an inch, mounted as shown at B in Fig. 3, was used to locate the vertical position of the microscope. Although the micrometer had a maximum travel of one inch, an extension rod allowed the entire vertical range of the microscope to be covered in one-inch intervals.

Figure 4 shows the mechanism used to compress the bed. It consisted of a piston with a platform for holding weights (D) and a counterbalance arm (F). The piston was hung from the counterbalance arm by means of two ball bearing snap swivels. By using the counterbalance arm, loadings on the bed less than the weight of the piston could be obtained. A calibrated roller chain was used to increase the loading on the bed by small increments which were determined by

the graduated dial. After the photograph of Fig. 4 was taken, a longer chain was added. It was 8-ft. long and hung downward through a hole in the table. By means of this chain, total loadings from 0 to 460 g. could be applied to the bed before it was necessary to add weights by hand to the piston. This was provided to minimize vibrations and to reduce lateral movement of the piston during determination of the compression-recovery curves. A screw was employed to allow the counterbalance arm to remain horizontal as the height of the bed was reduced. When photographs were to be taken during compression, a close-fitting piston guide was used to prevent lateral motion of the piston. The guide was positioned immediately above the observation cell and was supported like the index of the setting circle shown at E in Fig. 4. Provisions were made so that the vertical alignment of the piston could be adjusted.

Three one-inch steel rods supported the 3/8-in. steel plate holding the observation cell. The bottom plate was bolted to the plywood top of a steel-reinforced table which rested upon a concrete floor. This equipment was housed in a constant temperature room maintained at 72°F., which was necessary for control of the refractive index of the saturants.

The heights of the fiber beds during compression were determined using the microscope in its position for horizontal viewing. Using the dial micrometer and the center of the eyepiece scale, the distance between the face of the piston and the glass plate on the bottom was measured. Then the extension rod on the micrometer was freed, the microscope raised and focused on a reference mark on the shaft of the piston, and the extension rod again tightened. The height of the bed could then be calculated from the readings of the dial micrometer. As there was some backlash in the vertical rack and pinion mechanism, all readings were approached from the same direction. The compressibility of the beds was determined by slowly applying a known load to the beds and then measuring their height.

The design of the glass-sided box used to hold the fiber beds, which has been termed the observation cell, is shown in Fig. 5. The front glass plate through which the bed was studied is optical-grade glass. The glass plate upon which the bed rests and the bottom window were cut from Kodak Projector Slide Cover Glass. A Dow Corning self-curing Silastic compound was used to seal the glass plates to the frame of the box. Between these two glass plates below the bed, there was a spur gear with its center removed. Using the spur gear and the smaller gear it was possible to rotate the bed to bring any desired fiber into the plane of focus of the microscope. To relocate individual fibers, it was necessary that the rotational position of the bed be known. A setting circle on the piston, shown at E in Fig. 4, was used to measure rotation of the beds.

For optimum results a source of monochromatic illumination should have been employed while observing the beds. Owing to the difference in dispersion characteristics between the glass and the saturant, a perfect match of the indices of refraction is possible only at one wavelength. It was found, however, that the readily available sources of monochromatic light lacked sufficient intensity and that white light worked rather well. Cleanliness of the fibers and imperfect temperature control within the beds limited transparency more than did white light.

For horizontal viewing the light source was placed in back of the bed, and a pane of opal glass was placed between the lamp and the bed. Using this arrangement, the silvered fibers showed up black against a light background. A large heat-absorbing cell filled with a copper sulfate solution was positioned in the light path to reduce heating of the oil.

For vertical viewing the lamp was placed beneath the plate supporting the bed. In this position, the silvered fibers appeared bright against a black

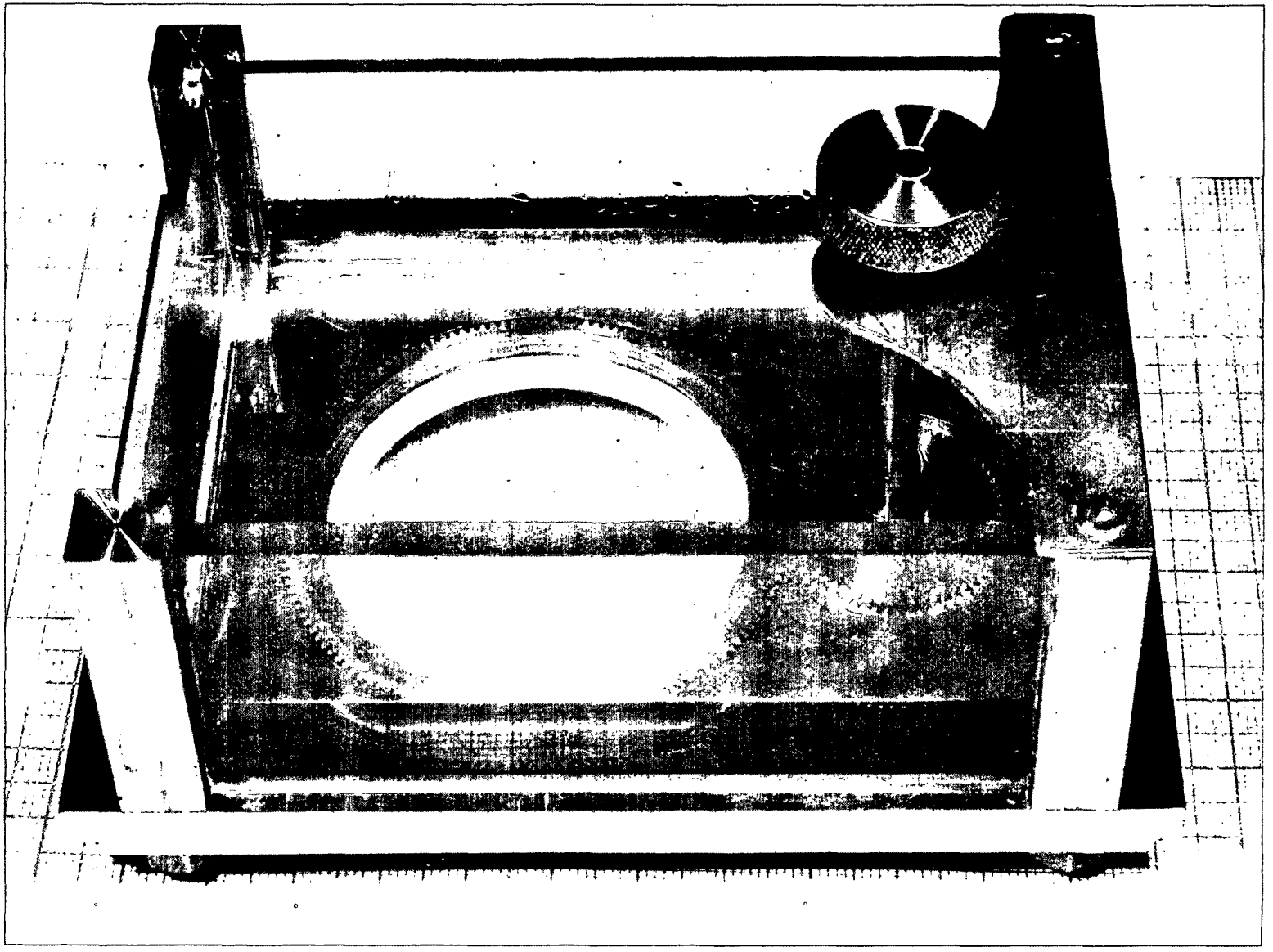

Figure 5. Cell Used to Hold Saturated Fiber Beds During Study. Bed Entirely Covers Glass Plate in Center. Light Area in Center of Opening is Due to Manner of Lighting

background, because the face of the piston was composed of a plate of black glass and the silvered fibers reflected light. As each fiber reflected only a small amount of light, the face of the piston had to be composed of a material which absorbed essentially all the light striking it.

Photographs of the fiber beds were taken using a Leica camera with the Micro-Ibso attachment. The Micro-Ibso and its 10X eyepiece replaced the usual lenses of the camera. Focusing was accomplished by means of a prism-type viewer on the Micro-Ibso.

To record the orientation of the fibers with respect to the plane of the mat it was necessary to locate the camera in the same position each time. This was achieved by taking the photographs always from the same eyepiece and with the eyepieces in their centermost position. When viewed from the front of the microscope, the camera was leveled using a bubble level which was adapted to fit the flash holder of the camera. In this position, the image of the glass plate on the bottom of the bed was not quite parallel with the edge of the film, and a small correction was necessary when measuring the orientation of the fibers. When this routine was followed the camera could be mounted in essentially the same position each time.

Kodak Plus-X film was used. Exposures varied from 10 to 40 sec. when viewing vertically, depending upon the lighting and magnification. When viewing from the front of the bed, exposures varied from 0.5 to 2 sec., depending primarily upon the degree of compression of the bed.

EXPERIMENTAL RESULTS

SCOPE OF WORK ACCOMPLISHED

Fiber beds were prepared using glass fibers of three different lengths, at one diameter, and fibers of a larger diameter for one of the lengths. The orientation and configuration of the fibers in freshly formed beds was studied for beds composed of the four different sizes of fibers. Special attention was given to the z-orientation of the fibers. The data were correlated with an empirical equation and transformed into probability density functions expressing the z-orientation distributions of the fibers. After accounting for the effect of compression on z-orientation, the probability density functions were used with the theory of Onogi and Sasaguri (31) to predict the number of fiber contacts per fiber within the compressed beds. These results were compared with the number of fiber contacts determined experimentally and the agreement was found to be good. In light of these findings, the compressibility equation of Wilder (32) was evaluated further.

The relationship between fiber dimensions and the mechanisms causing compaction was considered. Photographic evidence was obtained which showed the limits of possible fiber repositioning during compression. Several determinations were made of the compression response of beds under different conditions of interfiber friction. The results of the individual experiments were analyzed and summarized to present a clearer understanding of the compressive behavior of fibrous structures.

The presentation of the results of this study has been divided into two major sections. The first section describes the individual experiments and the results obtained. The second section contains an analysis and discussion of the experimental results taken together and considers their significance.

GROSS APPEARANCE OF BEDS

Before discussing the specific results of observing the interior of the beds, a few general comments are in order. The success of the technique for rendering the glass fibers invisible is indicated by Fig. 6 and 7. Figure 6 shows three fibers passing through an air bubble in the saturant and disappearing when they enter the liquid (oil). Essentially perfect transparency was obtained. Figure 7 shows a calibrated microscope slide photographed through the diameter of an unloaded bed containing about 0.2% silvered fibers. The smallest divisions represent thousandths of an inch. It can be seen that remarkably good resolution was obtained. A sodium vapor lamp was used for illumination in Fig. 6 and white light for Fig. 7.

The saturated fiber beds were not perfectly transparent. When observed against an illuminated background, the outline of the beds could be detected because they appeared slightly cloudy and possessed a light blue color. This was due to the fact that monochromatic illumination was not employed, and probably also to a slight contamination of the fiber surfaces. It could be seen that the edges of the beds remained straight both during compression and recovery. No increase in the diameter of the beds during compression could be detected.

When viewed vertically, all silvered fibers in the beds could be clearly observed. When viewed horizontally, fibers within 1 cm. of the edge of the bed could always be clearly seen. In most beds, fibers within 2 cm. of the edge could be studied. For beds with the highest percentages of silvered fibers (0.2 to 0.3%), this distance was reduced somewhat. It appeared, though, that fibers farther than 2 to 3 mm. from the edge were not influenced by the edge.

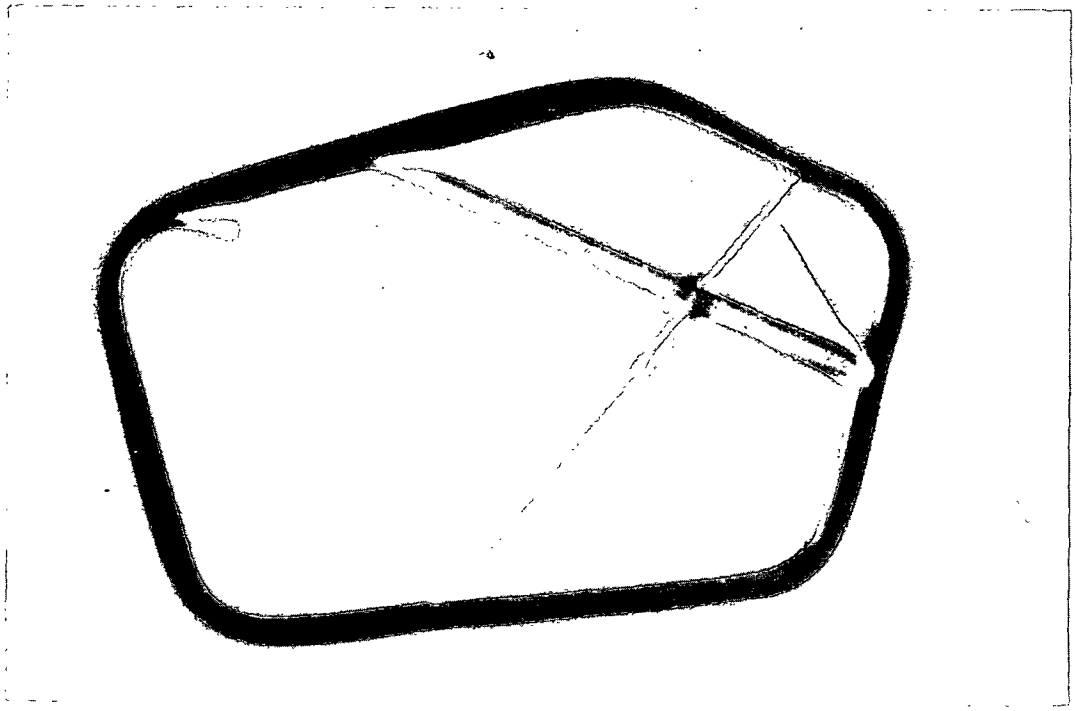

Figure 6. Glass Fibers Passing Through an Air Bubble and Disappearing When They Enter Oil Having the Same Refractive Index

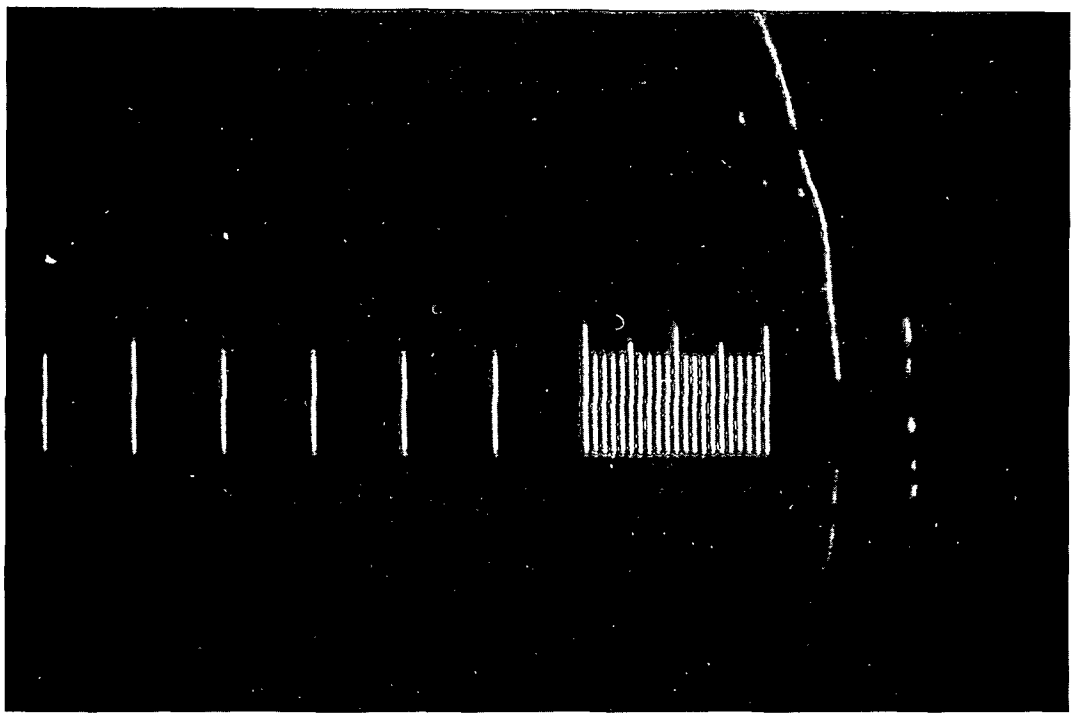

Figure 7. Calibrated Microscope Slide Photographed Through Diameter of Bed Containing Silvered Fibers. Smallest Divisions are 0.001 in.

Several differences were noted in the configuration of the fibers in the newly formed beds, depending upon the dimensions of the fibers. When viewed from the edge of the bed, the two fiber samples with a length-to-diameter ratio less than 200 were essentially straight. The 4.55 mm. by 7.22 μ fibers were somewhat bent, but not as greatly as the 2.26 mm. by 7.22 μ fibers. Some of the fibers of high orientation in the beds of 2.26 mm. by 7.22 μ fibers had the general shape shown in Fig. 8. No fibers were found which were concave upward. It would seem that, during formation of the bed, one end of these fibers pierced the portion of the bed previously deposited and that they were then bent over by the water flowing past them and were held in that position by other fibers which were subsequently deposited. The presence of these deformed fibers in the newly formed beds suggests that the structure of the freshly formed beds is somewhat dependent upon the velocity of the water flowing through the bed during formation, as well as on the pressure drop across the bed.

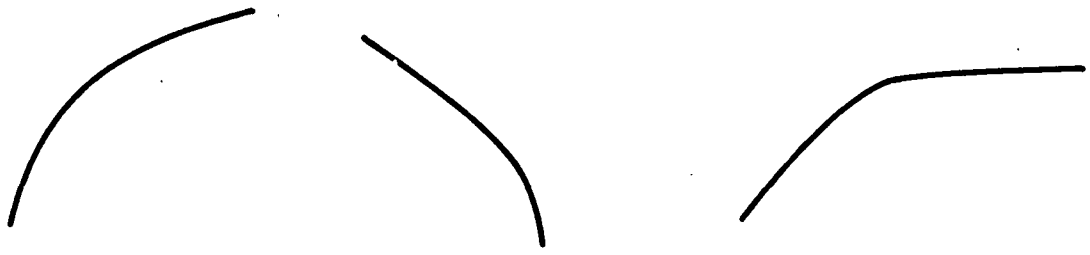

Figure 8. Configuration of Some 2.26 mm. by 7.22 μ Fibers in Freshly Formed Bed

When viewed from below, essentially all fibers were straight, regardless of their dimensions. Two minor exceptions were noted: Some of the 4.55 mm. by 7.22 μ fibers showed a very slight curvature in the x-y plane. In beds made of 2.26 mm. by 7.22 μ fibers, a few of the fibers with the configuration shown in Fig. 8 appeared curved when viewed from below.

COMPRESSION AND RECOVERY BEHAVIOR OF BEDS

Compressibility tests were used to characterize the compression and recovery response of the types of fiber beds which were studied visually. Beds of the 2.26 mm. by 7.22 μ fibers were studied more thoroughly than any of the others. A double logarithmic plot of mat solids, C, versus apparent applied stress, P, for one oil saturated bed of these fibers is shown in Fig. 9. A plot of solid fraction, σ, versus apparent applied stress, P, in rectangular co-ordinates is shown in Fig. 10. These curves are typical of those obtained for beds of the other sizes of fibers. Several features of these curves will be noted. Both the first and third cycles exhibited hysteresis. During the third compression, the bed responded somewhat more than during the first compression, but the recovery portions of the two cycles show little difference. It can be seen from Fig. 10 that this bed was essentially perfectly recoverable when compared in the uncompressed state. In fact, some of these beds had a slightly lower solid fraction at the end of the first recovery than they had immediately after saturation. The results of all compressibility tests are summarized in Table V. A comparison of beds numbered 1 and 2 shows that the reproducibility of the results was fairly good. Quantities chosen to describe the behavior of the beds are: work absorbed and returned during the cycle, solid fraction at an applied stress, P, of 100 g./sq. cm., and solid fraction at P equal to 70 g./sq. cm., both during compression and recovery.

If the height of a bed is plotted against the stress applied during compression, the area between the curve and the vertical axis, when multiplied by the cross-sectional area of the bed, equals the work absorbed by the bed. The area between the compression and recovery curves represents the work lost during the cycle. The values given in Table V have been expressed as work per gram of

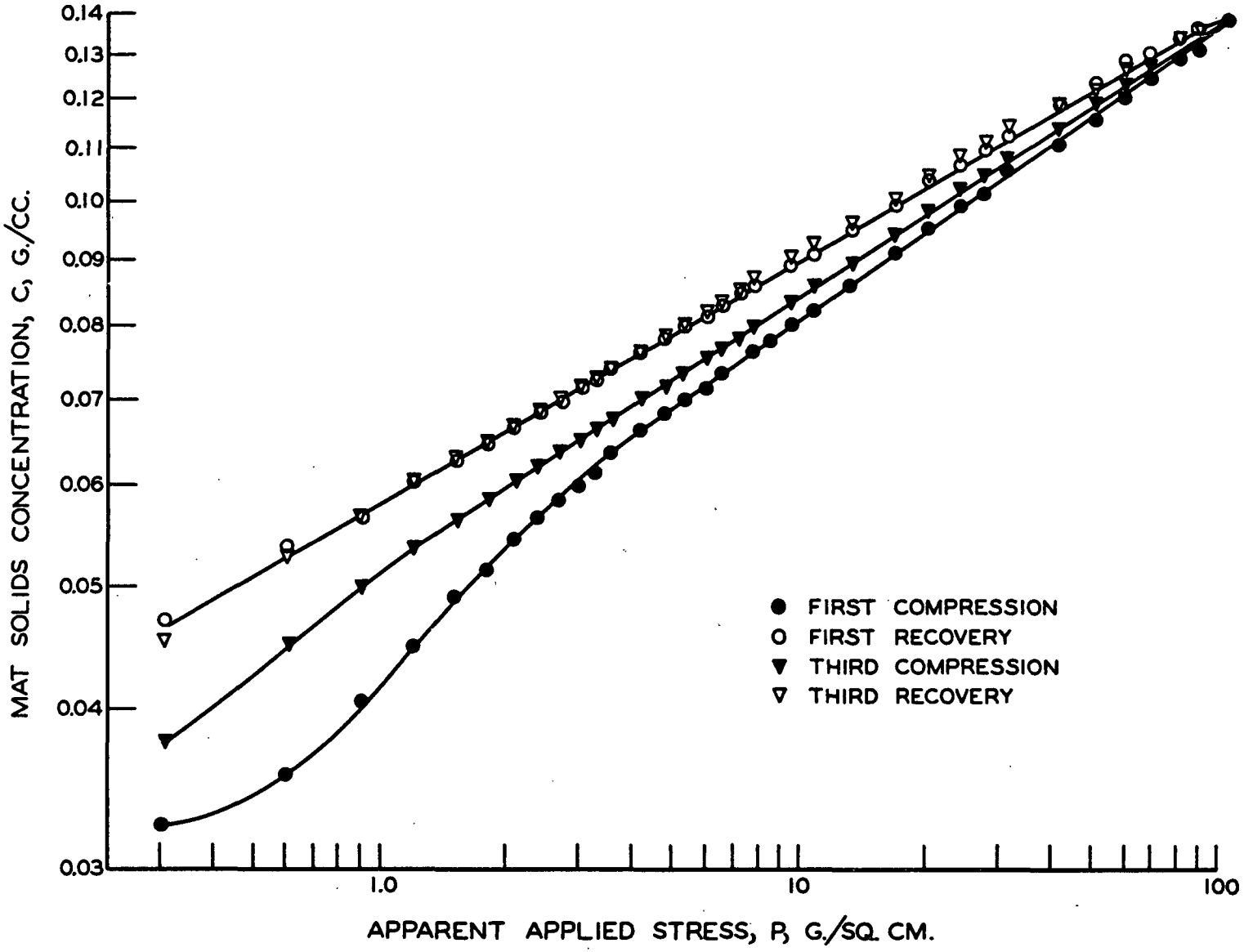

Figure 9. First and Third Compression and Recovery Curves for a Bed of the 2.26 mm. by 7.22 μ Fibers When Saturated With Oil

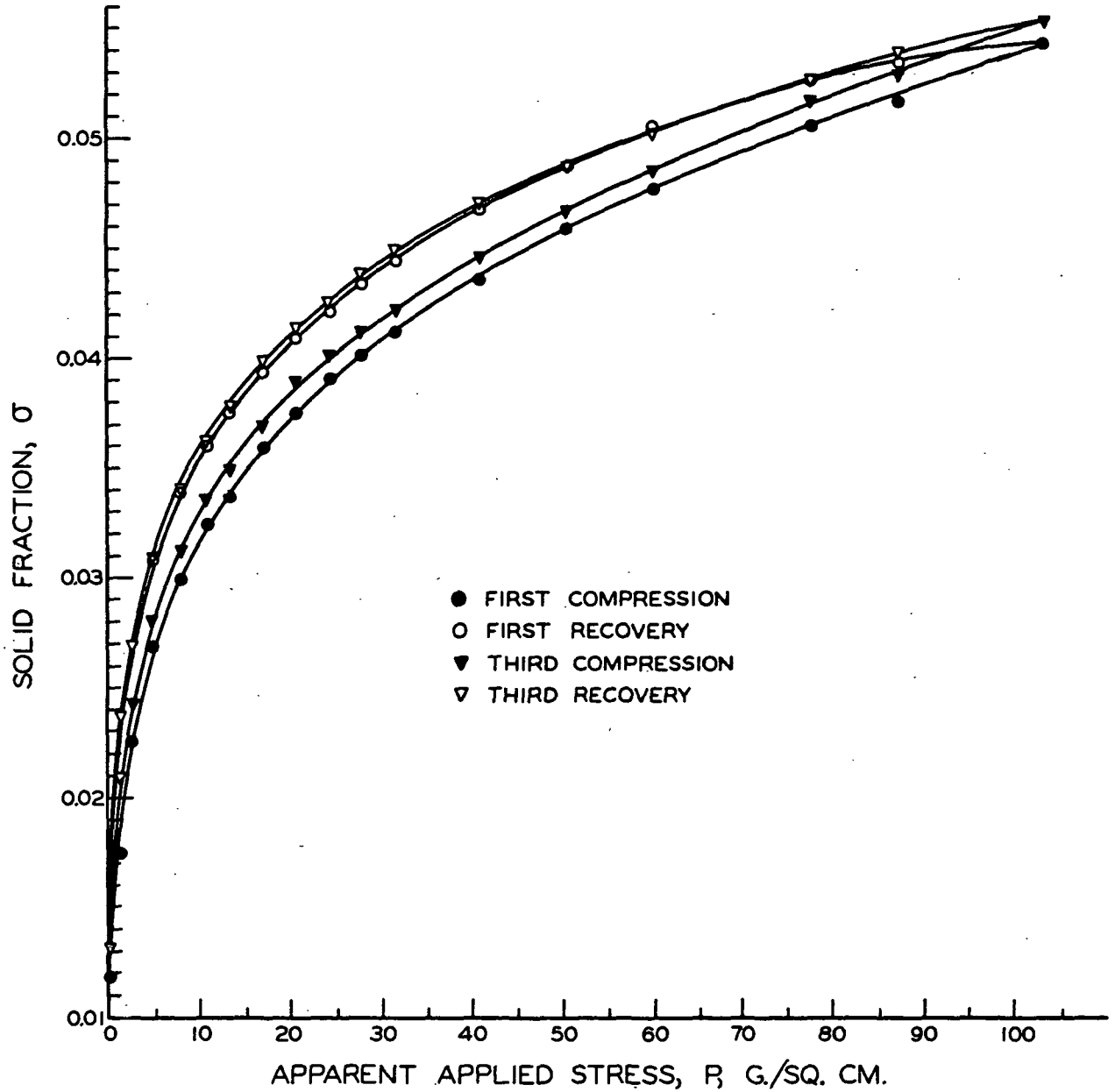

Figure 10. First and Third Compression and Recovery Curves for a Bed of the 2.26 mm. by 7.22 μ Fibers When Saturated With Oil

TABLE V

SUMMARY OF RESULTS OF COMPRESSIBILITY TESTS

Bed Number	Fiber Dimensions	Saturant	Cycle	Method of Drying	Work Absorbed During Comp., g.-cm./g.	Work Regained During Recovery, g.-cm./g.	Work Lost, g.-cm./g.	Solid Fraction at 100 g./sq.cm.	Solid Fraction at 70 g./sq.cm. During Compression	During Recovery	Hysteresis
1	2.26 mm. by 7.22 μ	Oil	1	Freeze dried	221	149	72	0.0538	0.0494	0.0516	0.0022
1	2.26 mm. by 7.22 μ	Oil	3	Freeze dried	200	154	46	0.0547	0.0505	0.0518	0.0013
2	2.26 mm. by 7.22 μ	Oil	1	Freeze dried	--	--	--	0.0537	0.0492	0.0511	0.0019
2	2.26 mm. by 7.22 μ	Oil	3	Freeze dried	--	--	--	0.0548	0.0506	0.0517	0.0011
3	2.26 mm. by 7.22 μ	None	1	Freeze dried	227	179	48	0.0547	0.0500	0.0514	0.0014
3	2.26 mm. by 7.22 μ	None	3	Freeze dried	208	177	31	0.0556	0.0509	0.0518	0.0009
4	2.26 mm. by 7.22 μ	Oil	1	Air dried	216	153	63	0.0510	0.0475	0.0491	0.0016
4	2.26 mm. by 7.22 μ	Oil	2	Air dried	202	152	50	0.0515	0.0482	0.0493	0.0011
4	2.26 mm. by 7.22 μ	Oil	5	Air dried	193	151	42	0.0517	0.0483	0.0493	0.0010
5	2.26 mm. by 7.22 μ	ODB[a]	1	Freeze dired	202	166	36	0.528	0.0488	0.0497	0.0009
5	2.26 mm. by 7.22 μ	ODB	2	Freeze dried	192	165	27	0.0549	0.0507	0.0517	0.0010
5	2.26 mm. by 7.22 μ	ODB	3	Freeze dried	187	166	21	0.0552	0.0512	0.0518	0.0006
5	2.26 mm. by 7.22 μ	Oil	4	Freeze dried	205	160	45	0.0550	0.0501	0.0519	0.0018
6	2.26 mm. by 7.22 μ	Water	1	Freeze dried	205	173	32	0.0541	0.0497	0.0512	0.0015
6	2.26 mm. by 7.22 μ	Water	3	Freeze dried	196	170	26	0.0544	0.0503	0.0512	0.0009
7	1.09 mm. by 7.22 μ	Oil	1	Freeze dried	168	116	52	0.0724	0.0662	0.0692	0.0030
7	1.09 mm. by 7.22 μ	Oil	2	Freeze dried	141	114	27	0.0724	0.0672	0.0688	0.0016
8	4.55 mm. by 7.22 μ	Oil	1	Freeze dried	212	172	40	0.0550	0.0508	0.0520	0.0012
8	4.55 mm. by 7.22 μ	Oil	3	Freeze dried	202	172	30	0.567	0.0520	0.0532	0.0012
9	4.55 mm. by 7.22 μ	ODB	1	Freeze dried	216	177	39	0.0502	0.0463	0.0471	0.0008
9	4.55 mm. by 7.22 μ	ODB	3	Freeze dried	202	176	26	0.0499	0.0466	0.0474	0.0008
9	4.55 mm. by 7.22 μ	Oil	5	Freeze dried	201	173	28	0.0565	0.0518	0.0528	0.0010

[a] o-Dichlorobenzene.

fiber. Because the total area of the hysteresis loop does not adequately describe the height of the hysteresis loop, particularly at high loadings, the solid fraction at P equal to 70 g./sq. cm. are given in Table V for compression and recovery.

One bed of the 2.26 mm. by 7.22 μ fibers was allowed to airdry after its edge had been cut off. It had been noticed earlier in this work that air drying the beds caused the fibers to adhere to each other. Actual glass to glass hydrogen bonding may have occurred. As wet silica glass is considered to be covered with a thin layer of silica gel (18), there is a possibility of bonding of the fibers at their points of contact upon drying. Another possibility is that a thin film of contamination caused the fibers to adhere to each other. At maximum loading, the solid fraction of this bed was considerably lower than that obtained for any of the freeze-dried beds, and this behavior persisted even when the bed was subjected to five compression cycles.

For future reference it should also be noted from Table V that the bed which was not saturated and the bed which was saturated with water compressed to nearly the same extent as the beds which were saturated with the oil. However, the areas of the hysteresis loops, expressed in Table V as work lost, for these two beds were less than for the oil-saturated beds. This was especially true for the water-saturated bed. Also observe that for oil-saturated beds of the 1.09 mm. by 7.22 μ and 4.55 mm. by 7.22 μ fibers the area of the hysteresis loops was less than for the corresponding beds composed of the 2.26 mm. by 7.22 μ fibers.

It had been anticipated from the work of Jones (1) that the glass fiber beds would exhibit some nonrecoverable deformation, i.e., they would not recover completely at the conclusion of the first compression-recovery cycle. None of the oil-saturated beds of 2.26 mm. by 7.22 μ fibers demonstrated any detectable

nonrecoverable deformation, however. To investigate if this result was due to a lubrication of the fibers by the oil, a different index matching saturant was prepared by adding a small amount of diethylbenzene to o-dichlorobenzene. It was expected that this liquid would be less of a lubricant than the oil. This combination was chosen because the o-dichlorobenzene had nearly the required refractive index and because the o-dichlorobenzene and diethylbenzene have about the same volatility. Table V shows the data obtained from the first and third compression cycles for a bed of the 2.26 mm. by 7.22 μ fibers saturated with the o-dichlorobenzene. Again no nonrecoverable deformation was found. At maximum loading essentially the same solid fraction was obtained as with the oil-base saturant. The area of the hysteresis loop, however, was considerably smaller. To learn whether the smaller hysteresis loop was due to some peculiarity of that particular bed, the o-dichlorobenzene was removed with acetone; the bed was dried and resaturated with the oil. It will be noted from Table V that the area of the hysteresis loop, for the first cycle after the bed was resaturated, increased to approximately the value obtained for a similar bed which had been initially saturated with the oil.

Similarly, the first and third compression-recovery curves were determined for an o-dichlorobenzene-saturated bed of the 4.55 mm. by 7.22 μ fibers. After removing the o-dichlorobenzene saturant with acetone, drying, and resaturating with the oil, the compression-recovery curve was again determined. The results of this procedure are also shown in Table V as bed number nine. With the o-dichlorobenzene saturant, the area of the hysteresis loop was essentially the same as for the first and third cycles of a similar oil-saturated bed, even though the width of the hysteresis loop at the higher pressures was appreciably less than for the oil-saturated bed. What is of greatest interest is the solid fraction at 100 g./sq. cm. When this bed was saturated with the o-dichlorobenzene, it

compressed significantly less at moderate loads than it did when saturated with the oil. After the bed was saturated with oil, its compression-recovery curves were nearly identical to those obtained for the third cycle of a similar bed (No. 8), which was initially saturated with the oil.

The oil had a higher specific gravity (1.82 vs. 1.31) and a somewhat greater viscosity than the o-dichlorobenzene, but these factors cannot account for the observed results. Viscosity effects were discounted primarily because the rate of loading was very low. Also, if the viscosity of the saturant had been important, the hysteresis of the unsaturated bed would have been much lower than for the oil-saturated beds. Viscosity effects would not be expected to produce the observed difference in hysteresis between beds of the 2.26 mm. and 4.55 mm. fibers. While it is known that some materials affect the mechanical properties of glass (19), it was considered unlikely that the saturants would change the modulus of elasticity of the fibers. The reduction in hysteresis caused by the o-dichlorobenzene can be explained (see p. 105 and Appendix III) in part if it is assumed that the coefficient of friction between the fibers is greater with the o-dichlorobenzene than with the oil. Partial confirmation of the validity of this assumption was obtained.

An estimation of the effect of the saturants used in this work on the coefficient of friction between glass surfaces was made using The Institute of Paper Chemistry friction meter (33). New polished plate glass was used for both surfaces. The surfaces were wetted with the desired saturant and the slider (39 mm. by 50 mm.) was allowed to stand in contact with the large plate at a pressure of 44.3 g./sq. cm. for at least 30 minutes. This was done to allow the film of saturant to reach an equilibrium thickness, after which the coefficient of static friction was measured. As soon as slippage occurred, the

film of saturant became continuous and the friction dropped to very low values. The oil and the o-dichlorobenzene gave reproducible values for the coefficient of static friction of 0.14 and 0.24, respectively. Dry glass and glass covered with a film of water gave values which varied greatly from one point to another along the bottom plate, regardless of the manner of cleaning the plates. Although the reproducibility was poor, the water-wetted glass appeared to have a static coefficient of friction in the range 0.4 to 0.8. The dry glass had a coefficient of static friction in the range 0.30 to 0.32. It was interesting to note that when the water was allowed to evaporate, the slider stuck to the bottom plate. The force required to initiate sliding was greater than three times the normal force. This agreed with the observation that the air-dried glass fibers tended to stick together.

These experiments were performed only to rank the lubricity of the saturants. Actual values for the coefficient of friction between the glass fibers may differ considerably from those obtained with the glass plates. Glass fibers have a fire-polished surface, as opposed to the mechanically polished surfaces of the plate glass. Moreover, the coefficient of friction between glass surfaces probably is some function of the normal force. It was concluded, however, that oil produced a lower coefficient of friction than did o-dichlorobenzene, and that both coefficients were less than for the dry fibers. Water may produce a coefficient of friction higher or lower than the organic liquids, depending on the condition of the glass surface.

EFFECT OF FIBER DIMENSIONS ON z-ORIENTATION

It has been suggested that when fiber beds are formed by filtration from dilute suspensions, the orientation in the x-y plane normal to flow is random and no (34) or very few (1) fibers are oriented in the z-direction, that is,

parallel to flow. It was noted early in this study that most of the fibers were oriented so that they were nearly parallel with the x-y plane. However, it was observed that a small percentage of the fibers were oriented at appreciable angles to the horizontal and that the percentage seemed to vary with the dimensions of the fibers used.

An investigation was undertaken to determine the effect of length-to-diameter ratio upon the z-orientation distributions. A reticle with a grid pattern was used in the eyepiece of the microscope to determine the orientation of the fibers. The angle of the fiber was calculated by measuring the horizontal and vertical distance between the ends of the fibers. Only those fibers which were oriented close to the plane of focus of the microscope were considered. Fibers in all areas of the bed except the edges were included. About 400 fibers of each size were measured. The 1.09 mm. by 7.22 μ fibers and the 2.30 mm. by 12.86 μ fibers were almost perfectly straight. The 2.26 mm. by 7.22 μ fibers were noticeably curved, but it was considered that this would not seriously affect the determination of their orientations.

The z-orientations of the fibers, or their deviation from horizontality, have been expressed in terms of the angle, θ, which they make with the z-axis. This was done so that the relationships developed would be compatible with those of Onogi and Sasaguri (31), which will be utilized in a later section. To conform with the generally accepted usage, fibers making small angles with the z-axis will be said to have a high degree of z-orientation. For a curved fiber, the average orientation, θ, is defined by

$$\theta = \frac{1}{L} \int_0^L \theta_i ds \qquad (5),$$

where θ_i is the angle with the z-axis along the incremental length ds. Unless the fiber is appreciably bent, θ will approximately equal the angle which a straight line drawn between the ends of the fiber makes with the z-axis.

The z-orientation distribution obtained for the 1.09 mm. by 7.22 μ fibers is shown in Fig. 11 as a histogram. Note that the relative frequency has been plotted on a logarithmic scale. The z-orientation distributions obtained for all three sizes of fiber are shown in a different form in Fig. 12, 13, and 14. The abscissae of the points are the midpoints of the intervals of the histogram. A least squares fit of the points to an empirical equation of the form

$$\ln F = a\ (\theta)^G + B \qquad (6)$$

was used to obtain the curves. In this equation, F is the relative frequency, θ is the angle the fiber makes with the z-axis, and a, G, and B are constants to be determined.

An equation of the form $\ln F = a(\theta)^G + B$ was chosen to correlate the data, as it appeared to be the simplest one which fit the data well. A least squares fit of the data was obtained by forcing the curve through the point of highest frequency and by using iterative methods to determine G and B to the nearest 0.01. Once the best values of G and B had been determined, a was known by virtue of the fact that the curve passed through the point of greatest frequency. Values of the constants for all three sizes of fibers are given in Table VI. The correlation index (35) is also given as an indication of the goodness of fit to the data. Scatter of the data in the region of low relative frequency can readily be attributed to the small size of the sample in that region.

A determination of the z-orientation distribution for the 4.55 mm. by 7.22 μ fibers was not attempted. Because a high percentage of the fibers was oriented

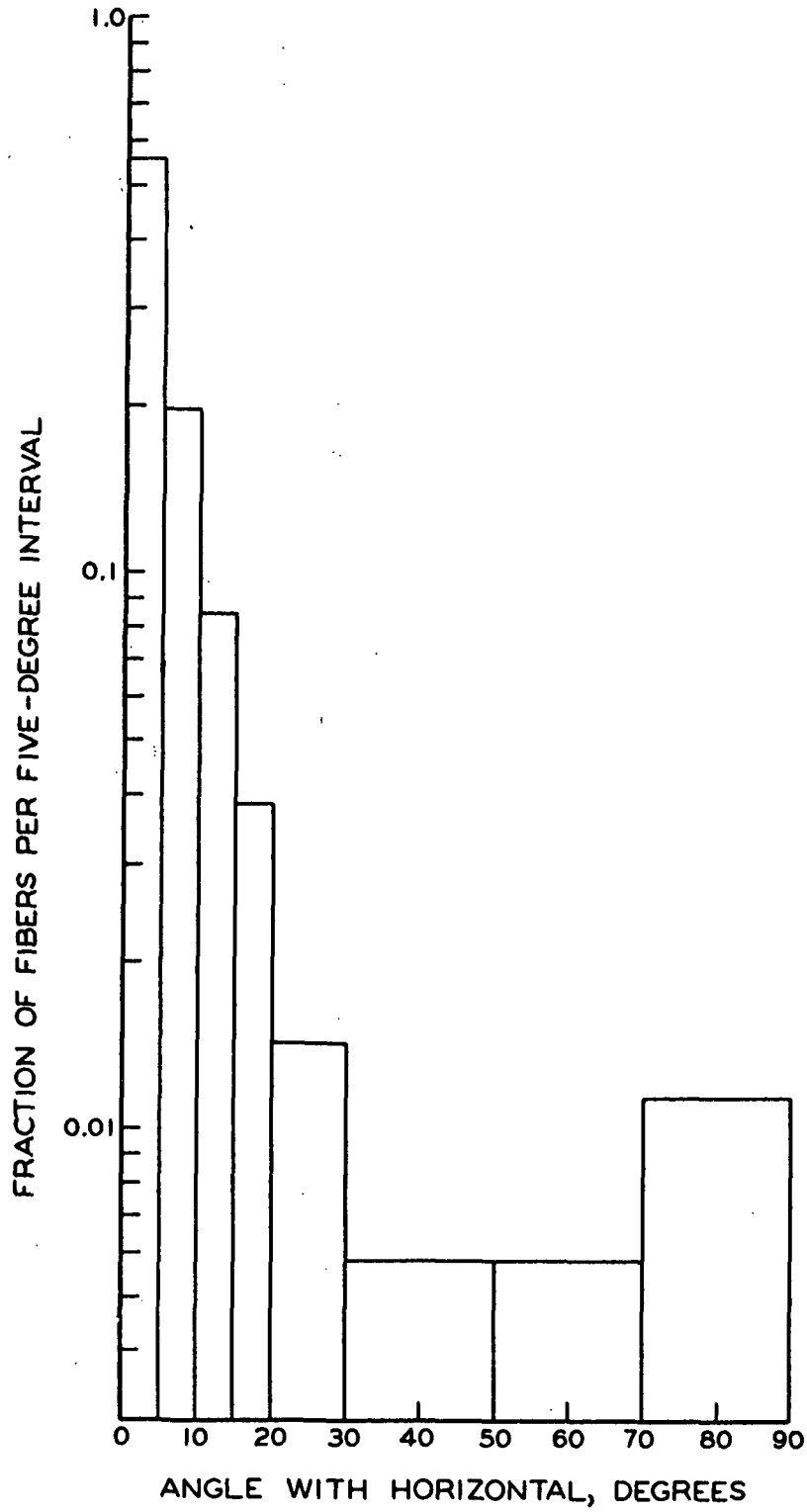

Figure 11. Fraction of Fibers (1.09 mm. by 7.22 μ) Per Five Degree Interval Having z-Orientation Within Indicated Limits

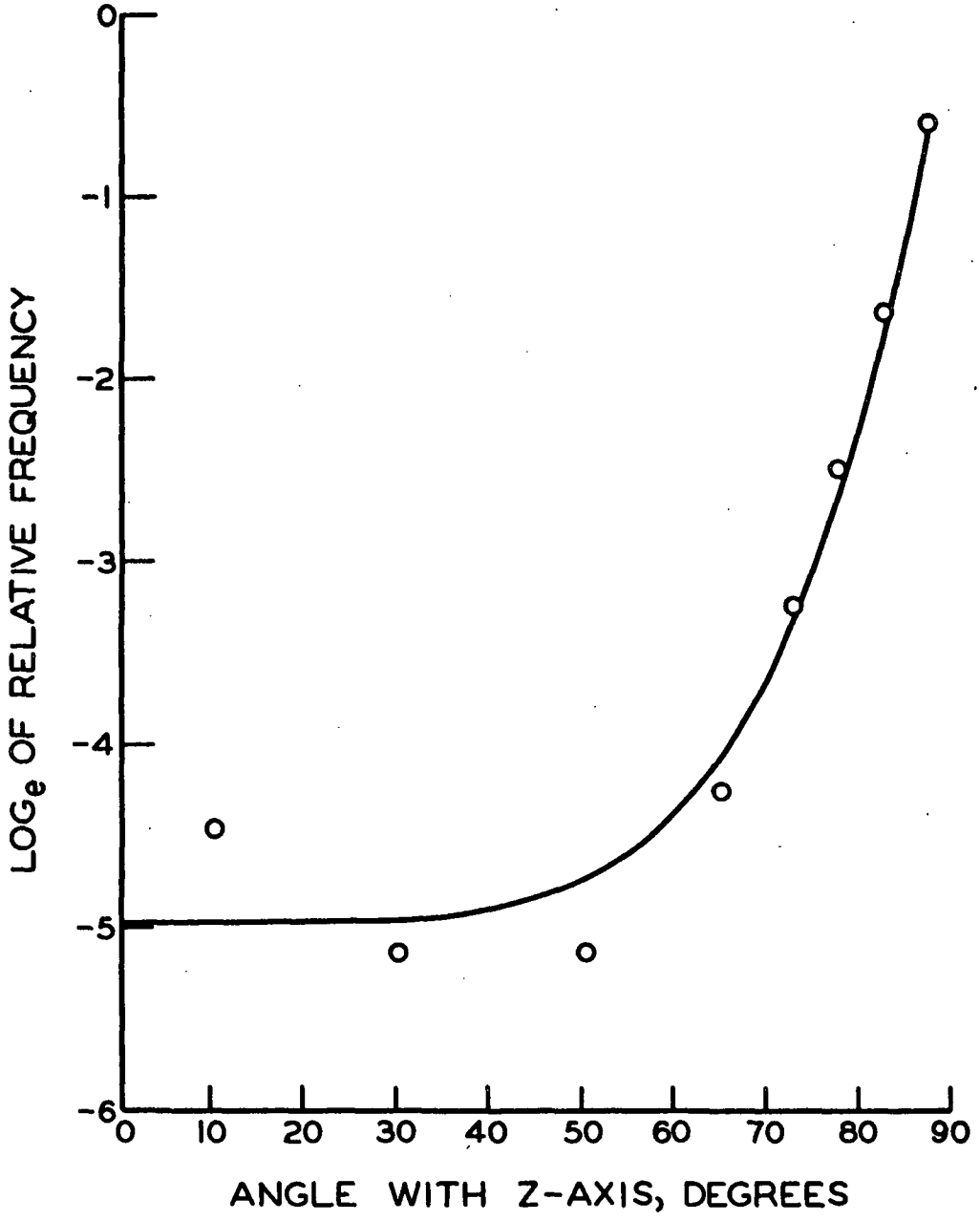

Figure 12. Initial z-Orientation Distribution of 1.09 mm. by 7.22 μ Fibers

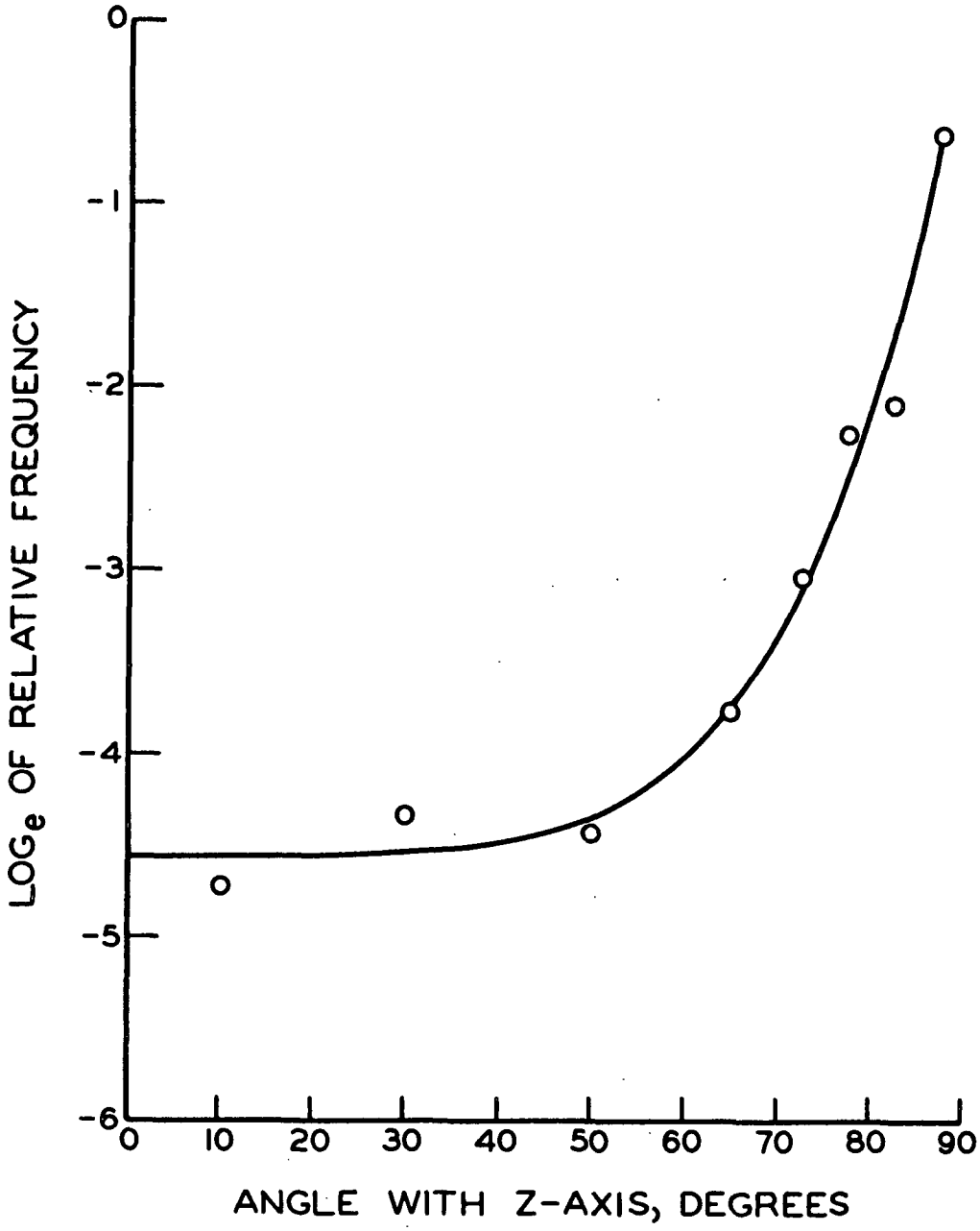

Figure 13. Initial z-Orientation Distribution of 2.30 mm. by 12.86 μ Fibers

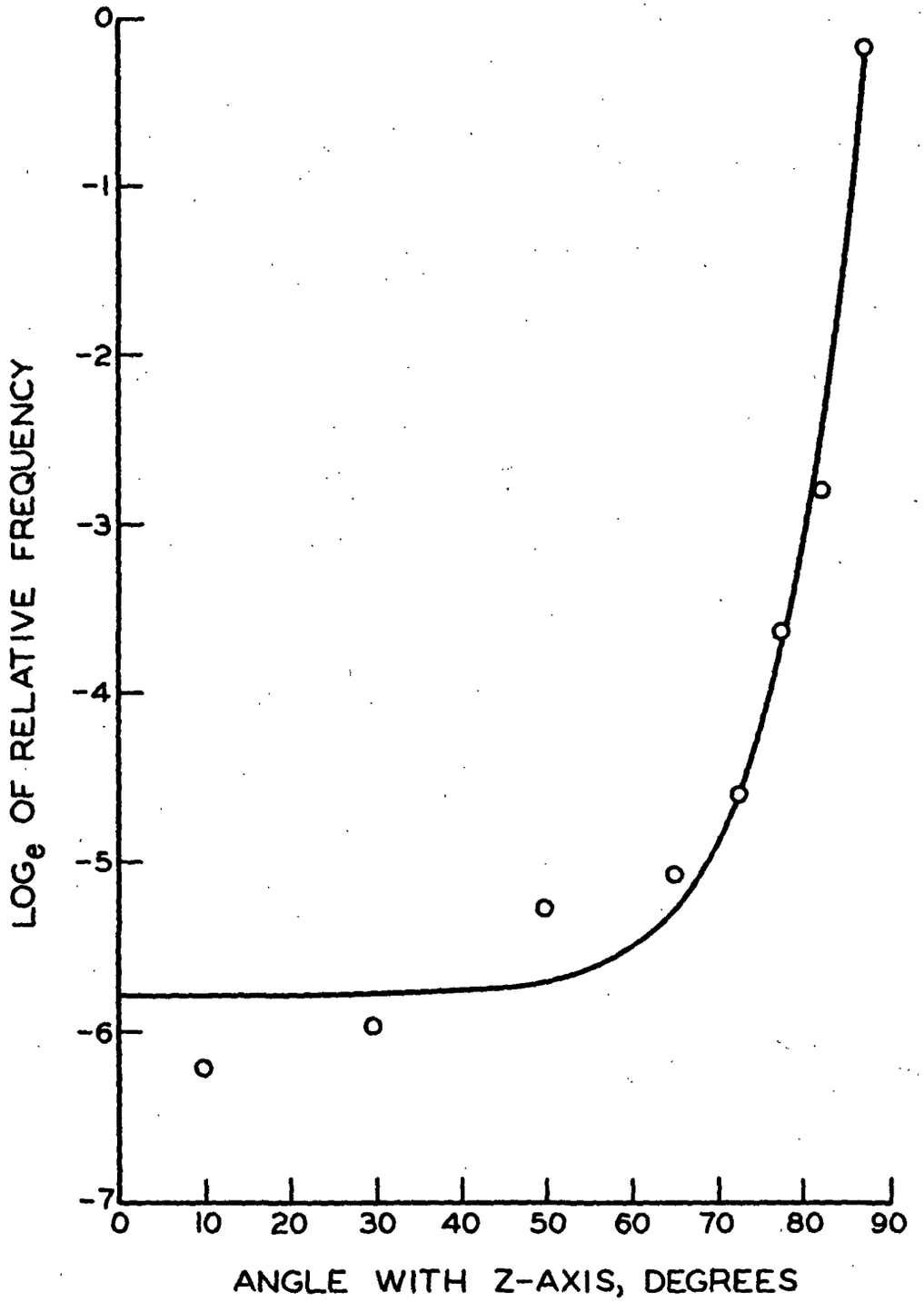

Figure 14. Initial z-Orientation Distribution of 2.26 mm. by 7.22 μ Fibers

nearly horizontally, a very large number of fibers would have had to be measured to get meaningful values for the fraction of the fibers oriented at appreciable angles to the horizontal. It was noted, though, that in the newly formed bed a few of the 4.55-mm. fibers were oriented at angles less than 45° with the z-axis. Even though the complete distribution was not determined, the z-orientation of thirty of the 4.55-mm. fibers was measured and their mean z-orientation was calculated.

TABLE VI

EMPIRICAL CONSTANTS FOR EXPERIMENTAL z-ORIENTATION DISTRIBUTIONS

Fiber Dimensions	a	G	B	Correlation Index
1.09 mm. by 7.22 μ	2.34×10^{-10}	5.29	-4.98	0.986
2.30 mm. by 12.86 μ	1.76×10^{-10}	5.33	-4.56	0.989
2.26 mm. by 7.22 μ	2.39×10^{-16}	8.43	-5.78	0.988

Likewise, the mean z-orientation for the other three sizes of fibers were calculated. Figure 15 shows the mean z-orientation plotted against the length-to-diameter ratios of the fibers. It can be seen that the average deviation from horizontality of the fibers increased as the length-to-diameter ratio of the fibers decreased, especially for values of the length-to-diameter ratio less than 300. It should be noted from Fig. 11 that, due to the shape of the distribution, the mean orientation is not the most probable orientation.

The values for the average z-orientations given in Fig. 15 are the arithmetic means. Out of curiosity, the weighted mean z-orientation for the four groups of fibers was calculated in the manner indicated by Equation (7)

$$\theta'_w = \sum_{i=1}^{i=N} \frac{\theta'^2_i}{\theta'_t} \qquad (7),$$

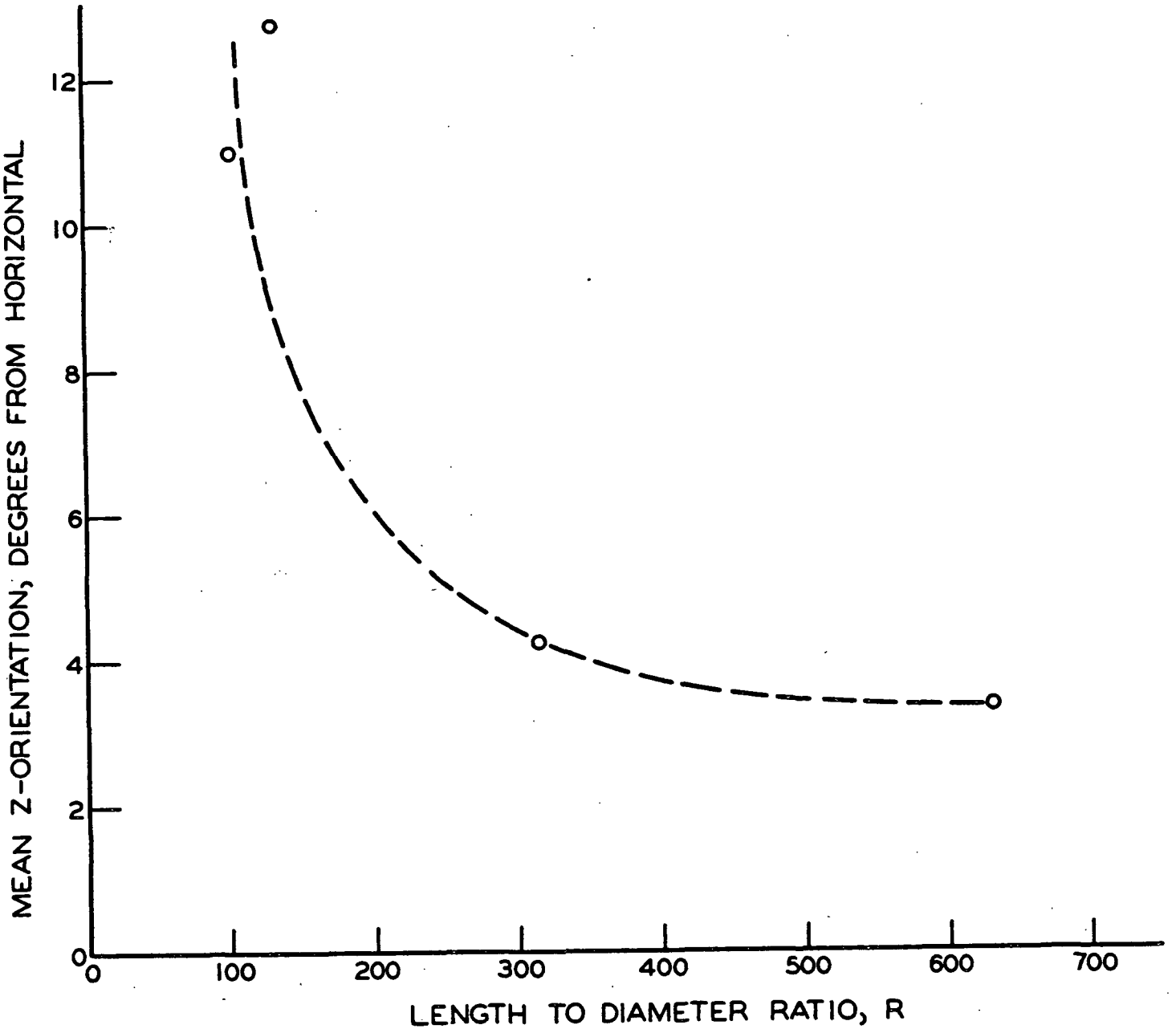

Figure 15. Number Average z-Orientation as a Function of Length-to-Diameter Ratio for Newly Formed Beds

where

$$\theta'_t = \sum_{i=1}^{i=N} \theta'_i \quad .$$

In this equation, $\theta'_{\underline{w}}$ is the weighted mean, $\theta'_{\underline{t}}$ is the total orientation of all fibers in the sample composed of $\underline{N}$ fibers, and $\theta'_{\underline{i}}$ is the orientation of the individual fibers with respect to the horizontal. Primes are used to indicate that, in this case, the fiber orientations were expressed in terms of the angle with the x-y plane rather than the z-axis. It will be noted in Fig. 16 that, in the range studied, there was a linear relationship between weighted mean z-orientation and length-to-diameter ratio. This result was not anticipated and no explanation is offered. The fact that the four data points fell so nearly on a straight line suggests that this result may have been more than merely fortuitous.

If this line is extrapolated to a length-to-diameter ratio of unity, the value for the weighted mean orientation is found to be 53°. It is interesting to note that even with this lengthy extrapolation, the value obtained is near the value (47°) for an isotropic distribution. It is not known, though, if a bed formed from cylindrical fibers having a length-to-diameter ratio of unity would actually have an isotropic z-orientation distribution. The significance, if any, of the observed linear relationship between weighted mean z-orientation in the freshly formed beds and the length-to-diameter ratio of their fiber is not known, and this result at present probably should be treated as a happenstance.

EFFECT OF COMPRESSION UPON FIBER BENDING AND NUMBER OF CONTACTS

Figure 17 illustrates the behavior of a typical 2.26 mm. by 7.22 μ fiber as the bed was compressed. The corresponding solid fraction of the bed is given

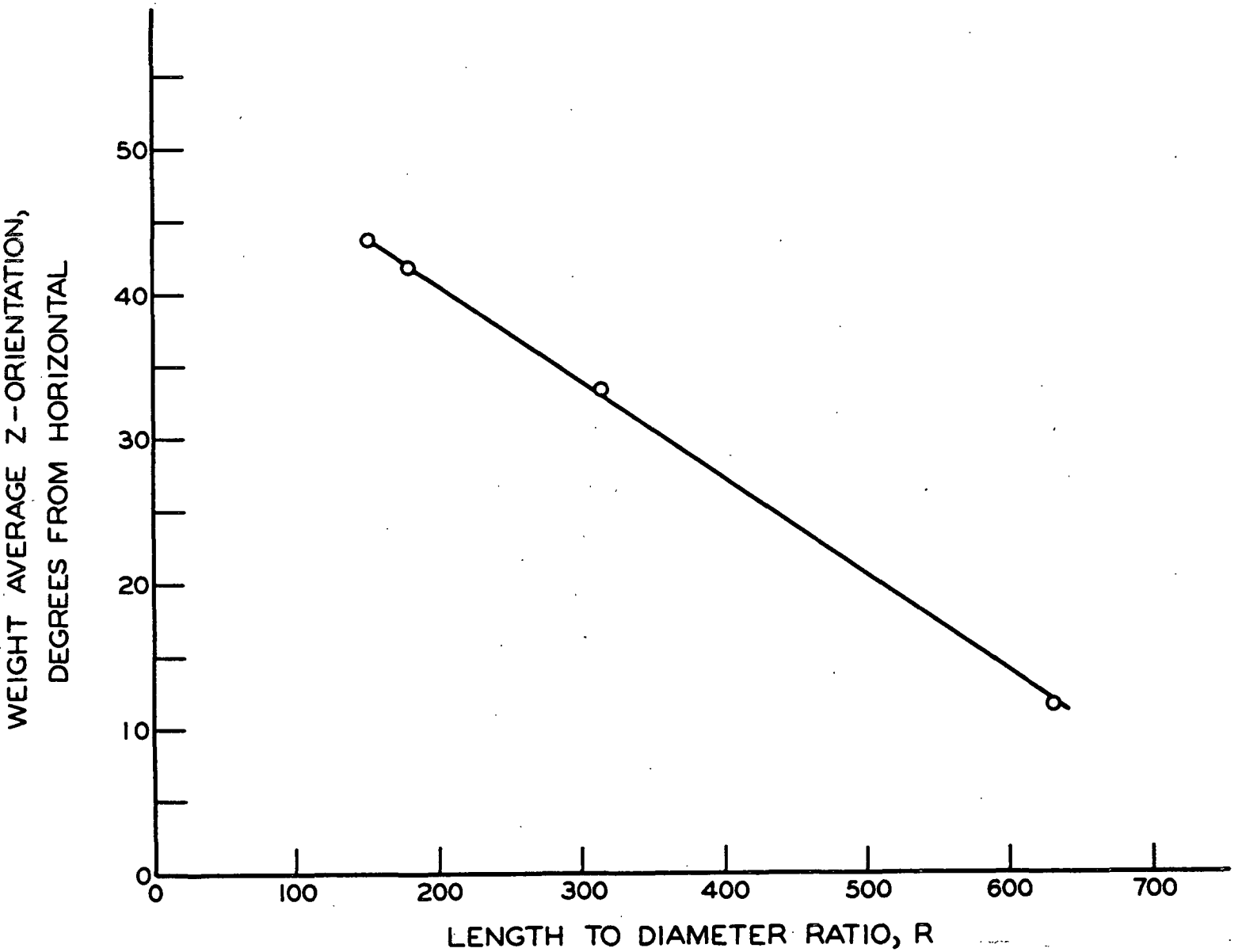

Figure 16. Weight Average z-Orientation as a Function of Length-to-Diameter Ratio for Freshly Formed Beds

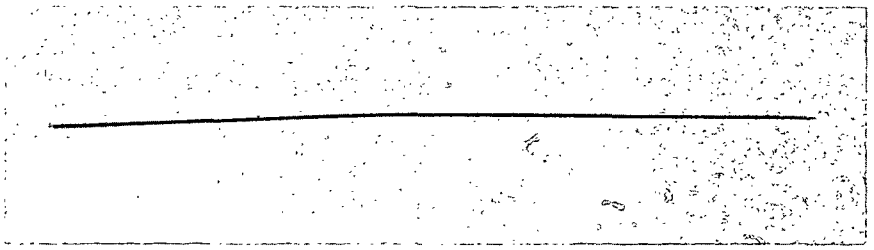

(A) Solid Fraction = 0.012

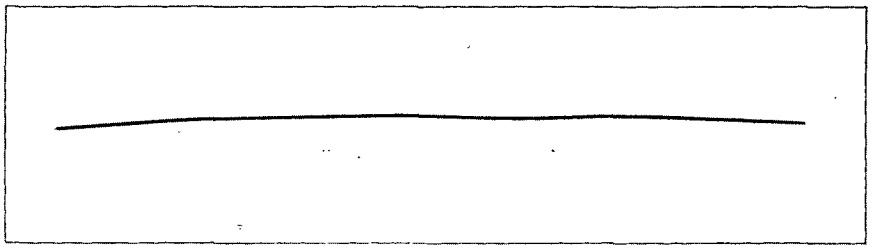

(B) Solid Fraction = 0.0310

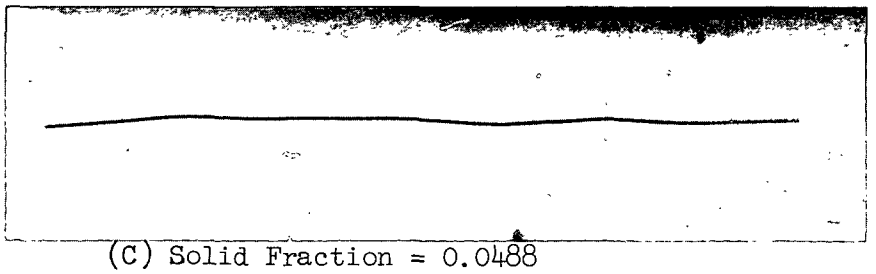

(C) Solid Fraction = 0.0488

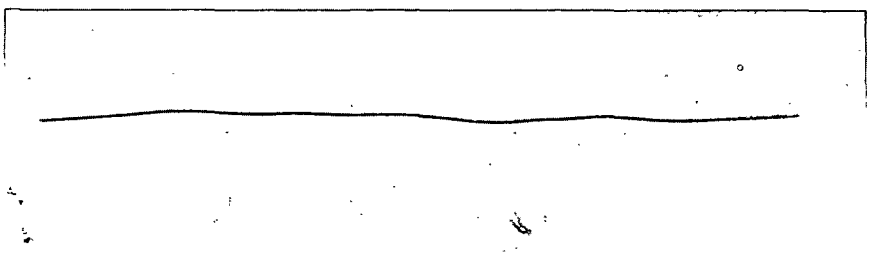

(D) Solid Fraction = 0.0545

Figure 17. Effect of Compression on Configuration of a Single 2.26 mm. by 7.22 μ Fiber

next to each frame. It is apparent that the bending of the fiber increased during compaction. Of particular interest are the facts that there are no abrupt changes in the configuration from one end of the fiber to the other, and that the maximum deflection of any portion of the fiber is about one to four fiber diameters. Photographs of the type shown in Fig. 17 were interpreted in several ways, one of which is presented below.

It has been recognized for some time that the number of contacts between the fibers must increase as a fibrous mat is compressed. The greatest single obstacle to describing the compression behavior of fibrous structures has been the absence of an adequate means of determining the number of contacts between the fibers. Without knowing the mean number of adjacent fibers in contact with an individual fiber, the unsupported fiber length or frictional interaction between the fibers cannot even be estimated with confidence.

Since the fibers were initially straight, their curvature, or configuration, could be used to obtain a value for the minimum number of contacts per fiber. This number exceeds by two the number of points along the fiber where the bending reaches a maximum. Except for the case where two successive contact points are on the same side of the fiber (top or bottom), the minimum number of contacts is greater by three than the number of inflection points. It was fairly easy to identify the inflection points, but it was not always possible to determine the points at which the bending reached a maximum. Consequently, the reported number of contacts is slightly greater than the number calculated by counting the number of inflection points.

A cylindrical lens (Edmund Scientific, Cat. No. 40,212, F.L. 4.38 cm.) was used as an aid in determining the number of contact points along the fibers. When the lens was supported 2.5 cm. above a photograph, with its axis aligned

with the axis of the fiber, a magnification of about 2.6 was obtained in the direction perpendicular to the fiber axis. It would have been difficult to produce a satisfactory negative to illustrate this effect (36). However, if the reader views the fiber of Fig. 17 through a large-diameter (1 to 2 in.) Lucite or glass rod, the increased ease of detecting inflection points will become obvious to him. Inspection of Fig. 17 with a cylindrical lens reveals that this fiber touched a minimum of seven fibers at a solid fraction of 0.0310 and at least thirteen fibers at a solid fraction of 0.0545. The results obtained for all fibers studied are given in Table VII.

TABLE VII

NUMBER OF FIBER CONTACTS PER FIBER

Fiber Dimensions	Mean No. of Contacts	Standard Deviation	Solid Fraction	Sample Size
2.26 mm. by 7.22 μ	7.3	1.10	0.0310	10
2.26 mm. by 7.22 μ	11.4	1.02	0.0488	10
2.26 mm. by 7.22 μ	12.6	2.00	0.0545	18
1.09 mm. by 7.22 μ	6.5	1.06	0.0601	42
1.09 mm. by 7.22 μ	6.5	1.29	0.0739	34
4.55 mm. by 7.22 μ	21.6	2.92	0.0575	20
2.30 mm. by 12.86 μ	7.2	1.06	0.0662	17

While a value for the minimum number of contacts along a fiber could be determined from the number of inflection points, it was not known how close this value was to the actual number of contacts. It was entirely possible that the observed minimum number of contact points could have been significantly less than the actual number.

An estimate of the actual number of contact points along a fiber was obtained by introducing a very flexible fiber into the bed of glass fibers. A 0.1-denier

dacron fiber (about 3 μ in diameter) with a circular cross section was used. Because its stiffness, $\underline{EI}$, was about one one-hundredth that of the glass fibers, it was assumed that this fiber would readily deflect when it encountered a glass fiber.

The dacron fiber was dyed black with Rit dye to improve its visibility. Attempts to form beds from suspensions of glass fibers mixed with a small percentage of the dacron fiber were unsatisfactory. However, it was found that the dacron fiber could be satisfactorily introduced into the dried beds before saturation. Single filaments of the dacron fiber were isolated and slightly stretched for several days to remove any kinks, after which they were inserted into the bed, using a fine glass needle. For beds of the 2.26 mm. by 7.22 μ fibers, this method of introducing the dacron filaments was compared with placing the dacron filaments between two similar beds. When compared at an apparent applied stress of 107 g./sq. cm., 6.4 contacts per millimeter were counted for the fibers placed between the two beds, and 5.9 contacts per millimeter for the fibers inserted with a glass needle. The agreement between these two methods was considered good enough to allow the needle to be used to introduce the dacron fibers into beds of the other fibers. As the magnification used during photographing the dacron filament was increased from 5.10 to 6.79, an increase in resolution was obtained and the number of observable fiber contacts increased slightly. This comparatively small difference between the magnification obtained on the film was increased by about a factor of four and one-half when the prints were made. Further increases in the magnification had little if any effect on the observable number of contacts.

Using the higher magnification and introducing the dacron filament into the beds with the needle, the frequency of contacts at an applied stress of 107

g./sq. cm. was determined for beds of the 1.09 mm. by 7.22 μ, 2.26 mm. by 7.22 μ, and 4.55 mm. by 7.22 μ fibers. The number of contacts per millimeter of filament was found to be 9.5, 7.3, and 9.0, respectively. This was only two to four more contacts per millimeter than observed for the glass fibers. Because the dacron filaments had a diameter less than half that of the glass fibers, were more flexible, and because they were not load bearing members of the fibrous structures, it is not possible to relate directly the frequency of contacts along the dacron filament with that of the glass fibers. It was considered noteworthy, though, that the frequency of contacts with the dacron filament was not greatly different from the observable number along the glass fibers. It was concluded from this work that, under the conditions which were employed, the number of contacts observed for the glass fibers was not greatly different from the true number of contacts.

At very low or high compacting pressures upon the beds, the technique of determining contact points from the configuration of the fibers probably is insensitive. The number of contacts determined by this method is more closely related to the degree of compression or solid fraction of the structure than to the load supported by it. Although under the conditions employed in this study, the minimum number of observable contacts for the glass fibers appears to have been near the true value, these results do not necessarily justify the extension of this technique to other fibrous structures.

FIBER REPOSITIONING

Previous evidence (1) has indicated that fiber repositioning or slippage is an important factor in determining the compression-recovery behavior of fibrous structures. A distinction will be made between the terms fiber repositioning and fiber slippage even though they are closely related. Fiber

repositioning will refer to translation or rotation of the fibers or fiber parts with respect to each other or some fixed point of reference. In contrast, fiber slippage will refer to slippage of one fiber surface across another. Depending upon how fiber repositioning might occur, there could be either a large or small amount of fiber slippage. For example, in a completely bonded structure, fiber repositioning, i.e., bending, could occur without slippage of one fiber across another. Likewise, it will be demonstrated that fiber slippage can occur without the need for movement of entire fibers.

It is taken for granted that during compression the fibers will be displaced in the direction of motion of the piston. Because the fibers are primarily in contact on their top and bottom surfaces, relative movement of the fibers in the direction parallel to that of the piston would result in little fiber slippage. What was of greatest interest was the amount of fiber repositioning in the plane of the mat (x-y plane). Unless specifically stated to the contrary, the terms fiber motion or repositioning will refer to displacement of the fibers in the direction normal to the direction of piston travel.

It was not possible to measure absolute movement of the fibers due to the lack of a fixed point of reference. For example, the microscope supports were not sufficiently rigid to permit utilization of the co-ordinate settings of the microscope as a fixed reference system. Furthermore, when it was determined that relative movement of the fibers with respect to each other could be determined with high precision, there was no need for a means of measuring absolute movement of the fibers.

TRANSLATION AND ROTATION

Whether repositioning of the fibers was occurring during compression was determined by photographing a given area of the bed before and after compaction

and comparing the photographs. If the corresponding images of the fibers superimposed exactly, it could be concluded that there was no fiber repositioning of an amount greater than the resolution of the technique. However, the converse did not apply. Failure of the corresponding images to superimpose did not necessarily confirm the existence of fiber repositioning.

Because lateral motion of the piston could have caused repositioning of the fibers which was not associated with compression, a close fitting piston guide was employed. Other problems which at first gave confusing results, such as movement of the cell containing the bed, were investigated and eliminated. Also when the optic axis of the microscope was not exactly aligned with the direction of motion of the piston, the corresponding images of the fibers did not superimpose. Alignment of the optic axis was accomplished by an adjusting screw on the support of the microscope and by rotation of the prism on the microscope. Correct alignment was indicated by viewing through the camera mounted on the microscope a reference mark on the face of the piston. When exact alignment was obtained, vertical movement of the piston in its guide caused no lateral motion of the reference mark with respect to the eyepiece scale of the camera. Due to backlash in the vertical rack and pinion mechanism of the microscope support, it was necessary, when photographing the beds, to approach the rest position of the microscope from the same direction used during establishing alignment. Correct alignment, although difficult to obtain was not difficult to maintain during a series of photographs.

After studying several hundred photographs, it has been concluded that very little slippage or repositioning of the fibers occurred during compression. Two sets of photographs which support this conclusion follow. These sets of photographs show two different areas of the same bed which contained about 0.2%

silvered fibers and was composed of the 2.26 mm. by 7.22 μ fibers. Figure 18 will be referred to as View A and Fig. 23 as View B. These two views are not entirely typical of the other photographs obtained but were chosen to illustrate particular features.

Figure 18 shows several fibers in the interior of a freshly formed bed as they appeared when viewed vertically. Figure 19 shows the same area after the first recovery, and Fig. 20 the same area at maximum load during the second cycle. The negative of Fig. 18 was superimposed on the negative of Fig. 19 to produce Fig. 21 and on the negative of Fig. 20 to produce Fig. 22. It will be noted that the corresponding images of the fibers superimposed essentially perfectly. Movement of the fibers colinear to their axes might have occurred without being readily detectable by the method of superimposing the negatives. That this was not the case can be demonstrated by the fact that the layer of silver was missing in certain areas along the fibers. As can be seen in View A, Fig. 21, the positions of the areas devoid of silver also superimposed, showing that any axial motion of the fibers was slight.

Figure 23 shows View B before the first compression. Figure 24 shows the same area at maximum load during the first compression, and Fig. 25 at maximum load during the second compression. The negatives of Fig. 23 and Fig. 24 were superimposed to produce Fig. 26, and Fig. 27 was produced by superimposing the negatives of Fig. 24 and 25. This series of photographs again shows that there was little lateral movement of the fibers. As indicated by the arrows in Fig. 27, though, the ends of two fibers did show a small amount of lateral bending.

Several features of these photographs which may not be obvious will be explained. Because these prints show the interior of a three-dimensional structure, only a portion of the fibers is clearly in focus. The fibers of View A

Figure 18. View A Before First Compression, $\sigma = 0.0101$

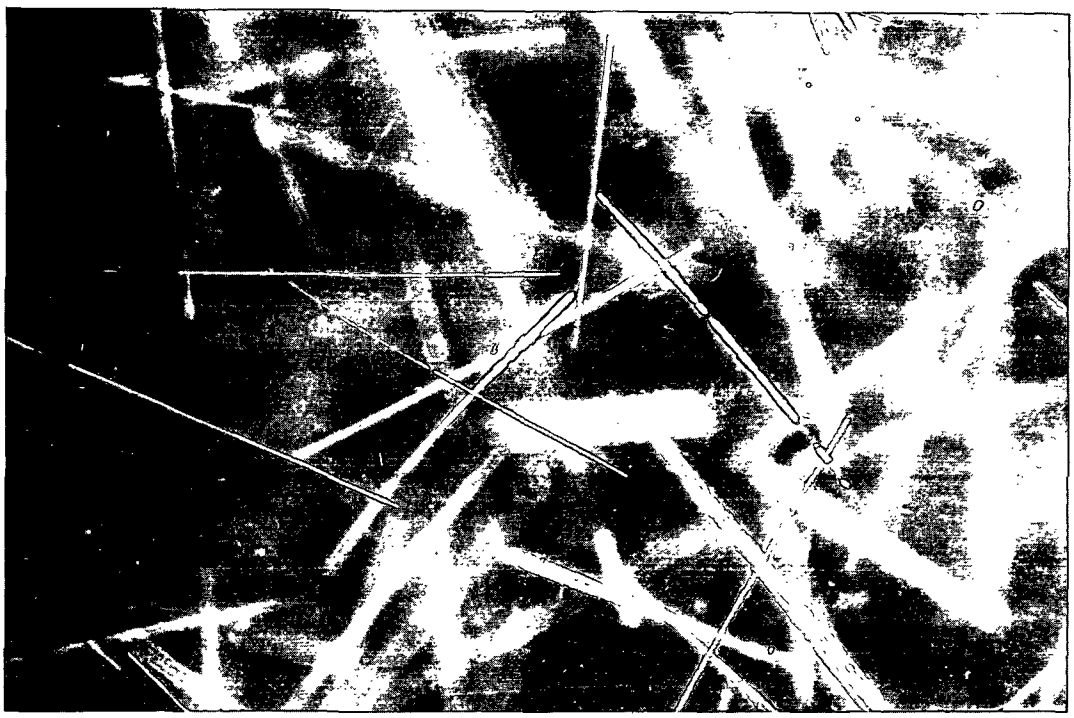

Figure 19. View A End of First Recovery, $\sigma = 0.0108$

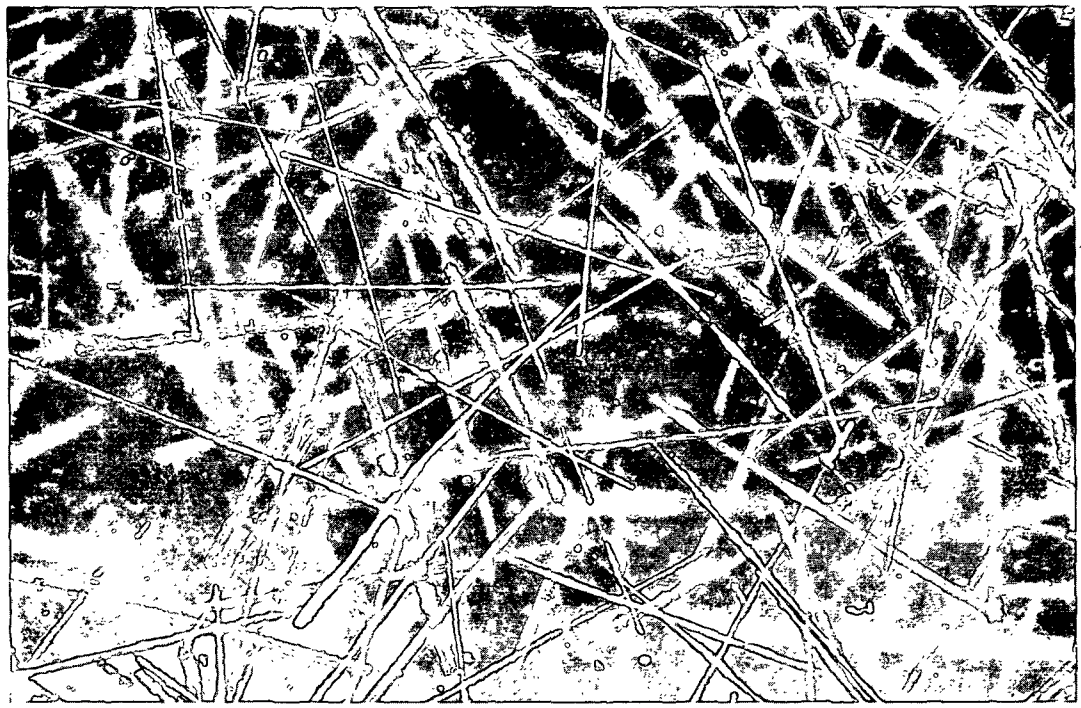

Figure 20. View A Maximum Load During Second Compression, $\sigma = 0.0604$

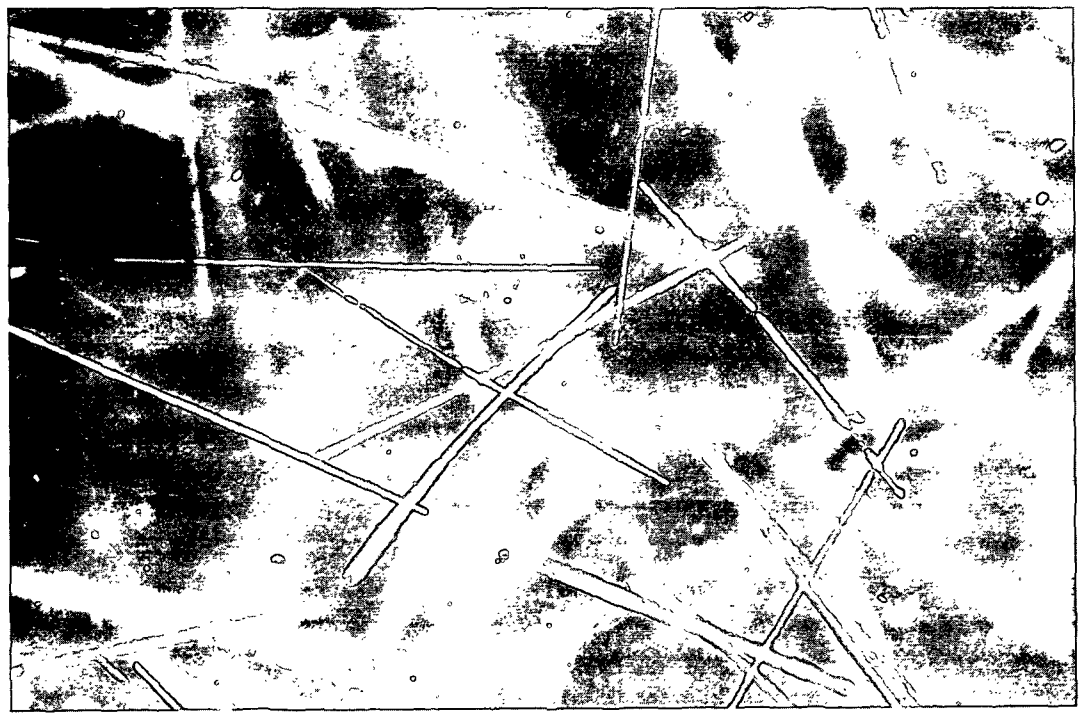

Figure 21. View A Composite of Fig. 18 and Fig. 19.
Note Absence of Fiber Repositioning

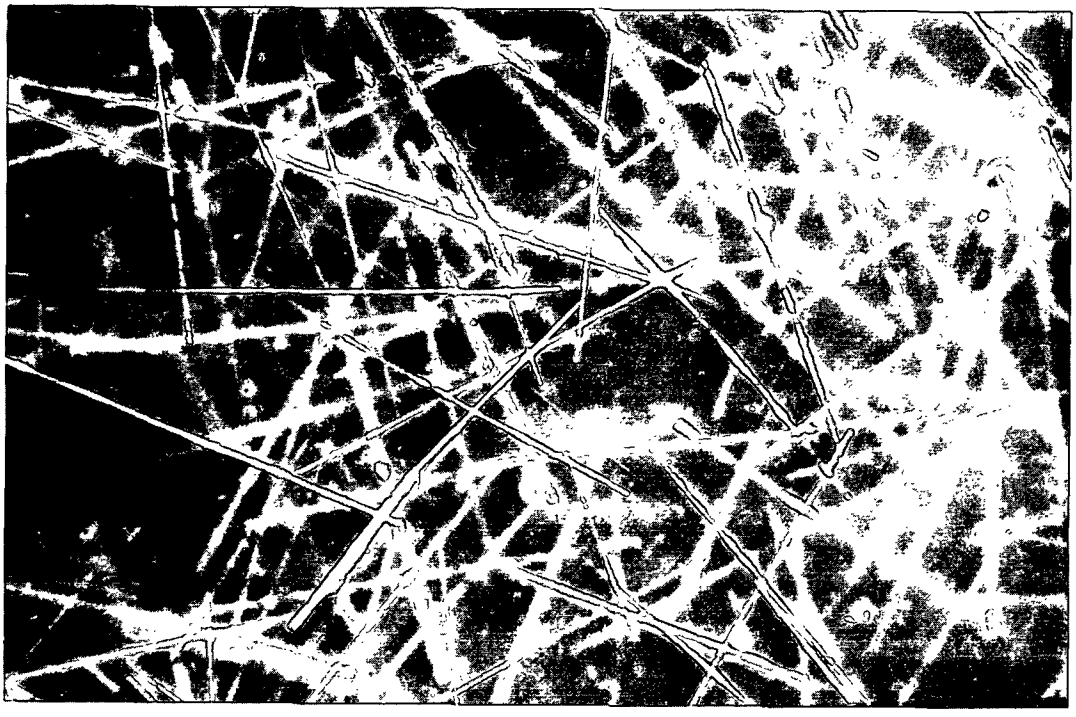

Figure 22. View A Composite of Fig. 18 and Fig. 20.
Note Absence of Fiber Repositioning

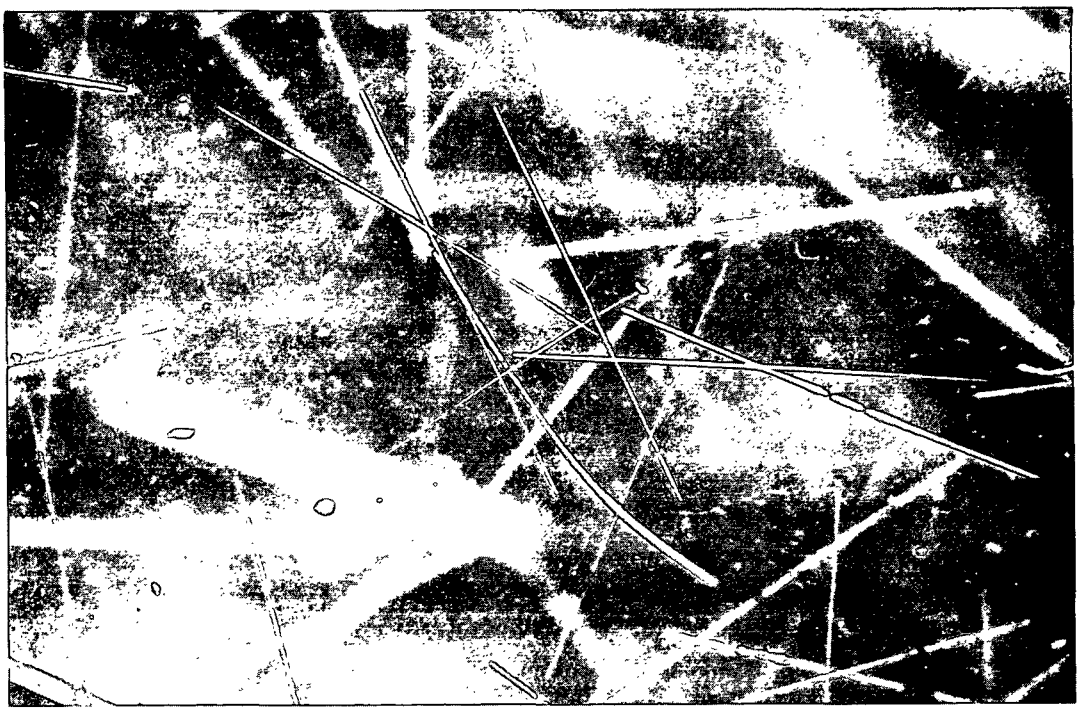

Figure 23. View B Before First Compression $\sigma = 0.0101$

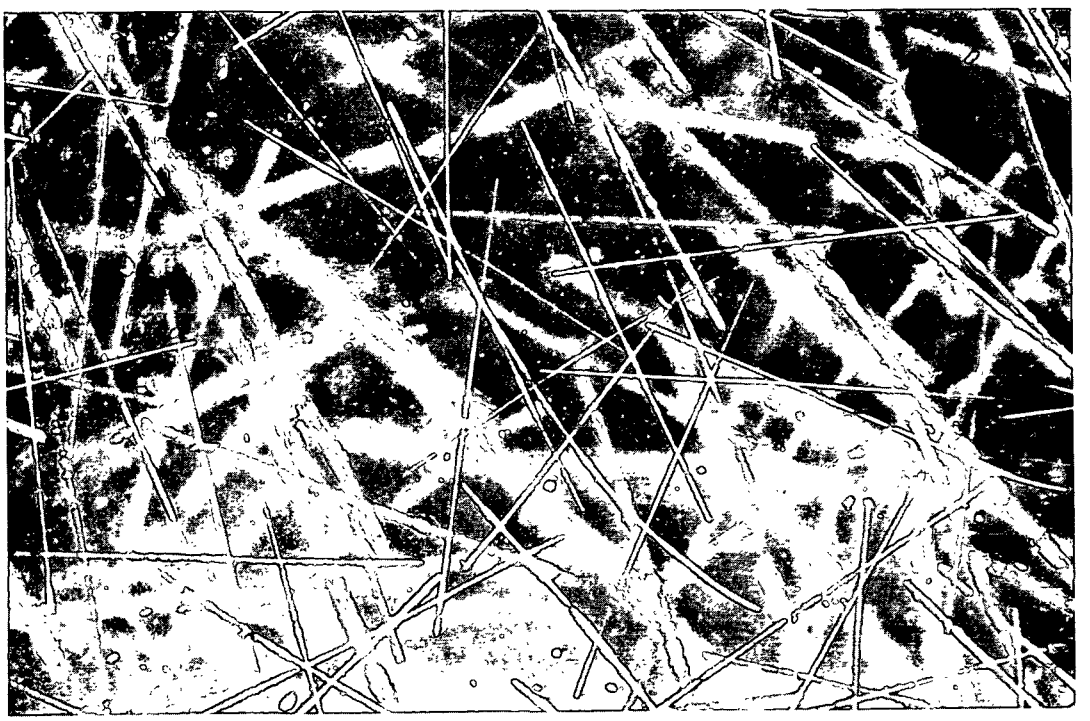

Figure 24. View B Maximum Load During First Compression $\sigma = 0.0559$

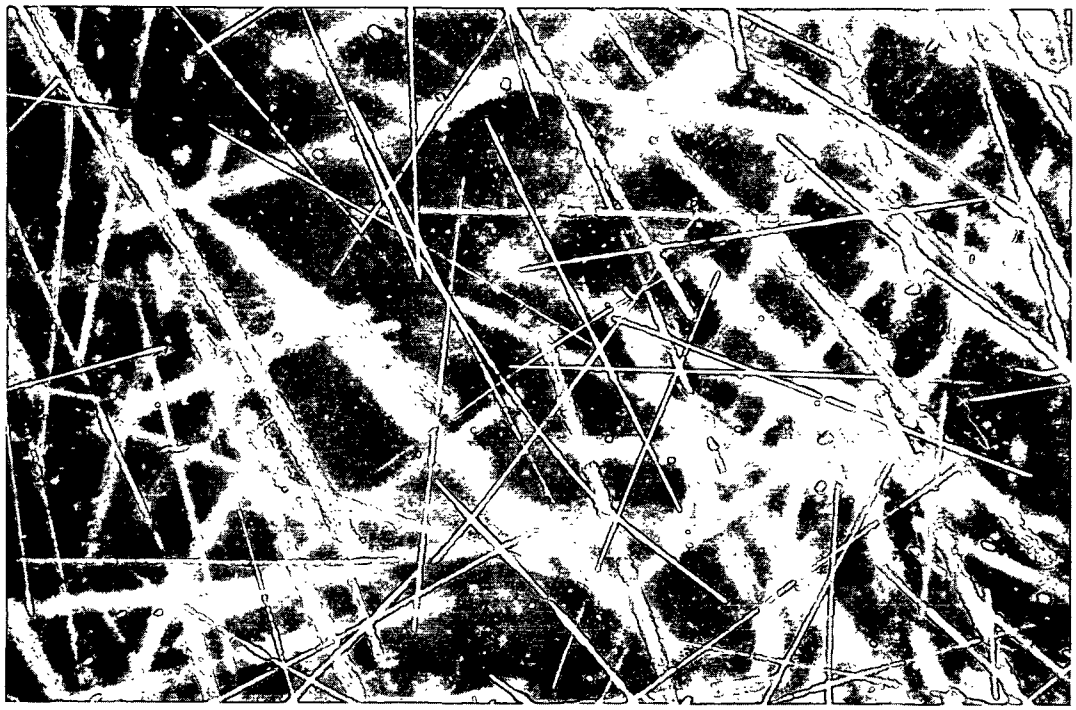

Figure 25. View B Maximum Load During Second Compression $\sigma = 0.0604$

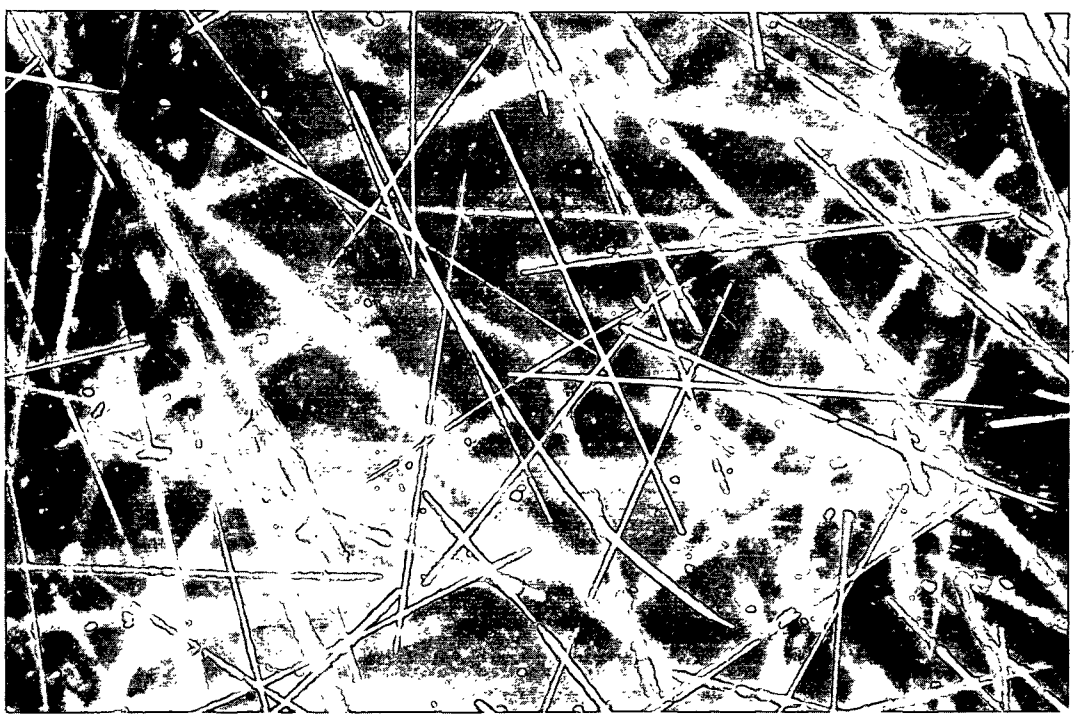

Figure 26. View B Composite of Fig. 23 and Fig. 24

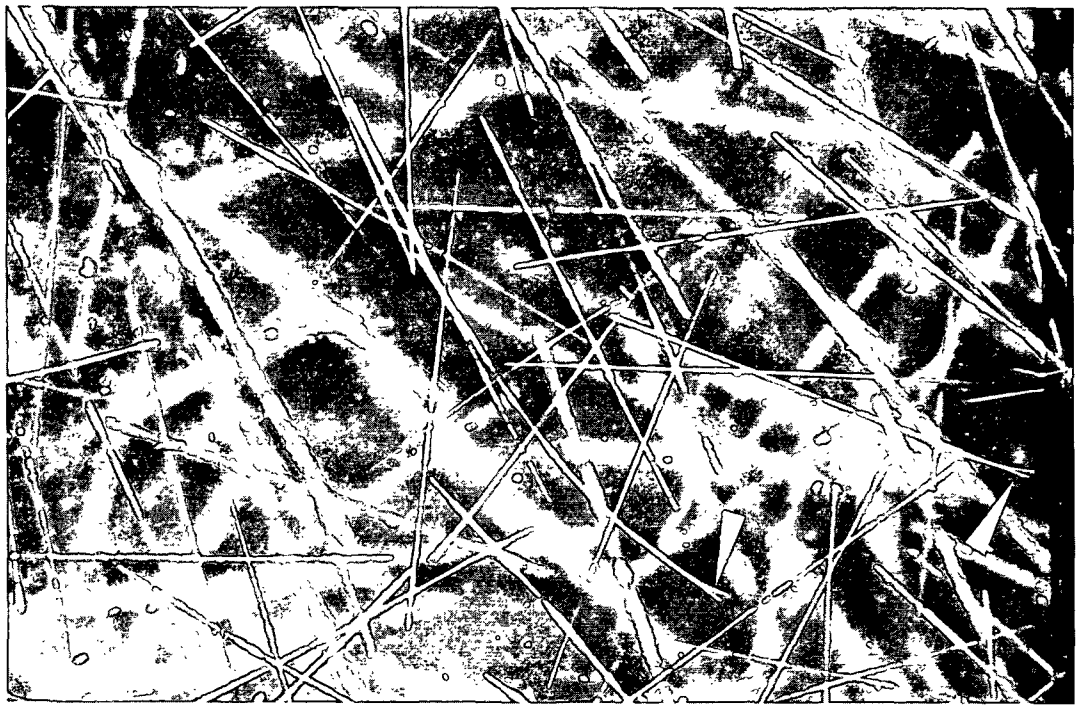

Figure 27. View B Composite of Fig. 24 and Fig. 25

which are clearly in focus were 1.2 mm. from the bottom of the bed when it was unloaded, while in the case of View B, this distance was 3.5 mm. These distances may seem small, but compared to the fiber diameter they are quite large. Many of the areas studied were farther from the bottom of the beds than these two, and the results were comparable. Fibers which were not in focus appear broad and semitransparent. Under the conditions employed in obtaining these photographs, the depth of focus is about 1 mm., but fibers within a vertical range of about 2 mm. are clearly discernible. As the bed was compressed, the vertical distance between the fibers decreased and more fibers were clearly in focus. Many fibers in the photographs of the compressed beds show areas where the fibers appear wider. This was due to bending of the fibers, which caused some areas of the fibers to be oriented so that they reflected more light than other areas. Those areas reflecting the most light appear widest.

Both View A and View B show fibers which appear curved. These fibers are not typical of the majority of fibers. It will be noted that in the unloaded beds (Fig. 18 and Fig. 23) both curved fibers have an end which is not clearly in focus. This is because both curved fibers were oriented so that they made appreciable angles with the plane of the beds. It was believed that these fibers with appreciable z-orientation would demonstrate the maximum amount of repositioning. Of the several areas studied (at least twenty), View B showed the maximum amount of repositioning which could be attributed to compression.

One bed of the 1.09 mm. by 7.22 μ fibers was examined for evidences of fiber repositioning. Due to experimental difficulties, such as failure to obtain exact vertical alignment of the optic axis, the results were not as conclusive as with the 2.26 mm. by 7.22 μ fibers. It can be said, though, that the shorter fibers showed no tendency to rotate or to move perpendicularly to their axes. There may have been a slight amount of movement of some fibers along the direction of their axes.

AXIAL SHORTENING

While there was only a slight amount of fiber repositioning, it can be shown that there was some slippage of fiber surfaces against each other. As a fiber bends during compression, either the ends of the fiber must move toward each other or the fiber must stretch between its points of support. Approximate calculations (see Appendix III) indicate that for the fibers used in this study the axial tension required to stretch the fiber the required amount was about an order of magnitude greater than the frictional forces preventing the ends of the fiber from moving together. Photographs showed that the projected length of a fiber on the x-y plane was perceptibly greater when the bed was unloaded than when it was fully loaded. The amount of axial slippage of the fibers

cannot be measured from these photographs, however, due to changes in the z-orientation of the fibers and to difficulty in precisely locating the ends of the fibers.

A determination of the amount of axial slippage of a small number of the 2.26 mm. by 7.22 μ fibers was made, though, from photographs taken through the edge of the bed. Photographs of individual fibers, taken when the bed was under maximum load, were projected onto a large sheet of paper to give a total magnification of 878, and their images were traced with a pencil. The distance between the ends of the fiber, as measured along the fiber and measured along a straight line between the ends, was obtained by using a map measure. Distances could be read to the nearest 0.1 in. and estimated to the nearest 0.01 in. The results are summarized in Table VIII. All of these fibers were cut from the same filament, which had a diameter of 6.42 μ. The fiber listed as No. 1 is the same fiber shown in Fig. 17.

TABLE VIII

DIFFERENCE BETWEEN ACTUAL AND PROJECTED LENGTH OF 2.26 MM. BY 7.22 μ FIBERS AT A SOLID FRACTION OF 0.0545

Fiber No.	Difference Between Actual and Projected Length, μ ± 0.15
1	3.8
2	5.6
3	6.9
4	2.5
5	3.8
6	3.8
7	9.0
8	3.6
9	4.0
10	2.4
Mean	4.5 μ

EFFECT OF COMPRESSION UPON z-ORIENTATION

It was anticipated that the fibers oriented at large angles to the horizontal would show some slippage and that they would become more nearly horizontal during compression of the bed. To show the behavior during compression of fibers having appreciable z-orientation, several fibers were photographed through the edge of the bed at four levels of compression during the first compression and also after the first recovery.

The behavior of a representative fiber is shown in Fig. 28 and 29 which were produced by photographing the same fiber at three stages during the first compression of the bed and superimposing the negatives before printing. At each stage of compression the bed was rotated to photograph other fibers. When the first photograph was taken the fiber was not quite perpendicular to the optic axis, which accounts for that image of the fiber appearing slightly shorter than the other two. These photographs were taken of the bed shown in Fig. 18-27. The bottom of the bed is parallel to the bottom edge of the photograph. It is apparent that the orientation of the fiber changed considerably during compression. It can also be seen that the lower end of the fiber with high orientation moved to the left and its upper end moved to the right. This movement was more pronounced in the photograph (Fig. 29) taken at the maximum pressure. When the bed was allowed to recover, the ends of the fiber moved back to essentially their original position. Lateral movement or lateral bending of the fibers crossing a fiber at high z-orientation, would have had to occur if slippage did not. This amount of lateral movement could have been readily detected when viewing vertically through the bed, but it was not observed. Thus, the movement of the ends of this and similar fibers certainly produced some fiber-fiber slippage.

Figure 28. Composite Photograph Showing Effect of Compression on z-Orientation. Individual Photographs Taken at $\underline{C}_o/\underline{C}$ = 1.0, 0.611, and 0.444

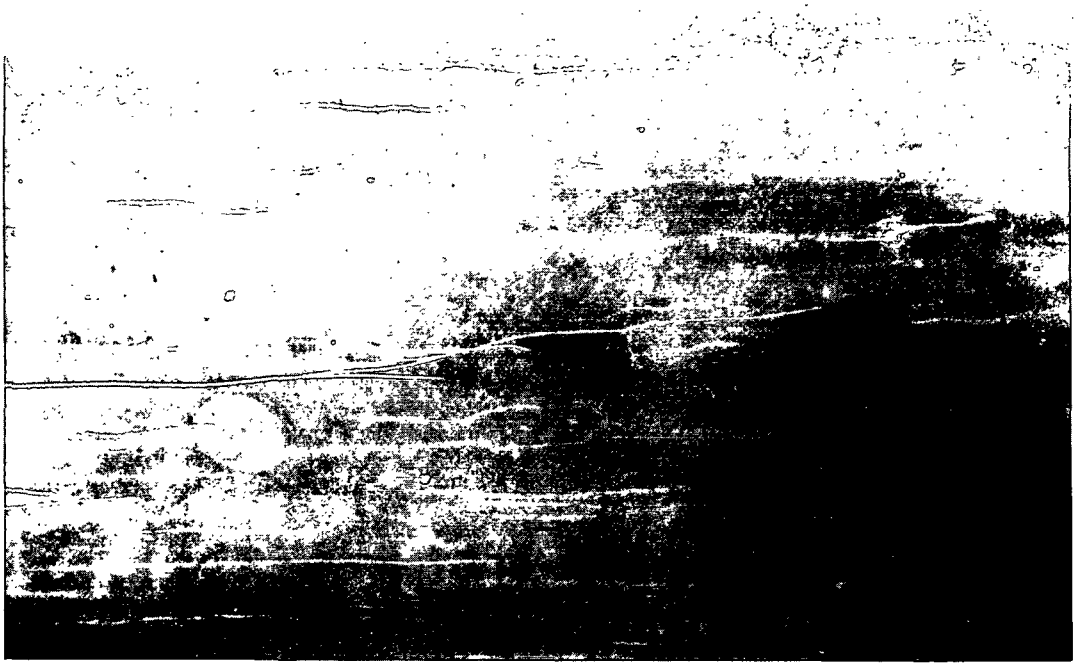

Figure 29. Effect of Compression on z-Orientation at Maximum Loading. Same Fibers as in Fig. 28. $\underline{C}_o/\underline{C}$ = 0.177

It was found that the change in z-orientation with compression occurred nearly as anticipated. To simplify the following discussion, let a parameter termed "degree of compression," $\underline{D_c}$, be defined. It is defined by

$$D_c = \frac{H}{H_o} = \frac{C_o}{C} = \frac{\sigma_o}{\sigma} \qquad (8),$$

where $\underline{H}$ is the height of the bed, σ equals the solid fraction, $\underline{C}$ equals mat solids concentration, and the subscript o refers to the unloaded structure. If the bed were a perfectly homogeneous material, then

$$D_c = \frac{Z}{Z_o} \qquad (9),$$

where $\underline{Z}$ is the distance between the bottom of the bed and any point on a fiber in the bed. Since fibrous structures are not homogeneous on a microscopic scale, Equation (9) does not hold exactly for these materials, but it applies well, especially at low degrees of compression. At higher degrees of compression, $\underline{Z}$ as calculated by Equation (9) will be too high for some points within the bed and too low for others, due to the bending of the fibers. This happens because, while bending, some portions of each fiber will be displaced upward and some portions downward with respect to the center of mass of the fiber. It can be seen from Fig. 28, though, that a fiber may experience a significant change in orientation before the configuration of any one fiber changes appreciably.

If a fiber makes an angle θ_o with respect to the z-axis in the unloaded bed, at any degree of compression, $\underline{D_c}$, it will make an angle approximately equal to θ as given by

$$\theta = \cos^{-1}(D_c \cos \theta_o) \qquad (10).$$

See Appendix I for the derivation of Equation (10) and a discussion of the implied assumptions.

The orientation of six fibers at four degrees of compression was measured from enlargements printed on film. Figure 30 shows the ratio of the measured orientation to the anticipated orientation [as calculated by Equation (10)] versus the degree of compression. In Fig. 30-31, the orientations of the fibers are expressed in terms of the angles they make with the x-y plane. It will be noted that three of the fibers changed their orientation approximately as predicted by Equation (10) up to D_c equal to 0.611, and that two of them agreed with Equation (10) up to D_c equal to 0.444. Because the fiber with the ratio less than unity at D_c equal to 0.444 had a low initial orientation, its deviation from the predicted orientation was only 1.30, which was not as great as it may at first appear from Fig. 30. The other three fibers showed significant deviation from the predicted orientation even at a degree of compression of 0.611. Figure 31 shows the ratio of the measured to the predicted angles, at a degree of compression of 0.444 versus the initial orientation of the fiber. There appears to have been a definite trend toward an increasing ratio as the initial orientation of the fiber increased.

This was probably due to the fact that the magnitude of the predicted change is greater for the fibers of highest orientation. Unless the fibers bend considerably, some axial slippage is necessary to allow the fibers to change their orientation appreciably. As slippage of the fibers is restricted, those with the highest orientation would be expected to show the greatest deviation from the predicted orientation.

Equation (10) takes into account only the changes in gross fiber orientation due to the over-all compaction of the mat. The mean orientation of a fiber [see Equation (5)], however, depends upon its configuration as well as upon the direction of its axis. Most of the fibers in the beds used had only

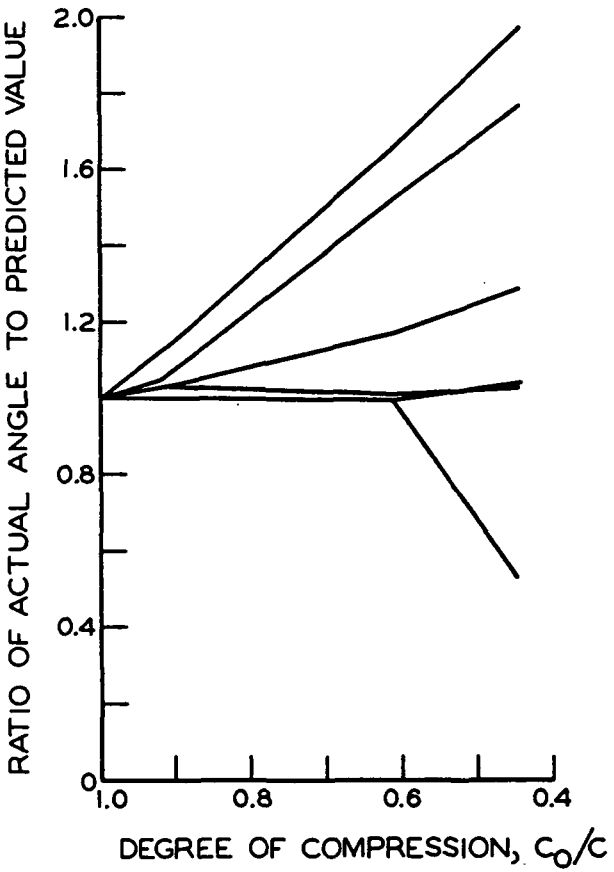

Figure 30. Effect of Compression on the Deviation From Predicted z-Orientation of Individual Fibers

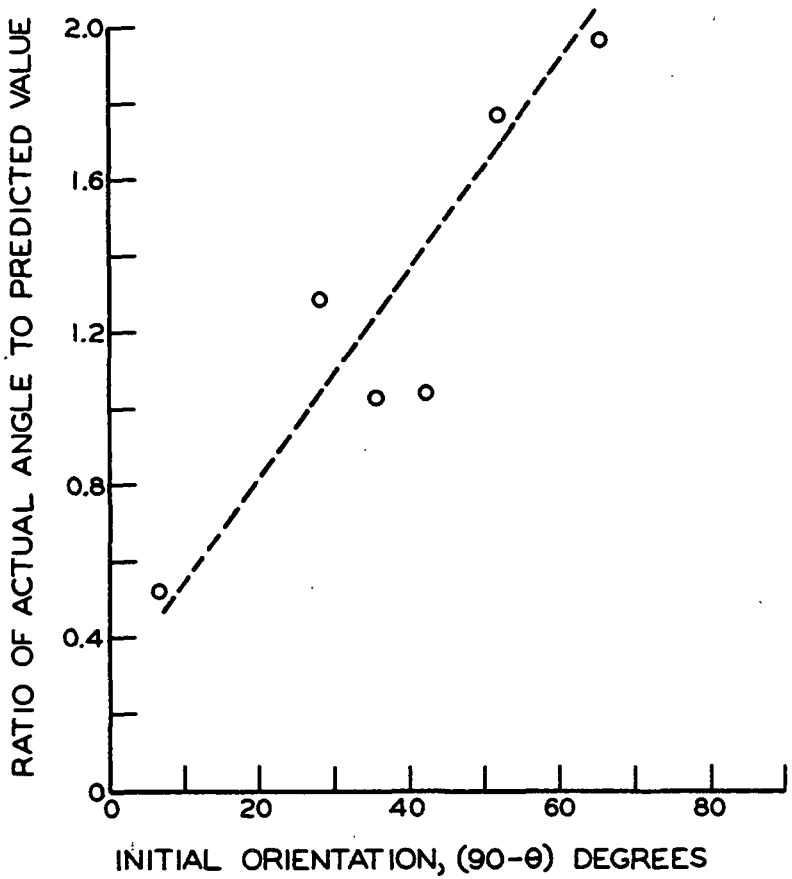

Figure 31. Deviation From Predicted Orientation (at $C_o/C = 0.444$) vs. Initial Orientation of Fiber

small amounts of z-orientation. Consequently, the mean orientation as predicted by Equation (10) will be too low for the majority of the fibers due to neglecting the bending of the fibers.

A somewhat better expression for the mean orientation, θ, of a fiber at any degree of compression might be

$$\theta = \cos^{-1}(D_c \cos \theta_o) + \left(\frac{\sigma - \sigma_o}{\sigma_o}\right) B' \qquad (11)$$

where B' is some function of the bending of the fibers. What form B' should take is not known, but it probably depends upon the dimensions and elastic properties of the fibers.

Of the three mechanisms which can cause compaction of fibrous structures, the results of studying fiber bending and fiber repositioning have been presented. The third mechanism, deformation of the fibers at their points of contact, was not significant as is shown in Appendix III.

ANALYSIS OF DATA

INTRODUCTION

Before the experimental results which were obtained can be discussed, a few terms must be defined. That portion of a fiber between adjacent points of contact with other fibers is defined as a segment. A span, however, is defined as that portion of a fiber between successive points of contact on a single side of the fiber, i.e., top or bottom. The mean number of fibers in contact with a single fiber, N_J, will be referred to as the mean number of fiber-fiber contacts per fiber or, more simply, contacts per fiber. Because two fibers participate in each fiber-fiber intersection, the mean number of contacts per fiber does not equal the ratio of the total number of intersections in a bed to the total number of fibers, but is twice this ratio. Consequently, contrary to published statements (1, 37, 38), the total number of fiber-fiber intersections in a bed is not given by the ratio of the total fiber length to the mean segment length, but is actually half this quantity. That is, the number of contacts per fiber, N_J, is given by

$$N_J = \frac{L_T}{N\ell} = \frac{L}{\ell} \qquad (12),$$

where N is the total number of fibers, L_T is the total fiber length, L is the mean fiber length, and ℓ is the mean segment length. Equation (12) applies regardless of the fiber length if the ends of the fibers (that portion from their termination to the first contact point) are regarded as only portions of a segment. The distinction between the mean number of fiber contacts per fiber and the number of intersections per fiber must be clearly understood if one wishes to calculate the normal load between the fibers at the points of contact or the surface area of the fibers in contact with each other.

EFFECT OF FIBER DIMENSIONS UPON COMPRESSIBILITY

A knowledge of the number of contacts per fiber, in a newly formed bed, is of considerable importance to an understanding of the compression behavior of fibrous structures, but the technique of estimating the number of fiber contacts, from the number of inflection points loses its sensitivity when the bed is not compressed. A value for the number of contacts in an ideal freshly formed bed can be obtained, though, from semitheoretical considerations. An ideal freshly formed bed will be defined as one formed at zero pressure drop from a liquid having the same density as the fibers. Under these conditions, the shape of the fibers in the bed will be identical with their configuration in a stationary suspension. The glass fiber beds used in the present study closely approximated this definition of an ideal freshly formed bed, since most of the glass fibers within the beds were almost perfectly straight.

During the formation of an ideal bed, as a fiber is deposited upon a partly formed bed it will be supported by two points, as it would be a rare coincidence for three or more points of suspension to occur in the same straight line. Since each fiber contact on the bottom of a fiber is paired with one on the top of another fiber, each fiber, except those on the very top of the bed, will also as a rule contact two fibers along its top surface. Each fiber then will touch on the average four other fibers. Undoubtedly, four contacts per fiber is the lower limit for fibers in a stable fibrous structure. Fibers which are deposited in the bed with appreciable z-orientation, or those which roll as they are deposited, may contact more than two fibers along their bottom sides, so that even in an ideal freshly formed bed the number of contacts per fiber might be slightly greater than four.

It would seem that in ideal freshly formed beds each fiber should contact about four other fibers, which leads to the generalization that the number of contact-points in a freshly formed bed is approximately proportional to the number of fibers and that the initial span length, ℓ_o, is approximately proportional to the fiber length, L.

FIBER LENGTH

Since the flexibility of a span is approximately proportional to the third power of its length (see Appendix II), these considerations allow a clearer interpretation of Jones' (1) data on the effect of fiber length upon compressibility. Jones found, for glass fibers with a diameter of 12.86 μ, that as the fiber length decreased from 6.3 mm. to 0.96 mm. the mat solids concentration at any compacting pressure increased. This effect of length on mat solids concentration was greatest for the shortest fibers. It would seem that this result was due partly to the effect of length-to-diameter ratio on z-orientation. Probably of greater importance is the fact that the distances between the points of contact was less for the shorter fibers, allowing them to pack closer together.

Jones' data show clearly that the slope of the compression and recovery curves is greater for the longer fibers. This is consistent with the argument that the initial span lengths are greater for the longer fibers. Consequently, structures formed from the longer fibers will compress more readily than those containing shorter fibers.

Jones found that nylon fibers with a diameter of 46.2 μ and lengths from 6.3 to 0.96 mm. showed a similar effect of length on the mat solids concentration and slopes of the compression-recovery curves. However, for 5.12 μ glass fibers he found that the effect of fiber length was less pronounced. The

shortest fibers (0.96 mm.) produced beds with higher mat solids concentrations than did the longer fibers (1.68, 3.13, 4.6, and 6.3 mm.), which produced beds with approximately the same mat solids concentration. The slopes of the compression-recovery curves were about the same for all five fiber lengths.

It is likely that the initial structure of the beds made from 5.12 μ diameter fibers was not as dependent upon the length of the fibers as were beds made with the 12.86 μ fibers. This could be due to the greater flexibility of the 5.12 μ fibers. It might be expected that, as deposited, the 5.12 μ fibers were not straight but were bent down against the surface of the mat by the water flowing past them. If this explanation is correct, the effect of fiber length for small diameter fibers becomes more important as the flow rate during formation and the total weight of the bed decreases. Also, the use of a higher density saturant to minimize the compressive effect of the weight of the bed should increase the effect of fiber length for small diameter fibers.

FIBER DIAMETER

In the past it has been somewhat difficult to explain why there is so little effect of fiber diameter upon the compression response of fiber beds (1), especially if fiber bending is the major mechanism producing the deformation. This seems particularly strange when one recalls that the stiffness of a beam with a circular cross section, EI, varies as the fourth power of the diameter. It has been suggested that the effect of the diameter of the fibers upon their stiffness is counterbalanced by the effect of fiber diameter upon the structure of the mats, but exactly how this happens has not been described. As will be discussed subsequently, Wilder (32) assumed that the initial thickness of a "layer" in a bed equals the fiber diameter. When this was done, fiber diameter cancelled out during the derivation of his compressibility equation, but the behavior of individual fibers cannot be readily determined from this treatment.

A consideration of the energy stored in the bed during compression will help to clarify this problem. Energy absorbed by means other than bending of the fibers will be neglected in this discussion. Consider two similar fiber beds of the same weight and cross-sectional area. The fibers in both beds are assumed to have the same length and modulus of elasticity, but the diameter of the fibers in one bed is assumed to be twice as great as in the other. As the beds have the same total weight, the number of fibers of large diameter, N_L, will equal one fourth the number of fibers of small diameter, N_S.

To explain how there can be so little effect of fiber diameter, it will be assumed that the compression-recovery curves for the two beds are, in fact, identical. Consequently the energy absorbed during compression by the two beds will also be equal. The energy absorbed by the bed equals the product of the energy absorbed per fiber and the number of fibers. The stored potential energy due to bending, W_b, of a beam is given by

$$W_b = \int \frac{M^2 dx}{2EI} \qquad (13),$$

where M is the bending moment over the elemental length dx of the beam (39). The bending moment is given by

$$M = \frac{EI}{r_c} \qquad (14),$$

where r_c is the radius of curvature of the neutral axis of the beam. Equating the energy content of the two beds gives

$$\frac{N_L E I_L}{2} \int \frac{dx}{r_{cL}^2} = \frac{N_S E I_S}{2} \int \frac{dx}{r_{cS}^2} \qquad (15),$$

where I is the moment of inertia and the subscripts L and S refer to the large and small diameter fibers, respectively. Treating the radius of curvature as

equal to its mean value along the fiber (as a constant to simplify integration) and substituting the proper values for N_S and I_S, gives

$$r_{cS} = r_{cL}/2 \qquad (16).$$

Note that for the smaller fibers the mean radius of curvature along the fiber axis, r_{cS}, is one-half that of the larger, r_{cL}. Since the fibers are initially straight, the radius of curvature decreases as the beam is bent. It is clear that the larger fibers do not bend as much as the small diameter fibers even though the compression response of the two beds is identical. If the large diameter fibers did bend as much as the small diameter fibers, the compression-recovery curves for the two beds would be considerably different.

While the relationship between the mean radius of curvature of a fiber and the number of contacts per fiber, N_J, is not known, it is interesting to note that, at P equal to 107 g./sq. cm., the mean observed number of contacts for the 2.26 mm. by 7.22 μ fibers was 12.6, while for the 2.30 mm. by 12.86 μ fibers this value was 7.2. For these two types of fibers, the observed number of contacts per fiber was inversely proportional to the fiber diameter, within the limits of experimental uncertainty. It would seem that the ratio of the work absorbed in bending per fiber, W_b, to the fiber stiffness, EI, gives a better indication of the behavior of the fibers during compression than does the change in solid fraction of the bed for a given change in applied pressure.

INITIAL STRUCTURE OF BEDS

In this investigation no attempt was made to predict the initial structure of the beds, although the initial structure of three of the beds was determined experimentally. Most of the effort was directed toward an understanding of how the initial structure changes with compression.

Kallmes, et al. (41, 42) have made some progress in describing the structure of thin fiber assemblages. The principal limitation of this work is that the fiber assemblages are considered to be two-dimensional or a composite made from two-dimensional layers. Such a model may satisfactorily describe some of the properties of thin, well-consolidated fibrous structures such as paper (42), but it does not apply to thick filtration formed mats of high porosity. In particular, it appears that this treatment does not satisfactorily account for the effect of fiber length. For example, the number of contact points for a two-dimensional sheet is independent of fiber length and depends only upon the total fiber length per unit area. This result is contrary to the evidence obtained in the present investigation for three-dimensional structures.

It might be quite difficult to derive theoretically the relationship between fiber characteristics and the initial structure of filtration formed fibrous mats. It is conceivable, though, that an empirical relation between these two quantities could be obtained quite readily for fibers of uniform dimensions. Until this is done, it will be necessary for studies similar to this present investigation to determine experimentally the initial structures of the beds.

COMPARISON OF EXPERIMENTAL AND PREDICTED FREQUENCY OF CONTACT POINTS

Probably the most important single factor which determines the compressive behavior of a fibrous structure is the manner in which the frequency of contacts changes with increasing density of the structure. By combining (1) the z-orientation distributions determined for the freshly formed beds with (2) the relationship which was developed to account approximately for the effect of compression on z-orientation, and (3) a theory developed by Onogi and Sasaguri (31), it has been possible to compare the experimentally determined and the theoretically

predicted effects of compression and fiber dimensions on the frequency of contact points. The agreement between theory and experimental data was found to be quite good. Furthermore, some of the calculated results will be used as additional evidence for certain conclusions previously arrived at by a different approach.

To show how the z-orientation distributions were used to calculate the frequency of contact points, it is necessary to develop briefly the equations employed. For a complete derivation of the following theory, the reader is referred to the original paper (31).

Onogi and Sasaguri (31) have derived a relationship for the density of a fibrous mat in terms of the free segment length and the orientations of the segments. The basic equations are almost the same as those of Nimura and Kido (43) except that the thickness of the fibers was taken into account. Certain criticisms of the development of Onogi and Sasaguri for forces in the x-y plane have been reported (44), but they do not affect the present discussion.

The apparent density of a fibrous structure is the product of the total volume of segments in a unit volume and the density of the fiber itself, ρ. It was expressed by Onogi and Sasaguri as

$$C = N_x N_y N_z \int_0^\infty \lambda(\ell) \int_0^\infty \psi(A) A \ell \rho dA d\ell \qquad (17),$$

where the number of segments in the x, y, and z directions are given by N_x, N_y, N_z, and $\lambda(\ell)$ and $\psi(A)$ are the frequency probabilities to represent the distributions of the segment length, ℓ, and the cross-sectional area of the fibers, A. The values of N_x, N_y, and N_z depend upon the orientation of the segments and to a lesser extent their thickness. The orientation of a segment, which is assumed to be straight, is defined by the angle it makes with the z-axis,

θ, and the angle its projection makes with the x-axis, ϕ. Frequency probabilities $\Theta(\theta)$ and $\Gamma(\phi)$, are similarly used to represent the distributions of θ and ϕ.

The effect of the thickness of the fiber is taken into account by considering what contribution the thickness of the fiber makes to the total fiber length in each of the three directions. When segments are randomly distributed with respect to ϕ, the average value of the z-component of the direction cosine of the normal between two segments, $\bar{n}'$ is given by

$$\bar{n}' = \frac{1}{\pi}\sin^{-1}(2\overline{\sin^2\theta}_o - 1) + 1/2 \qquad (18),$$

where

$$\overline{\sin^2\theta}_o = \int_o^{\pi/2} \Theta(\theta)\sin^2\theta d\theta \qquad (19).$$

However, the average value of the x and y components, $\bar{\ell}'$ and $\bar{m}'$, is given by

$$\bar{\ell}' = \bar{m}' = \frac{2}{\pi}\int_o^{\pi} \Gamma(\phi)\sqrt{1-n^2}\, d\phi \qquad (20)$$

and

$$\bar{\ell}' = \bar{m}' = \frac{2}{\pi^2}\int_o^{\pi} \frac{\overline{\cos\theta}_o}{\sqrt{1-\overline{\sin^2\theta}_o \sin^2\phi/2}}\, d\phi \qquad (21),$$

where

$$\cos\theta_o = \int_o^{\pi/2} \Theta(\theta)\cos\theta d\theta \qquad (22).$$

The reader is referred to the original paper (31) for the derivation of the above expressions. If all segments have a circular cross section, and the frequency probability of the radius, r, is represented by $\chi(r)$, the contributions of their

thickness to the x, y, and z-directions are given by:

$$\bar{\ell}' \int_0^\infty 2r\chi(r)dr, \quad \bar{m}' \int_0^\infty 2r\chi(r)dr, \text{ and } \quad \bar{n}' \int_0^\infty 2r\chi(r)dr \tag{23}$$

The effect of these contributions need not always be taken into consideration, however. For example, when two segments belong to the same fiber, the interaction of the thickness of one on the other need not be considered. It is not presently possible to predict what portion of these contributions to the thickness is actually effective; consequently, Onogi and Sasaguri multiplied expressions (23) by a factor, β, equal to or less than unity. When the number of junctions is large, it was reported that statistical considerations show the lower limit of β to be 0.25.

If one accounts for the effect of the fiber thickness in this manner, the expressions for the number of segments in each direction are as follows:

$$1 = N_x \left[\int_0^\infty \lambda(\ell) \int_0^{\pi/2} \Gamma(\phi) \int_0^{\pi/2} \Theta(\theta) \ell \sin\theta \cos\phi \, d\theta d\phi d\ell + \beta\bar{\ell}' \int_0^\infty 2r\chi(r)dr \right] \tag{24}$$

$$1 = N_y \left[\int_0^\infty \lambda(\ell) \int_0^{\pi/2} \Gamma(\phi) \int_0^{\pi/2} \Theta(\theta) \ell \sin\theta \sin\phi \, d\theta d\phi d\ell + \beta\bar{m}' \int_0^\infty 2r\chi(r)dr \right] \tag{25}$$

$$1 = N_z \left[\int_0^\infty \lambda(\ell) \int_0^{\pi/2} \Theta(\theta) \ell \cos\theta \, d\theta d\ell + \beta\bar{n}' \int_0^\infty 2r\chi(r)dr \right] \tag{26}$$

Assuming that the fibers have a circular cross section of constant radius, are randomly oriented in the x-y plane, and that the free segment length at any density is constant, Onogi and Sasaguri have solved Equation (17) for three hypothetical distributions of θ. When the quantities represented by the

distributions are constant, the frequency probabilities take the form of delta functions. For example, when all segments have a uniform length ℓ_o,

$$\lambda(\ell) = \delta(\ell - \ell_o).$$

When all segments are assumed to lie in the plane of the sheet and the effect of the thickness of the fibers is neglected,

$$\Theta(\theta) = \delta(\theta - \pi/2) \qquad \text{(Case I)} \qquad (27)$$

and

$$C = \frac{3}{8}\left(\frac{r}{\ell}\right)\rho \qquad (28)$$

where r represents the radius of the fiber, ℓ the free segment length, ρ the density of the fiber, and C the density of the structure. Due to its simple form, Equation (28) has been used by a number of investigators, (1, 37, 38, 40) to estimate the importance of fiber-fiber interaction.

Two additional examples for

$$\Theta(\theta) = \frac{6\cdot 4\cdot 4\sin^6\theta}{5\cdot 3\ \pi} \qquad \text{(Case II)} \qquad (29)$$

and

$$\Theta(\theta) = \sin\theta \qquad \text{(Case III)} \qquad (30),$$

which is the case for a uniform distribution with respect to θ, were also solved and lead to equations of the form:

$$C = \left\{\frac{1}{K_1(\ell/r)+K_2\beta}\right\}^2 \left\{\frac{1}{K_3(\ell/r)+K_4\beta}\right\}\pi\left(\frac{\ell}{r}\right)\rho \qquad (31)$$

where K_1, K_2, K_3, and K_4 are constants. Equation (31) can be solved, but not explicitly, for the mean segment length, ℓ. Thus, when the orientation of the fiber segments in a bed is known and the fibers have uniform dimensions, the mean segment length can be calculated as a function of the mat density.

To calculate the segment lengths for the glass fiber beds, the fundamental equation of Onogi and Sasaguri, Equation (17), was solved to give an expression having the form of Equation (31), using the experimentally determined forms for $\Theta(\theta)$. This required substituting the experimental expressions for $\Theta(\theta)$ into Equations (18), (20), and (24)-(26) and numerically integrating them. These calculations were performed using an IBM 1620, Model II, computer. The method of numerical integration was checked by numerically integrating the required expressions containing the two hypothetical forms of $\Theta(\theta)$ given by Onogi and Sasaguri. For the hypothetical distributions, numerical integration agreed with integration by formula to the fourth significant digit.

After the four constants of Equation (31) were calculated, the free segment length and number of contacts per fiber were calculated for the three sizes of fibers. Figure 32 gives a comparison of the number of contact points per fiber, for the 2.26 mm. by 7.22 μ fibers, calculated for the three hypothetical frequency probabilities of Onogi and Sasaguri and calculated for the experimentally determined distribution for this fiber. Also shown are the values for the number of contact points experimentally determined for this fiber at three solid fractions, and in addition their 90% confidence limits. All curves shown in Fig. 32 are for β equal to 1.00. The number of contacts per fiber calculated by Equations (29) and (30) are considerably greater than the experimentally determined number. However, the number of contacts as calculated by Equations (6) and (27) give about equally good agreement with the experimental values. At the solid fraction of the newly formed bed (0.012), though, Equation (27) predicts that each fiber will contact fewer than two others. This is only about half as many as would be needed to produce a stable structure.

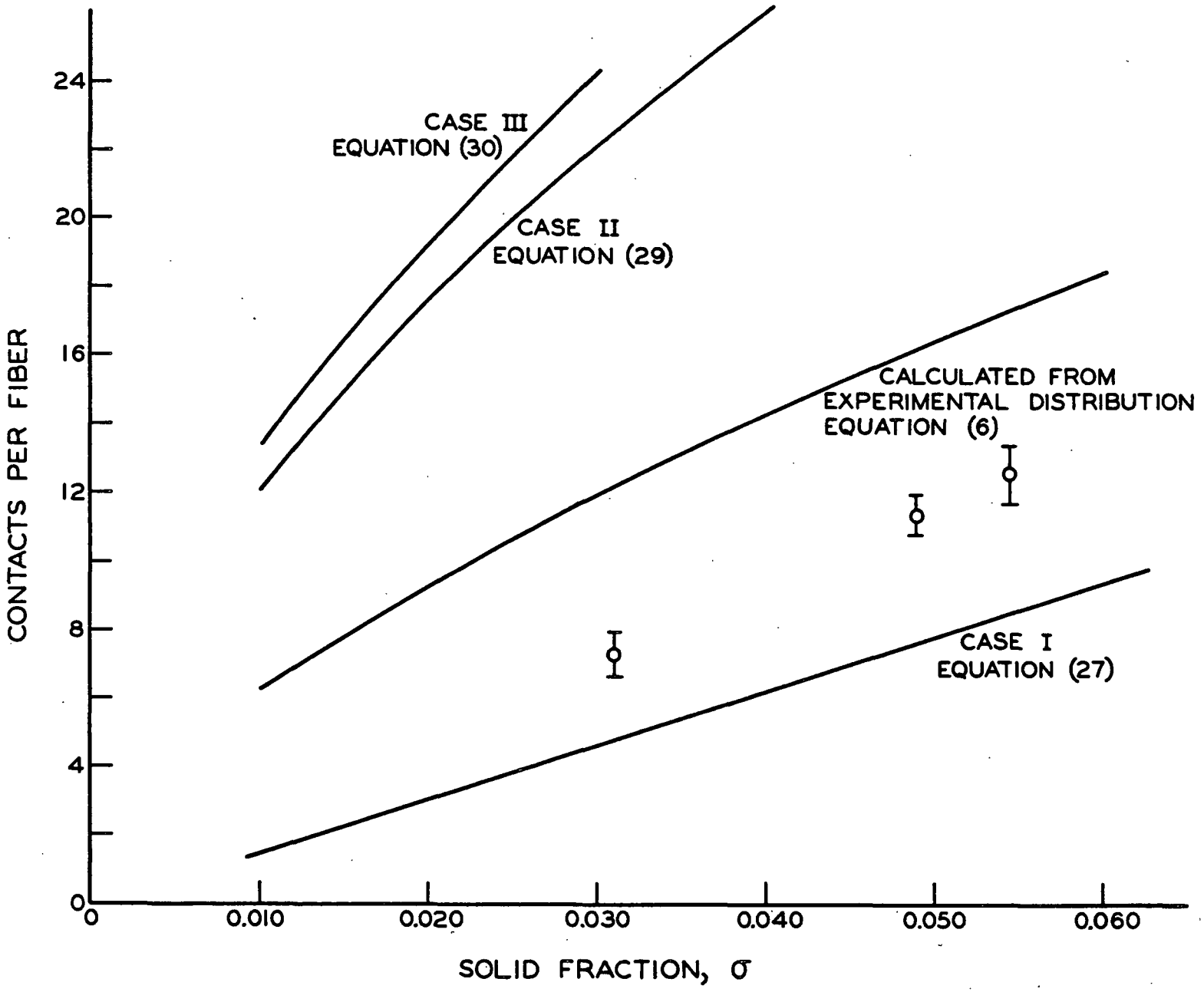

Figure 32. Effect of Form of z-Orientation Distribution on Calculated Number of Fiber Contacts for 2.26 mm. by 7.22 μ Fibers, When Distributions are Assumed to be Independent of Solid Fraction

The difference between the two frequency probabilities of Onogi and Sasaguri and the three experimental distributions are shown by the cumulative forms of these distributions in Fig. 33. It is apparent that all three experimental distributions have a higher portion of their fibers within 30° of horizontal than would be predicted by the hypothetical distributions. However, the hypothetical distributions predict a smaller portion of the fibers will be within 10° of vertical than do the experimental distributions. Comparing Fig. 32 with Fig. 33, it can be seen that the segment length is greater at any solid fraction as the fibers become more nearly horizontal.

The curves of Fig. 32 were calculated on the assumption that $\Theta(\theta)$ does not change with increasing solid fraction. As previously discussed though, the z-orientation of the fibers does change with compression, and at each degree of compression, $\Theta(\theta)$ takes a different form. The effect of compression on $\Theta(\theta)$ was evaluated by using Equation (10). At any degree of compression, the frequency of fibers between θ and $\theta + d\theta$ is given by the frequency of fibers between θ_o and $\theta_o + d\theta_o$ in the newly formed bed. As before, θ_o and θ are related by Equation (10). After the effect of compression upon $\Theta(\theta)$ was accounted for in this manner, the segment length, $\underline{\ell}$, for several degrees of compression was calculated for each of the three types of fibers. This necessitated the calculation and renormalization of a new value for $\Theta(\theta)$ at each degree of compression. These results are given in Fig. 34.

Figure 34 shows the calculated number of contacts per fiber versus solid fraction for the three sizes of fibers. Note the change in scale, of the vertical axis from Fig. 32 to Fig. 34. Also shown are the experimental data for these fibers and again the 90% confidence limits. While Fig. 34 may appear confusing at first glance, this combined presentation of calculated and

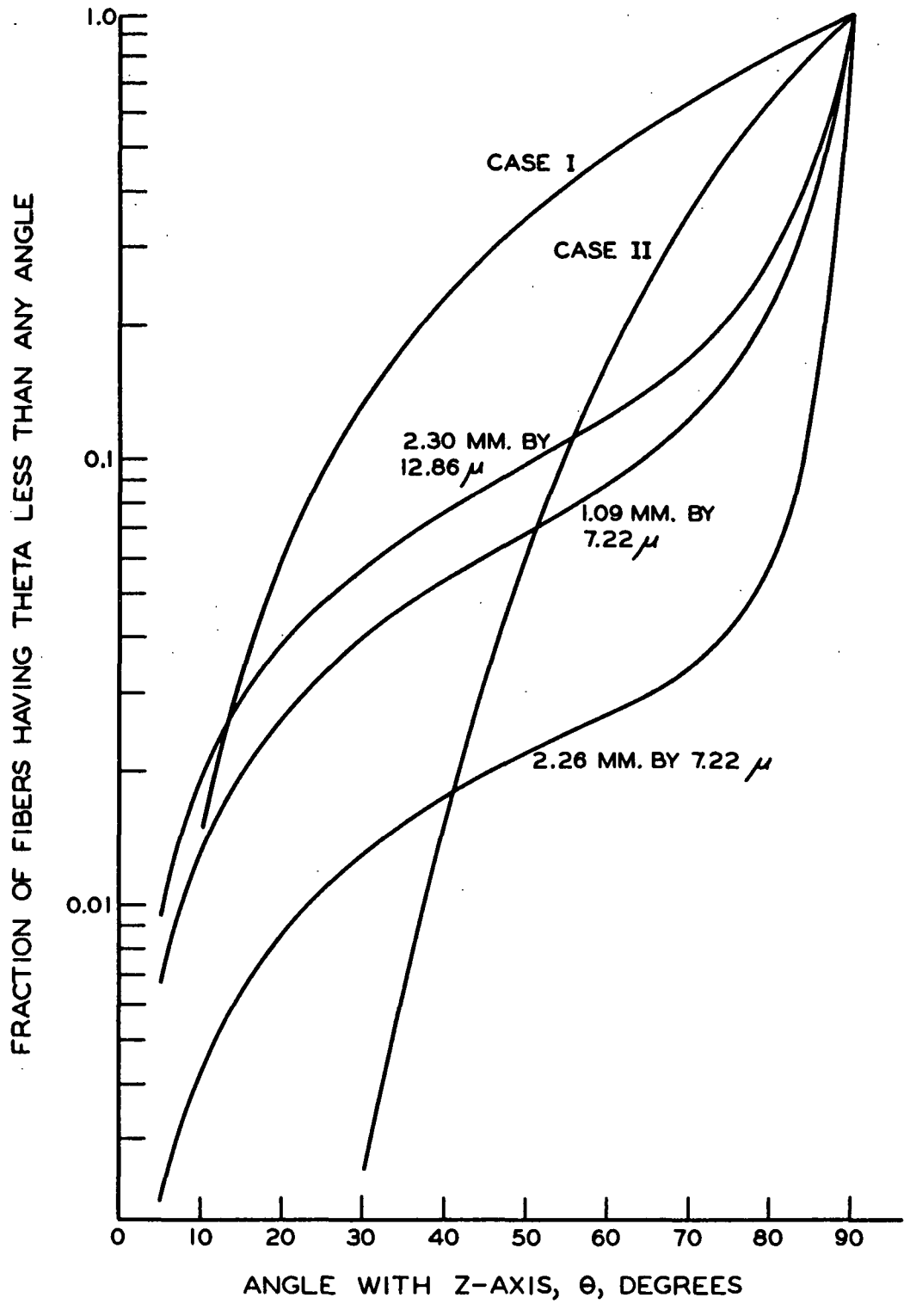

Figure 33. Comparison of z-Orientation Distributions

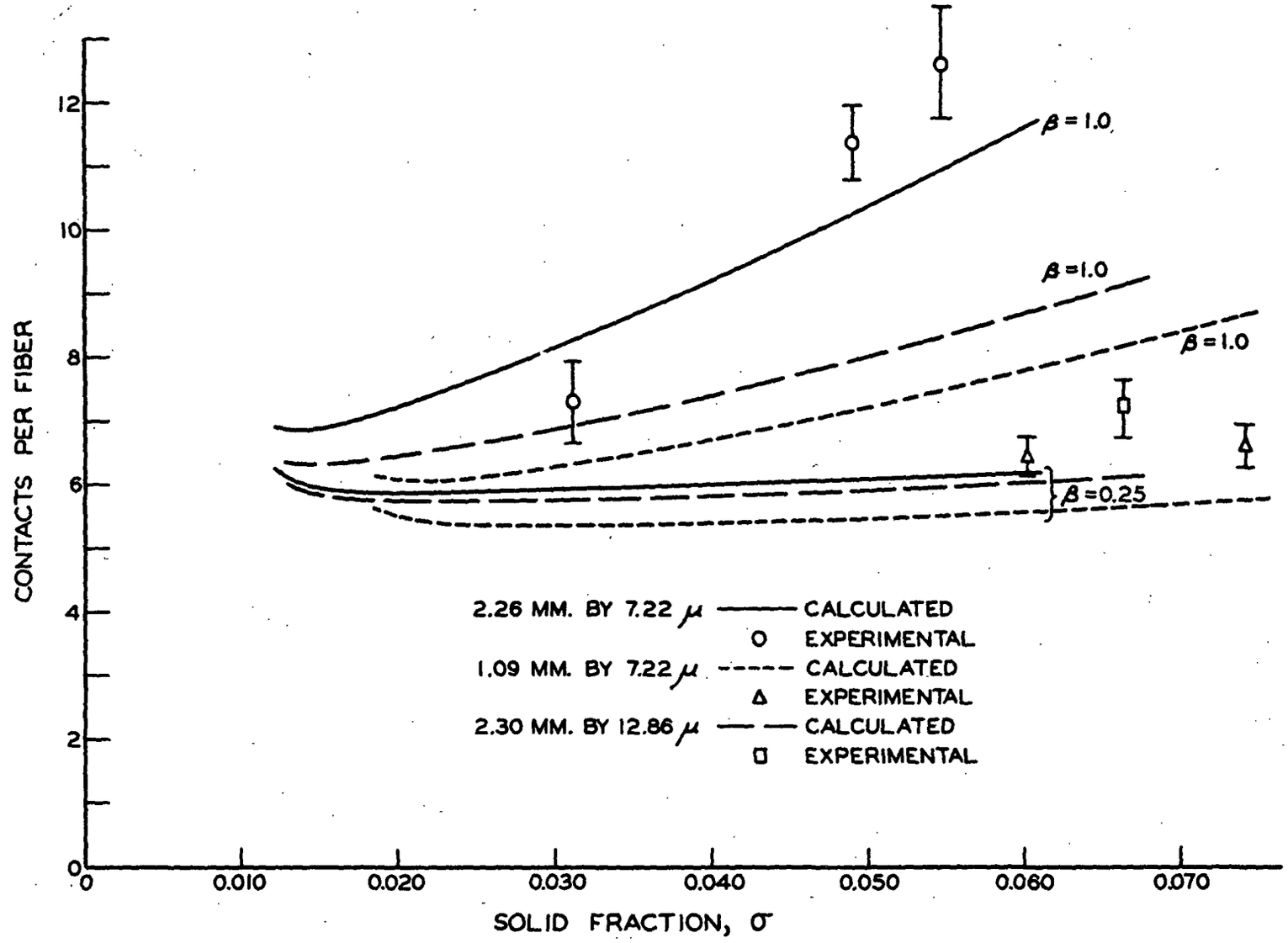

Figure 34. Comparison of Calculated Number of Fiber Contacts and Experimental Data

experimental results is necessary to allow the desired comparisons to be made. Even allowing for the uncertainty of β, one must consider the agreement between the theory and experimental results as good. It would appear that at the solid fractions corresponding to the data points, the best value of β for the 1.09 and 2.30 mm. fibers is somewhat greater than 0.5. Both the theory and the data show that the number of contacts for the 2.30 mm. by 12.86 μ fibers is significantly less than for the 2.26 mm. by 7.22 μ fibers even though they have nearly the same length. Also, the calculated number of contacts at the lowest observed solid fraction for beds of each size fiber is nearly independent of the fiber length. As previously discussed, this result was anticipated. It was expected, however, that there would be about four contacts per fiber for the newly formed beds rather than the approximately six as calculated. Part of the explanation could be that these beds were not formed at zero pressure drop. It has been noted that the 2.26 mm. by 7.22 μ fibers in the unloaded bed were not perfectly straight. This could account for the fact that the initial number of contacts calculated for this fiber was somewhat higher than for the other two sizes.

It is particularly interesting to compare the initial number of contacts calculated for the 1.09 mm. and the 2.26 mm. fibers since they have the same diameter. As the initial number of contacts is nearly the same for the two beds, the initial segment length is almost proportional to the fiber length. Note from Equations (18)-(31) that the calculated values of the segment length in no way depend upon the fiber length except as it influenced $\Theta(\theta)$.

When the manner in which a fiber is supported as it is deposited in a bed under ideal conditions was considered earlier, it was speculated that the segment length in an unloaded bed would increase with increasing fiber length for fibers of the same diameter. The calculated values for the segment length provide

additional evidence for this belief. As a bed is compressed, the segment length should tend to become less dependent upon fiber length. For the extreme case of a two-dimensional structure, the number of contact points per unit cross-sectional area of the bed is totally independent of fiber length (41).

Figure 35 shows the observed minimum number of contacts per millimeter of fiber length as a function of the fiber length-to-diameter ratio for the 1.09, 2.26, and 4.55 mm. by 7.22 μ fibers when the beds were subjected to an applied pressure of 107 g./sq. cm. It will be noted that the number of contacts per unit length of fiber increased slightly with decreasing fiber length even at this moderately high pressure.

Both the calculated and experimental data (Fig. 34) indicate that the 1.09 mm. fibers experience a smaller change in their number of contacts, for a given change in solid fractions, than the 2.26 mm. fibers. In addition, both the calculated and experimental data indicate that, at comparable solid fractions, each 2.30 mm. by 12.86 μ fiber contacted slightly more fibers than did the 1.09 mm. by 7.22 μ fibers.

The minimum in the curves of Fig. 34 is real and is not due to a lack of precision in calculating the number of contacts. It is not reasonable, though, that there would be any decrease in the number of contacts as compression increases. It is probable that in this region β is not constant but is increasing. The minimum in the curves could also be due to an overcorrection for the effect of compression upon z-orientation. There is no minimum when the change in z-orientation is not taken into account (Fig. 32).

In the case of the 2.26 mm. by 7.22 μ fibers, correcting for the effect of compression on the z-orientation predicts fewer contacts at high solid fractions

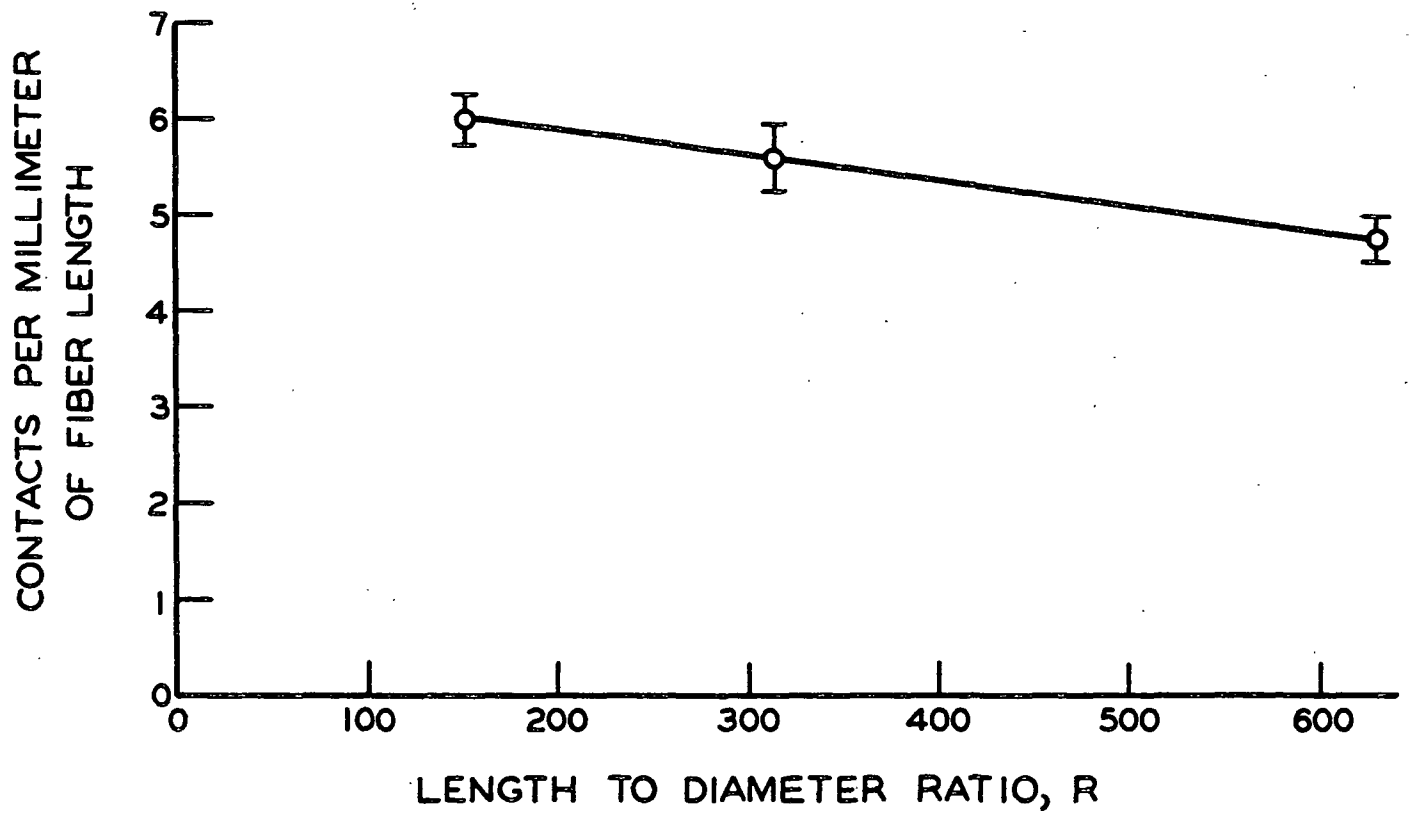

Figure 35. Contact Points vs. Length-to-Diameter Ratio at Constant Apparent Applied Stress (107 g./sq. cm.) for 7.22 μ Fibers

than were observed. It is likely that this was due to neglecting the contributions of fiber bending to the z-orientation. Accounting for the effect of compression on z-orientation gives values nearer to the experimental data than when this effect is neglected. Neglecting bending for the 1.09 and 2.30 mm. fibers appears not to have been important. However, as indicated by the number of contacts per fiber, these fibers had not bent as much as the 2.26-mm. fibers. At higher solid fractions the effect of bending would probably become more important for the 1.09 and 2.30 mm. fibers.

If the orientation of a fiber at any degree of compression is given by Equation (11) rather than Equation (10), when $\underline{B}'$ equals 1.5°, for example, the calculated number of contacts is shown in Fig. 36. This means that at a degree of compression of 0.25 the average z-orientation added by the bending is assumed to be 4.5° and proportionately less at lower levels of compression. This is about the amount of bending of the fibers which was observed (Fig. 17). It will be noted that even accounting for bending in this oversimplified manner gives results which agree with the data within the experimental limits.

If the effect of bending on the average orientation of the segments could be predicted and if the proper values of β were known, it appears it would be possible to calculate very closely the number of contacts at any solid fraction from the orientation of the fibers in the newly formed bed. The desirability of being able to predict the initial z-orientation distributions from the known fiber dimensions is obvious.

EMPIRICAL RELATIONS BETWEEN SEGMENT LENGTH AND SOLID FRACTION

In this work some consideration has been given to simpler expressions, than those of Onogi and Sasaguri (31), to predict the relation between contacts

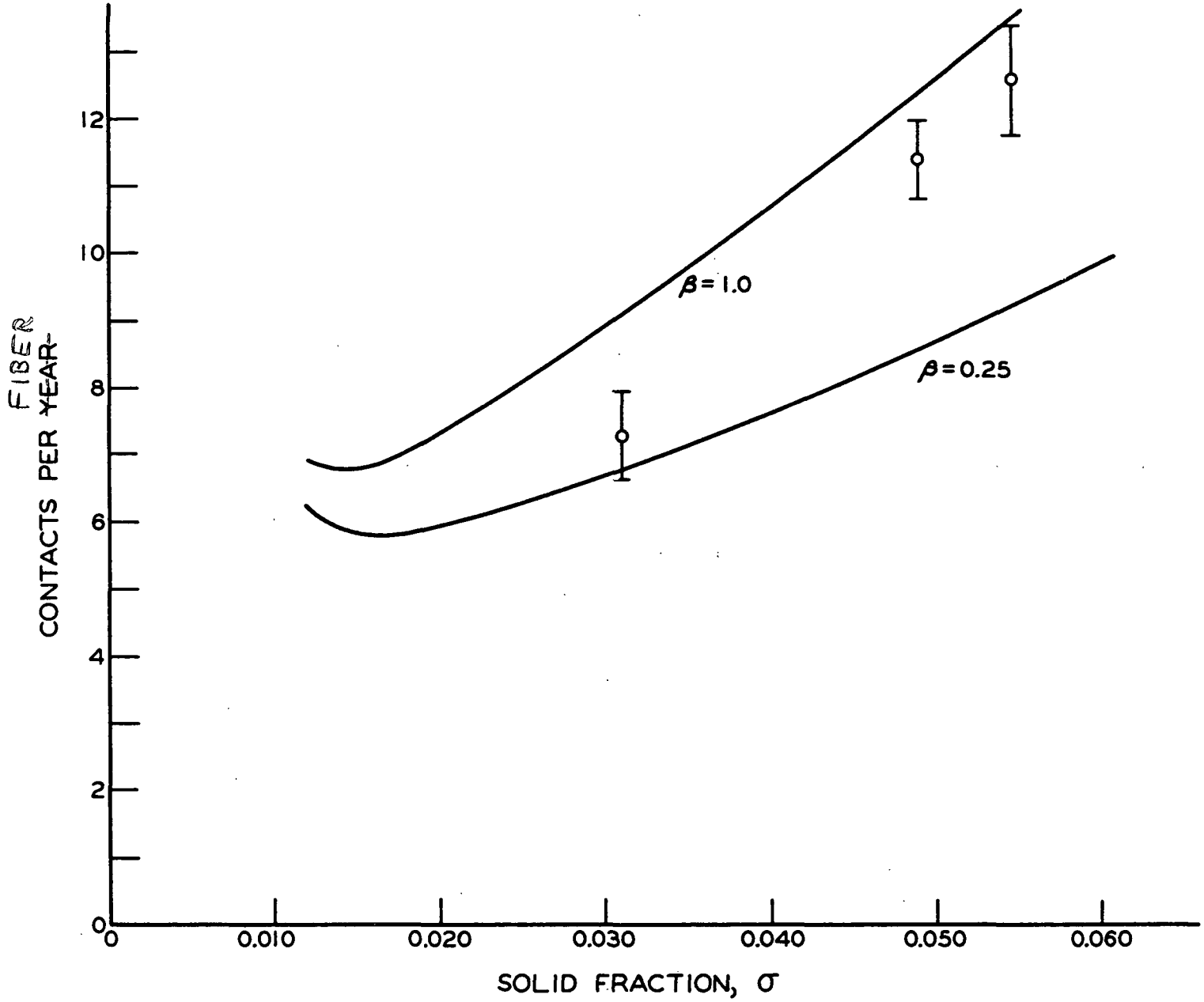

Figure 36. Accounting for Effect of Orientation Caused by Bending on Calculated Number of Contacts for 2.26 mm. by 7.22 μ Fibers

and solid fraction. Wilder (32) in the development of his compressibility equation utilized a relation of the form

$$\frac{\ell}{\ell_o} = \left(\frac{C_o}{C}\right)^{\alpha} = \left(\frac{\sigma_o}{\sigma}\right)^{\alpha} \qquad (32),$$

where α is a constant, C is the mat solids concentration, ℓ the mean segment length, and the subscripts refer to the conditions existing in the unloaded bed. Using experimental data for the 2.26 mm. by 7.22 μ fibers and values of ℓ_o calculated from the theory of Onogi and Sasaguri, it has been possible to test the applicability of Equation (32). A value for α was determined from the experimental data and from the calculated values of ℓ_o for β equal to 0.25 and 1.00 at a solid fraction, σ, equal to 0.012. The values of α obtained were 0.465 and 0.394, respectively. The closest fit to the data was obtained for α equal to 0.465, and this curve is shown in Fig. 37. As was done previously, the values of the segment length, ℓ, are expressed in terms of the number of contacts per fiber, N_J. It is not certain how close the calculated values of ℓ_o are to the true value of ℓ_o or how near C_o is to its true value. It can be seen, though, that no combination of values of ℓ_o greater than $L/4$ and σ_o less than 0.012 allows Equation (32) to agree well with the experimental data for the 2.26 mm. by 7.22 μ fibers. The maximum value of ℓ will not be greater than $L/4$, because each fiber must contact at least four other fibers. Because the 1.09 mm. by 7.22 μ fibers showed a more nearly linear increase in contacts with increasing solid fraction, Equation (32) describes the behavior of these fibers fairly well.

The utility of a second empirical relation between ℓ and σ was also considered. As the mean distance between the fibers decreases with increasing solid fraction, it seemed reasonable to try a relationship of the form

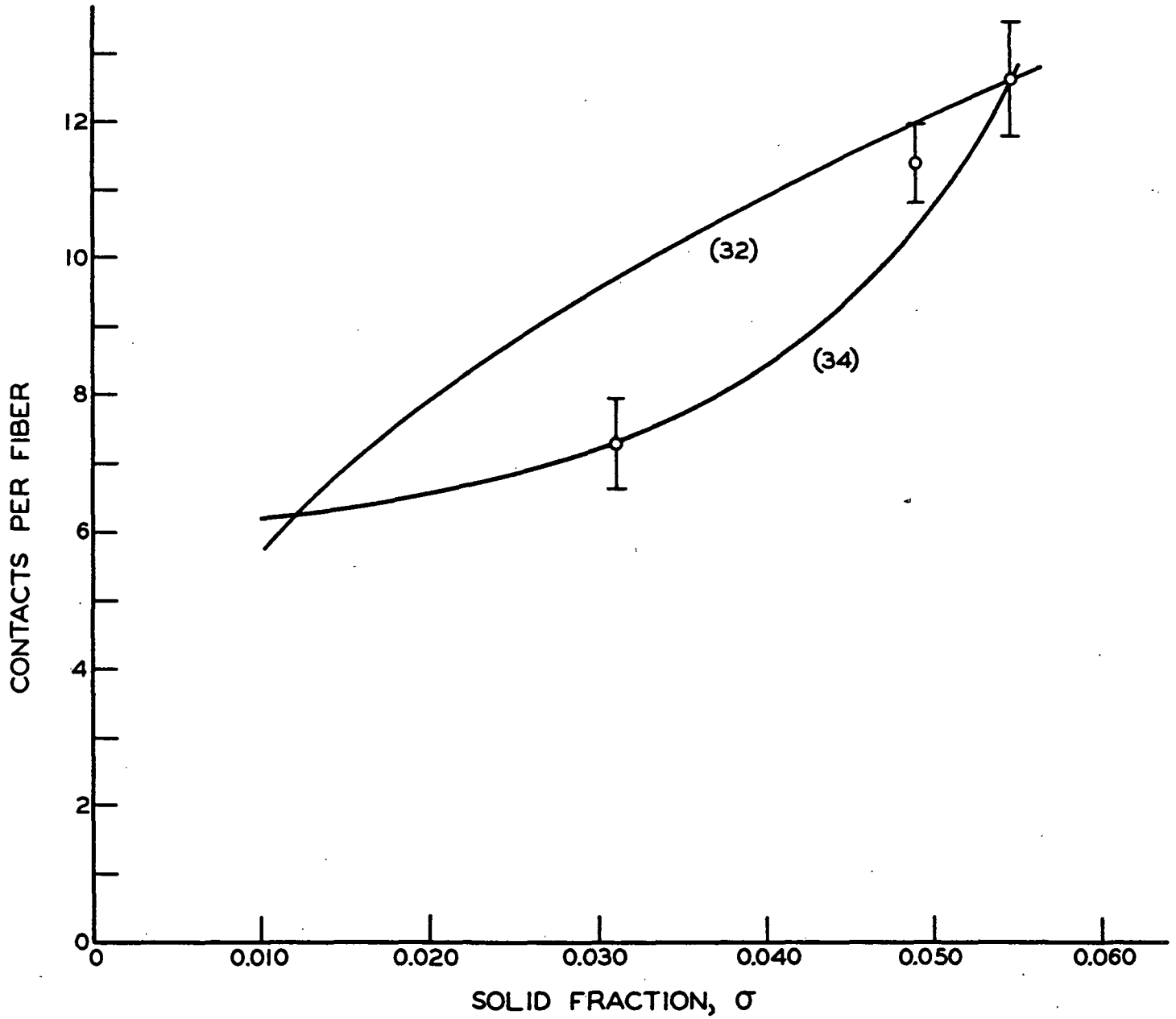

Figure 37. Comparison of Two Empirical Expressions Relating Solid Fraction and Contacts Per Fiber for 2.26 mm. by 7.22 μ Fibers

$$\frac{d\ell}{d\sigma} = -K'\sigma \qquad (33),$$

where K' is a constant, to calculate the effect of compression on segment length. Using the same boundary conditions used for Equation (32), the differential form, Equation (33), was solved (for β equal to 0.25) to give Equation (34).

$$\ell = -64.7\ \sigma^2 + 0.371 \qquad (34)$$

A graph of this function is shown in Fig. 37. Equation (34) appears to represent the experimental data better than Equation (32) for the 2.26 mm. by 7.22 μ fibers, but it does not seem to be entirely satisfactory. Equation (34) appears to predict a more rapid increase in the number of contacts, beyond solid fractions of 0.0545, than indicated by the experimental data or by the equations of Onogi and Sasaguri (31).

EFFECT OF AXIAL FORCES UPON FIBER BENDING

In previous treatments of the compression response of fibrous networks (32, 45), the deflection of a span of a beam (representing a simple fiber model) was considered to be proportional to the load upon the span. This proportionality applies for simple beams not experiencing an axial force. An axial force is defined as a tensile or compressive force directed along the axis of the beam. The effect of an axial force must, however, be taken into consideration to account for the observed hysteresis in the compression-recovery curves of fiber beds and to explain the effect of the saturants.

As a beam deflects, either the length of the neutral axis must increase or the ends of the beam must move closer to each other. In either case, unless the beam rests on frictionless supports, the beam will experience an axial force. As previously noted, a slight decrease in the distance between the ends of the

2.26-mm. fibers was observed during compression. In the event the ends did not move together, the axial force necessary to lengthen the fibers the required amount would have to be greater by about an order of magnitude than the frictional force which these fibers can provide. Lateral bending of the supporting fibers would tend to reduce the axial tension, but this mechanism could affect only the end spans of the fiber. It appears, therefore, that some axial slippage of the fibers must have occurred.

Consider the case of a simple beam resting on two supports and supporting a load concentrated at its midpoint. If an incremental load is slowly added, the axial force in the beam will increase until it equals the product of the reactive force at the points of support and the coefficient of friction between the beam and its supports. Then the beam will slip over one or both of its points of support. If the incremental load is removed, the situation will be reversed, except that the axial force will then be compressive rather than tensile.

By employing two of the expressions given by Morley (46), the magnitude of the effect of axial forces can be assessed. The maximum deflection, Δ_b, of a simple beam with freely hinged ends and supporting a concentrated load, W, at its midpoint and an axial load, p, is given by Equation (35) when the axial force is tensile and by Equation (36) when the axial force is compressive.

$$\Delta_b = \frac{WL}{4p} - \frac{W}{2p}\sqrt{\frac{EI}{p}}\tanh\frac{L}{2}\sqrt{\frac{p}{EI}} \qquad (35)$$

$$\Delta_b = -\frac{WL}{4p} + \frac{W}{2p}\sqrt{\frac{EI}{p}}\tan\frac{L}{2}\sqrt{\frac{p}{EI}} \qquad (36)$$

Figure 38 compares the effect of two levels of axial force with the absence of an axial force. It shows the deflection in fiber diameters as a function of the

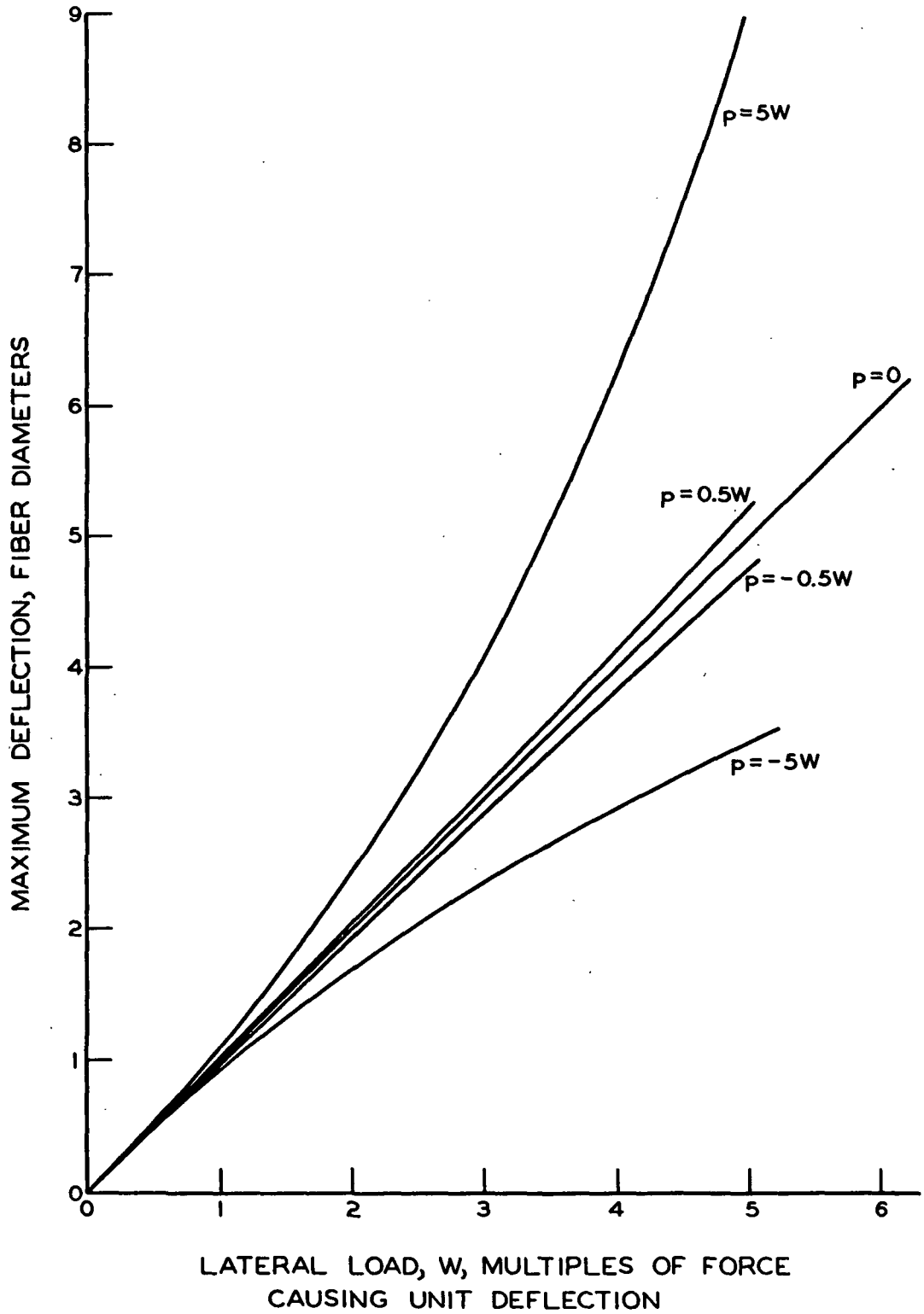

Figure 38. Effect of Axial Force on Deflection of a Simple Beam

lateral load, W, expressed in multiples of the lateral load required to produce a deflection of one fiber diameter in the absence of an axial force. When the force is directed away from the center of the beam, its sign is considered to be negative. At a given lateral load, axial tension reduces and axial compression increases the deflection, compared to a beam with no axial force. If the coefficient of friction is unity, as it is for clean glass on glass, the response of a simple beam during compression will be given by the curve p equal to -0.5W. During recovery, when the axial force is compressive, the response is given by the curve denoted by p equal to 0.5W. In the case of a center span of a fiber loaded at several points, the axial force might reasonably be expected to be several times the concentrated load on any one span. It will be noted that the hysteresis increases rapidly with increasing axial force as shown by the curves for p equal to 5W.

If the fibers are infinitely long, as for the case of Jones' (1) model structures, they may well be supported at a sufficient number of points to prevent slippage. Then the fibers will be forced to stretch between their points of contact. In this situation, if the fibers are not viscoelastic, the axial tension will be the same at equivalent loads during compression and recovery and no hysteresis would be anticipated. Jones found that his model structures exhibited no hysteresis.

In general, it might be expected that the hysteresis will be small for short fibers, because of the low axial force which can be maintained, whereas for very long fibers the hysteresis will be reduced because the fibers are restrained at so many contact points that axial slippage does not occur readily. A reduction in the coefficient of friction between the fibers will have about the same effect upon hysteresis as a reduction in fiber length (see Appendix III).

Jones' studies of the effect of fiber length for both nylon and glass fibers show a maximum in the relationship between hysteresis and fiber length. As shown previously in Table V, a similar result was obtained in the present study for the 7.22 μ diameter fibers. It appears that the hysteresis in the compression-recovery behavior of fibrous structures containing elastic fibers is due primarily to axial slippage of the fibers.

At this point it is possible to discuss in greater detail the compression-recovery behavior of some of the beds which were mentioned in an earlier section. As shown in Table V, an air-dried bed composed of 2.26 mm. by 7.22 μ fibers demonstrated greater resistance to compression than similar freeze-dried beds. Likewise, a bed of 4.55 mm. by 7.22 μ fibers saturated with o-dichlorobenzene compressed significantly less than when saturated with the oil. In both of these instances, there is little doubt that the reduction in compressibility was caused by an increased resistance to axial slippage.

For the 4.55 mm. by 7.22 μ fibers, the o-dichlorobenzene did not cause as pronounced a reduction in hysteresis as it did for the 2.26 mm. by 7.22 μ fibers. With both saturants, however, the area of the hysteresis loop was smaller for the 4.55-mm. fibers than for the 2.26-mm. fibers. No significant decrease in the compressibility of beds of the 2.26 mm. by 7.22 μ fibers was caused by o-dichlorobenzene. Because the 4.55-mm. fibers have about twice as many contact-points as the 2.26-mm. fibers, beds composed of the longer fibers would be expected to be more responsive to changes in the coefficient of friction between the fibers. The bed of the 2.26 mm. by 7.22 μ fibers which was not saturated, and the water-saturated bed, showed less hysteresis than did similar oil-saturated beds, but their compressibility was not greatly affected. It appears that increasing the coefficient of friction between the fibers had a greater effect on the recovery

portion of the cycle than upon the compressibility. Evidently, the axial tension of the 2.26-mm. fibers was not increased sufficiently by o-dichlorobenzene or water to decrease the compressibility of the beds.

The true value of the coefficient of friction between the fibers with any of the saturants is not known, but it seems probable that it was less than unity, even for the unsaturated bed. In fact, it is likely that the coefficient of friction was not constant but varied in some manner as a function of the normal load at the point of contact (47). Consequently, even for the 2.26-mm. fibers, the frictional force between the fibers may have had a significant effect upon the compression response of the beds. That is, the differences in the coefficients of friction caused by the various saturants may not have been sufficiently great to be detected. It appears that any factor which affects the condition of the surface of the fibers could influence the compression response of unbonded fibrous structures.

ANALYSIS OF COMPRESSIBILITY IN TERMS OF MECHANISMS

It was not possible to determine what effect the freezing and subsequent resaturation of the beds had upon their internal structure. This may have caused some mechanical conditioning of the beds to low stresses. It is believed, though, that this did not seriously affect the internal structure of the beds. If the beds had been appreciably mechanically conditioned, they would have been expected to show a smaller difference between the first and second compression cycles. Another indication that the beds were not mechanically conditioned to any appreciable extent is the curved lower portion of the log C vs. log P plots for the first compressions which becomes less pronounced as the beds are cycled. It is believed that the fiber beds as studied in this investigation were representative of the beds as formed.

Whether the beds were in the "as formed" condition did not particularly affect the studies of the mechanisms causing compaction of the beds. These beds demonstrated almost the same behavior as those of Jones (1), which were studied without the need for handling or resaturating them. Except for nonrecoverable deformation, the beds studied in the present investigation demonstrated the compression-recovery characteristics which had been attributed to fiber slippage.

Photographic evidence has demonstrated that there was only a small amount of fiber repositioning and an appreciable amount of fiber bending during the compression of glass fiber mats. Undoubtedly fiber bending is the primary mechanism responsible for the compaction of these mats. Before it can be concluded, though, that fiber slippage is unimportant other than as it affects bending of the fibers, satisfactory explanations are needed for the compression-recovery characteristics which have been attributed to the fiber-fiber slippage.

Repositioning of the fibers during compression could take several forms. Movement of the fiber centers in the direction of the stress applied to the mat is taken for granted. It is repositioning of the fibers or fiber parts in the plane of the mat which is in question. Movement of entire fibers may have been perpendicular or parallel to their axes or they may have rotated. No evidence was found which indicated that entire fibers rotated or that they translated perpendicularly to their individual axes. The ends of some of the fibers with high z-orientation moved appreciably in the direction of the fiber axes, but their midpoints showed little or no movement. Because of the small percentage of fibers with appreciable z-orientation, it is thought that the contribution of this effect was not great. It appears that, in terms of total distance, most of the slippage which occurred, was axial slippage which was associated with the bending of the fibers.

Although the mean difference between the length along the 2.26 mm. by 7.22 μ fibers and their projected length was 4.5 μ, the average slippage per contact point would have been only a fraction of this amount. The amount of slippage at any contact point would be approximately proportional to the distance between the contact and that point along the fiber where no slippage occurred. If one end of the fiber were fixed, the total amount of slippage would be about twice that which would occur if the center remained stationary. Thus, it is likely that the fixed point along the fiber occurred near its midpoint, and that the mean slippage per contact point was one-fourth the change in length or about 1.1 μ. This slippage due to bending would be in addition to any caused by repositioning of the entire fiber. While the amount of slippage caused by bending of the fibers was small, it can be demonstrated (Appendix III) that it was sufficient to account for most of the hysteresis in the compression-recovery curves.

The evidence indicates that horizontal movement of parts of a fiber was an unusual occurrence. When this was detected it was only the extreme end of a fiber which changed position. No signs of horizontal bending of the center spans of the fibers could be found, although horizontal fiber movement of an amount less than the diameter of a fiber, about 7 μ, probably could not have been detected by the photographic methods employed. To determine whether this small amount of slippage could significantly affect the compaction of a mat, it is necessary to consider in detail how slippage can contribute to compaction.

In addition to the effect of slippage on axial tension, slippage could contribute to compaction in only a limited number of ways. If a fiber slips so that a point of support is at a lower position on the supporting fiber, compaction will be favored. For this to be significant, the supporting fiber must be oriented at an appreciable angle to the horizontal. For example, if the supporting fiber

is oriented at five degrees to the horizontal and the supported fiber moves laterally 7 μ, it will be displaced downward by only 0.61 μ. Even if the fibers did move this much, it would be a small amount compared to the downward displacement caused by bending of the fibers.

Small amounts of slippage could possibly change the span length distributions enough to have some influence upon compressibility. This could result only if the majority of the slippages favored increasing the longer spans at the expense of the shorter ones. This in itself appears unlikely. Also, the minimum detectable slippage is small compared with the mean span length. It is considered improbable that slippage significantly changes the span length distribution.

Fiber repositioning could contribute to compaction by one fiber slipping off another and eliminating some contact points. Figure 27 showed two fibers whose ends bent horizontally. This photograph was the only one of several hundred, however, which showed this behavior. Evidently, horizontal bending of the ends of a fiber is not an important factor in the elimination of contact points. There is, though, another mechanism which probably does lead to a slight reduction in the number of contact points. As the fibers show little tendency to move sideways, elimination of a contact point can occur due to the ends of a fiber moving toward each other during compression. As noted, the total inward movement of either end of the 2.26 mm. by 7.22 μ fibers was about 2.2 μ. Then, a contact point would have to be within 2.2 μ of one end of either of the fibers for it to be possible that the contact point would be lost. Consequently, the probability that any contact along an individual fiber can be eliminated is $4.4\ \mu/L$, assuming that contacts occur with equal frequency along all portions of the fiber. For the 2.26-mm. fibers, then, about one contact in every 513 (about 0.2% of the total number) will be eliminated, probably during the first compression.

Once lost, contact between a given pair of fibers probably will not be re-established at compacting pressures less than or equal to that which caused its elimination. Unless this effect causes a disproportionately large change in solid fraction between the first and second compressions, the elimination of contact points can be ignored.

When compared at zero applied stress, oil-saturated beds of the 2.26 mm. by 7.22 μ fibers showed essentially no nonrecoverable deformation, and some of them even had a slightly lower solid fraction after the second recovery than they had before the first compression. Thus, for these beds it is not necessary to explain the existence of nonrecoverable deformation in the absence of fiber repositioning. Of all the beds studied, only the dry and the water-saturated beds of the 2.26 mm. by 7.22 μ fibers and the two beds composed of the 4.55 mm. by 7.22 μ fibers showed any indication of having a higher solid fraction at the end of the first compression compared to the solid fraction before the first compression.

Jones (1) reported a maximum in the relationship between "nonrecoverable deformation" and the length-to-diameter ratio of the fibers, which was attributed to fiber slippage. However, because the atypical edge of the beds was not removed before the first compression, these results are somewhat questionable. In addition, the nonrecoverable deformation as reported actually represents the width of the hysteresis loop at an applied stress of 10 g./sq. cm. for the first compression-recovery cycle (48). This suggests that the reported nonrecoverable deformation may have been due partly to the effect of axial slippage on axial tension.

Since the small amount of repositioning of entire fibers which does occur is primarily associated with fibers having appreciable z-orientation, it is not surprising that, beyond some point, beds with fibers of decreasing length-to-diameter

ratio might show increasing nonrecoverable deformation. z-Orientation decreases, however, with increasing length-to-diameter ratio and some other explanation is needed for the nonrecoverable deformation of beds with long fibers.

It is believed that the nonrecoverable deformation of beds having fibers with high length-to-diameter ratios is better accounted for by nonrecoverable bending than by slippage. Because of friction, within the beds, nonrecoverable bending may occur even for perfectly elastic glass fibers. There is no justification for thinking that, when the bed is unloaded, the forces between the fibers at the points of contact are also zero. On the contrary, the very fact that some curved fibers were found in the newly formed beds proves that the forces between fibers at the contacts were not all equal to zero. Therefore, especially for the longer fibers, the axial compressive force due to friction might not return to zero during recovery. No nonrecoverable bending of any of the fibers could be detected, but none of the beds studied showed appreciable nonrecoverable deformation.

Although the oil-saturated beds of 2.26 mm. by 7.22 μ fibers showed essentially no nonrecoverable deformation when unloaded, the first compression-recovery cycles were not identical with subsequent ones. Part of the reason for this difference in cycles may be experimental. When the compression-recovery curves were being determined, the close-fitting piston guide was not used. Consequently, there probably was slightly more repositioning of the fibers during these measurements than occurred when the photographs were being taken. This effect could contribute toward making the beds more compressible after the first compression. It is also possible (14) that there was a small decrease in the stiffness of the fibers as a result of the first compression. In addition, it should be mentioned that no breaking of the fibers was observed. Even if a very small fraction of the fibers had broken, it would have been detectable. This, of course, assumes that the unsilvered fibers showed no greater tendency to break than the silvered ones.

Another possible reason for the nonreproducibility of the first compression cycles is suggested by several features of the curves of Fig. 9-10. It is the compression portion of the cycles which shows the greatest change from the first to later cycles. Recovery curves generally show a smaller change from cycle to cycle. Therefore, even though the beds may reach slightly greater solid fractions during the second or third cycles, the energy expended compressing the beds is less than for the first compression. An abrading or smoothing of the contact areas on the glass (at the submicroscopic level) during the first compression would tend to make the beds more compressible during subsequent cycles and to reduce the energy required to reach a given solid fraction. Unlike a gross slipping of the fibers, this effect would allow the beds to recover completely at an apparent applied stress at zero. Whether this effect actually was significant could not be determined.

To summarize, photographic evidence showed that there was very little repositioning of the fibers during compression. An analysis of the ways slippage can affect compression has shown that slippage of an amount less than could be detected would not have significantly affected the compressibility of the beds. The small amount of axial slippage which does occur caused most of the hysteresis and is important chiefly because it affects fiber bending. This form of slippage probably results in the elimination of a small fraction of the contact-points and may contribute slightly toward the lack of reproducibility of the first compression-recovery cycle, although factors other than slippage can cause a similar effect. Repositioning of entire fibers makes some contribution to the hysteresis, but this occurs only for the small percentage of fibers having appreciable z-orientation. Nonrecoverable deformation of unloaded beds having fibers of moderate length is primarily due to nonrecoverable bending of the fibers, although for beds composed of short fibers, the chief cause is probably repositioning of the fibers

with high z-orientation. For initial stresses in excess of 1 g./sq. cm., and probably appreciably lower initial pressures, compression response of glass fiber mats may be thought of as determined entirely by fiber bending and the associated small amount of axial slippage.

DISCUSSION OF WILDER'S COMPRESSIBILITY EQUATION

One of the first attempts to explain the compression response of fibrous structures in terms of the behavior of individual fibers was that by Wilder (32). The basis of this derivation was that mat deformation is due entirely to bending of the fibers. This derivation produced the relationship

$$C^{4\alpha-1} - C_o^{4\alpha-1} = \frac{\pi^8 \rho^5 (4\alpha-1)P}{4096KEC_o^{6-4\alpha}} \qquad (37),$$

where C, ρ, E, and P have their usual meaning and the other symbols are constants. By proper selection of the constants C_o, α, and K, Equation (37) correlates experimental data well except at low compacting pressures, P. Whereas C_o actually represents the mat solids concentration of a bed which has not been subjected to a compressive stress, its value is usually uncertain, and C_o is often treated as an adjustable constant. The constant K occurs because, in the derivation of the compressibility equation, each segment of the fiber was regarded as behaving like a simple beam. It is defined by

$$K = \frac{\ell^3 W}{\Delta_b EI} \qquad (38),$$

where Δ_b is the central deflection of the span and W is the concentrated load. While Wilder did not attempt to predict the values of the constants, it has been possible from the present study to estimate values of α and C_o, for beds having fibers of two different lengths. Equation (37) then was used to estimate K.

The diameter and modulus of elasticity of the fibers were known. The values of C_o used were the mat solids concentration of the fiber beds obtained after freeze drying. For the 2.26 mm. by 7.22 μ fibers, the value used for C_o (0.030) was undoubtedly too high. As previously noted, these fibers in the newly formed beds were somewhat bent. The 1.09 mm. by 7.22 μ fibers were essentially straight in the newly formed beds, and consequently the value of C_o used for this bed (0.047) probably was near its true value.

Several values of α were calculated from Wilder's equation,

$$\frac{\ell}{\ell_o} = \left(\frac{C_o}{C}\right)^{\alpha} \qquad (32),$$

which was used to define α. In this equation, ℓ_o is the initial span length corresponding to the initial mat solids concentration, C_o. The values of α were calculated by using the experimentally determined values of ℓ and C, at the highest compacting pressures, and the values of ℓ_o calculated at C_o by using the theory of Onogi and Sasaguri (31). After determining appropriate values for α, K was calculated from Equation (37) using the experimental compressibility data for two of the beds.

Figure 39 shows K as a function of pressure, P, for the third compression of a bed of the 2.26 mm. by 7.22 μ fibers and for the second compression of a bed of the 1.09 mm. by 7.22 μ fibers. Figure 40 shows K as a function of the solid fraction, σ, for the same data. It is apparent that K, rather than being constant, increased with σ and P. Since the compressibility equation was developed on the assumption that K is constant, it appears that some modification of this derivation is needed. It will be noted that for both beds K increased almost linearly with P over a substantial range of pressures. The two curves shown are for the case of β equal to 0.25 which gave slightly higher values of α (0.465 and 0.119,

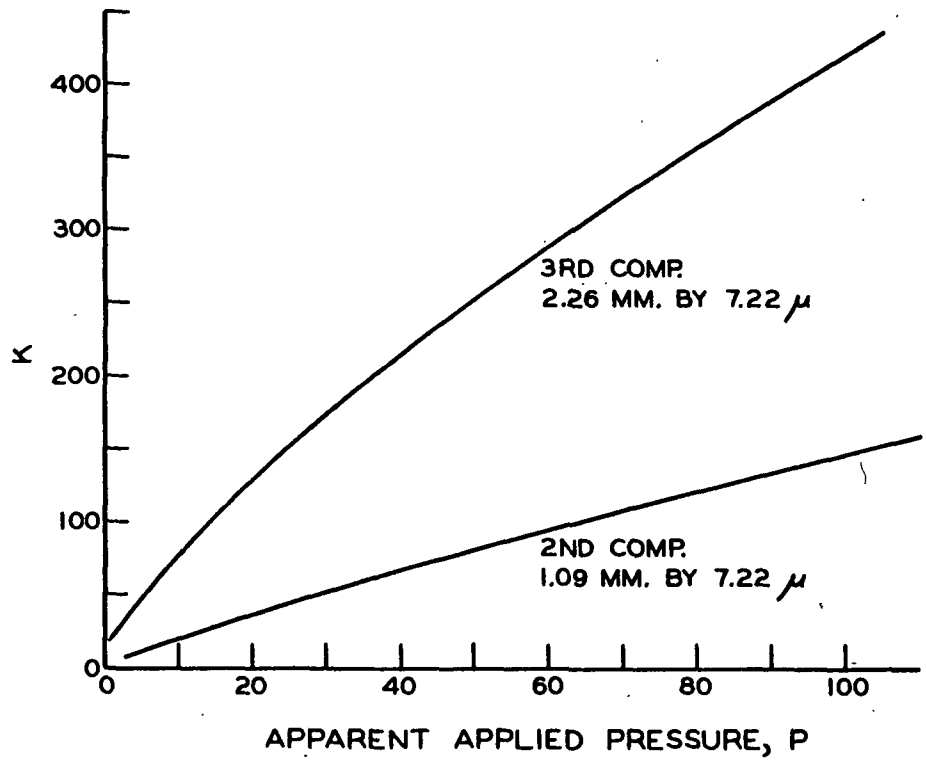

Figure 39. Two Tests of Wilder's Compressibility Equation

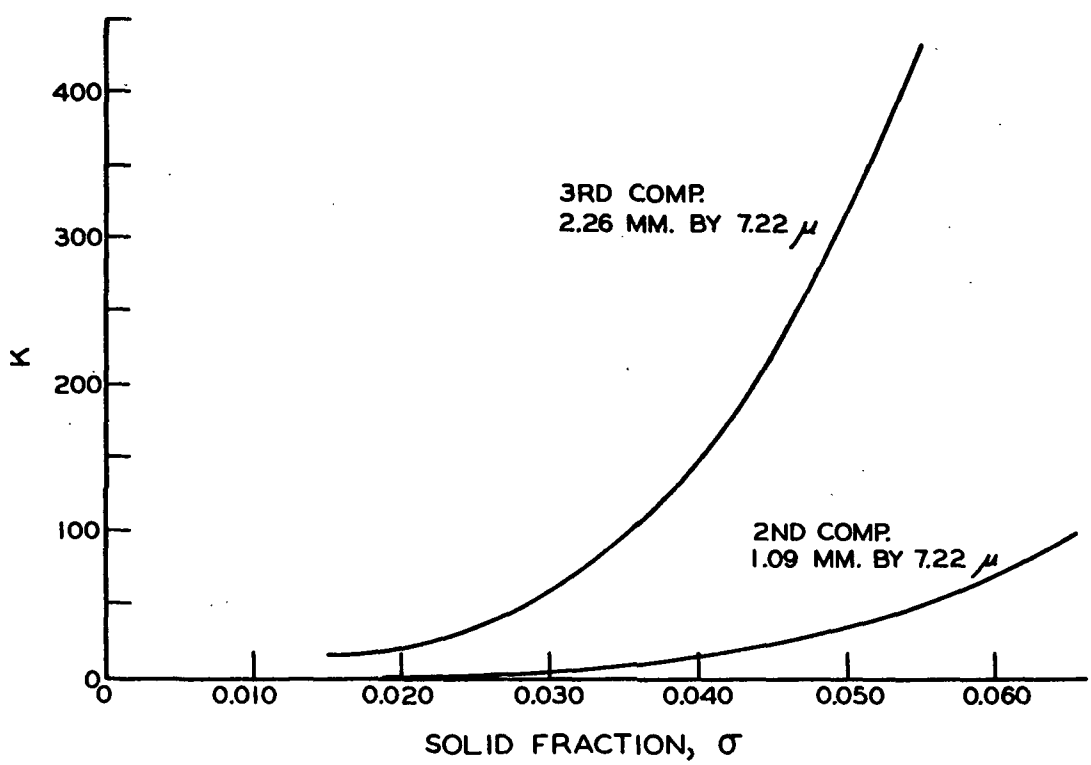

Figure 40. Two Tests of Wilder's Compressibility Equation

respectively, for the 2.26 and 1.09 mm. fibers) and a smaller change in $\underline{K}$ than for β equal to 1.00. Lower values of $\underline{C}_o$ than those used give even greater changes in $\underline{K}$. Much higher values of α (1.0 to 2.0) reduced the calculated magnitude of $\underline{K}$ and made it more nearly constant. However, these values of α predict a greater change in $\underline{\ell}$ with $\underline{C}$ than can possibly be consistent with the data obtained. Because the fibers must have at least four contacts, the maximum value of $\underline{\ell}_o$ is one-fourth the fiber length. The lower limit of $\underline{\ell}$ was established experimentally by using the 0.1-denier dacron fiber. Even when α was calculated from these extremes, it was not large enough to make $\underline{K}$ constant.

It is interesting to note that the calculated values of $\underline{K}$ are of the same order of magnitude as those obtained for simple beams. For a cantilever beam with a concentrated load at its end, and for a simple beam with free ends, and for a simple beam with restrained ends, each with a concentrated load at its center, the values of $\underline{K}$ are 3, 48, and 192, respectively. For the center spans of a continuous beam, the values of $\underline{K}$ may be at least as high as 480 (see Appendix II). The calculated value of $\underline{K}$ is quite sensitive, though, to the particular model which is employed for a continuous beam. Axial tension in the fibers will also tend to increase $\underline{K}$ beyond the values calculated for a simple beam. The calculated values of $\underline{K}$ (Fig. 39, 40) are quite large, but they are not unrealistically high.

It would seem that the theory represented by Equation (37) is basically sound, but that it requires some modification to explain adequately the compression response of fibrous structures. To suggest possible improvements of this theory, the assumptions which led to its development will be reconsidered. Refinements of these assumptions frequently lead to relationships which cannot be readily manipulated. However, because these assumptions illustrate areas of this subject where our knowledge is deficient, they are listed in the next section.

ASSUMPTIONS AND DISCUSSIONS

The principal assumption of this derivation is that fiber bending is entirely responsible for compaction of fibrous structures. This assumption appears justified, at least for glass fiber beds. The other assumptions required for this derivation are given below, followed individually by a brief discussion of them in light of the results of the present study.

No. 1. "At any degree of mat compaction, a constant distance exists between all fiber-fiber contacts within the mat (i.e., a constant free fiber segment length is assumed at any particular degree of compaction)." Especially in the newly formed bed, the free segment length is not constant. As a bed is initially compressed, the longer segments will be responsible for most of the deflection. As the compacting pressure is increased, the segment length would be expected to become more nearly uniform, and then all the fibers would participate in the compaction. The phase of bending when only the longer segments are being deflected may partially account for the curved lower portion of log P vs. log C plots. This assumption does not appear to be a serious limitation as long as the correct mean value for the segment length can be utilized. However, the problem arises in defining the correct mean value.

No. 2. "The contact points along any individual fiber consist of an alternate above-and-below arrangement. Therefore, the distance between points of support (located on the lower side of the fiber in question) is equal to twice the free fiber segment length." This assumption does not appear to be a serious limitation. Adjacent contacts on the same side of a fiber would probably only increase the mean segment length.

No. 3. "The fibers are cylindrical in shape and are not significantly deformed in cross section during the loading process (point contact between fibers)" applies well for glass fibers.

No. 4. "The fibers can be treated as simple beams and satisfy all assumptions inherent in the development of the simple beam deflection equations (this implies that we are dealing with relatively small deformations)." Photographic evidence indicates that the assumption of small deformations is not in itself a serious limitation. Treating the fibers as simple beams, however, places several restrictions on their behavior. For long fibers with a high coefficient of friction, treating the projected length and the actual length of the fibers as identical may be a significant error as shown by the 4.55-mm. fibers in o-dichlorobenzene. This assumption also precludes the possibility of an axial tension in the fibers. For shorter fibers with a low coefficient of friction, the axial forces will be fairly small and the limits of the error in neglecting axial tension are probably indicated by the size of the hysteresis loop. For long fibers, neglecting the axial forces in the fibers may cause appreciable error.

This assumption also implies that the deformation of a segment is proportional to ℓ^3. This relation holds for all simple beams and at least in some cases for continuous beams (see Appendix II). Whereas the deflection of a segment of a continuous beam may be proportional to the applied load, at a constant segment length, it is likely that, as the length changes and loading upon the beam becomes more complex, the proportionality constant ($1/K$) decreases (see Fig. 39, 40). That is, as a bed is compressed, not only do the lengths of the segments decrease, but the resistance to bending for a given length increases. While there are other factors which may cause an apparent change in K, it is probable that treating K as a constant is a weakness of this theory which will require some improvement.

No. 5. "A definite relationship [Equation (32)] exists between the mat solids concentration, C, and the free fiber segment length, ℓ." As was discussed,

this relation does not accurately predict the change in ℓ for fibers of moderate length. However, even for the 1.09-mm. fibers where this relation appears to apply, the value of K was not constant.

No. 6. "Each fiber-fiber contact supports the same fraction of the total applied load." This assumption is closely related to No. 1. Although the photographic evidence demonstrates that the stress at each contact point is not the same, it is not presently possible to assess the effect of the use of a mean contact load in place of a distribution of loads.

No. 7. "The structure of the mat can be described by use of the horizontal 'layer' concept, each 'layer' consisting of that portion of the bed cross section which supports the total load applied to the bed."

No. 8. "Each 'layer' behaves exactly the same as all other 'layers,' contains the same number of contact points, and is deformed by the same amount under any applied load as all other 'layers.'" The concept of a layer is useful and is justified. A layer can be defined unambiguously at any P. However, in the course of the derivation, the thickness of a layer in the uncompressed bed was taken as equal to the fiber diameter, and the number of layers for all values of P was treated as constant. In addition, it was necessary to consider the deformation of each layer as equal to the deformation of a segment. These parts of this assumption are likely to be oversimplifications. Also, the number of contacts between two layers was considered to be the projected number of intersections. If the thickness of a layer is greater than the fiber diameter, the actual number of contacts may not be identical with the projected number. For example, it seems equally likely that the thickness of a layer is at least as great as the mean vertical distance between successive contacts along a given fiber. In this case the thickness of a layer would depend upon the mean

z-orientation of the fibers and consequently upon the length-to-diameter ratio of the fibers.

If a reasonable value is chosen for K, one may estimate the thickness of a layer, calculate the deflection of the fibers, and compare the results with the photographs obtained in this present work. When this is done, as shown in Appendix III, it appears that the thickness of a layer is not greatly different from the fiber diameter.

It would be possible to calculate the thickness of a layer at moderate pressures from measurements made on the photographs of the fibers. This would require calculating the stresses at the points of contact from the shape of the fibers using the first area-moment theorem (49). Knowing the distribution of stresses at the points of contact, one could calculate the thickness of the layers from Equation (36). Time did not allow this to be done. Quite likely one of the areas of this theory which needs some improvement is the description of a layer, but this is not a simple task (50).

No. 9. "Fibers in the bed are essentially infinite in length (i.e., fiber ends and segments at fiber ends do not influence the mat behavior)." As indicated by Jones' data, the effect of fiber length should be taken into account. It has been shown in the present study that the number of contact points at any solid fraction and the effect of axial tension depend largely on the fiber length. While the effect of fiber length upon the axial tension can probably be ignored except in the most sophisticated treatments (and perhaps for very long fibers), the effect of fiber length upon the segment length is of major importance. To account for the effect of fiber length would be a beneficial extension of this theory.

Wilder's treatment is a major step toward improving our understanding of the compression response of fibrous structures, even though the need for certain improvements has been indicated. Incorporating these modifications into the theory would undoubtedly lead to cumbersome expressions. With ready access to high-speed computers, though, numerical solutions may be readily obtained. An exact theory would be desirable to evaluate approximate treatments of this subject. An exact theory, while still a difficult problem, may not be as difficult as previously anticipated, due to the apparently minor contribution of fiber slippage.

RELATION OF THIS WORK TO PULP FIBER MATS

As with other investigations which utilize model fibers, care must be exercised in extending the results to pulp fiber systems. However, some of the general conclusions probably apply universally to fibrous structures.

It would be expected that the structure of filtration-formed pulp mats is also influenced by the dimensions of the fibers. While the amount of z-orientation obtained with pulp mats may be considerably different from that obtained with glass fibers, it is likely that the amount of z-orientation increases with decreasing length-to-diameter ratio. Compared to most glass fibers, pulp fibers have quite a low length-to-diameter ratio. Consequently, even though wood fibers are more flexible and experience rather high fluid drag forces, when pulp mats are formed at low flow rates, the mean z-orientation of the fibers is probably greater than a degree or two and some of them may have quite high orientations. For fibers with different lengths and about the same diameters, at equal compacting pressures, the beds composed of the longer fibers probably have fewer contacts per unit length of fiber than beds composed of shorter fibers.

It is probable that there is no large amount of fiber repositioning during the compression of pulp fiber mats. The glass fiber mats possessed lower initial

solid fractions than usually obtained with pulp mats, and the glass fibers had circular cross sections. Both of these factors would be expected to produce more fiber repositioning in the glass fiber mats than in pulp mats. It should be noted, though, that while the glass fiber mats did not increase their diameter by a measurable amount during compression, the edges of unrestrained pulp mats do bulge somewhat (51). This suggests that for pulp mats there must be some repositioning of the fibers. It is not known, though, whether the bulging occurs throughout the mats or is localized on their edges as a result of a wall effect during formation of the beds.

With wood pulp fibers there are other factors, in addition to those discussed for glass fibers, which may cause the initial compression cycles to differ from the later ones. Pulp fibers are not perfectly elastic and when strained in tension they do not recover completely (52). Bending of pulp fibers, also, is probably not entirely recoverable. If the fibers can be considered hollow elliptical cylinders, two additional causes of nonrecoverable deformation become possible: Rotation of part of a fiber so that its major axis lies more nearly horizontally will increase the solid fraction and decrease the resistance of the fiber to bending. Even a partial collapse of the fiber at its points of contact or areas of greatest bending moment would greatly reduce the ability of a fiber to recover from bending. It is not presently possible to determine the extent of fiber repositioning in wood fiber mats. Care must be exercised, however, in attributing changes in the behavior of a bed during successive compression cycles to slippage or gross rearrangement of the fibers.

The present work also indicates that the method of pulping and extent of bleaching may influence the compressibility of saturated mats by changing the

surface characteristics as well as the stiffness of the fibers. Differences in the surfaces of the fibers, for example, could result from variations in the distribution and nature of the hemicelluloses. Being more flexible than glass fibers, at a given pressure the pulp fibers probably have more contact points per fiber than do similar glass fibers. Consequently, the nature of the surface of pulp fibers could become important to the compressibility of the mats at smaller length-to-diameter ratios than was important for the glass fibers. Walker (53) found that the compressibility of water-saturated mats of cotton linters was increased by the sorption of a 4-O-methylglucuronoarabinoxylan. This was attributed to a lubrication effect of the hemicelluloses. This present study lends additional evidence for the lubrication effect.

In at least one respect, pulp mats probably behave quite differently from glass fiber mats. It is entirely possible that deformation of the fibers at their points of contact is important for pulp mats even at compacting pressures of 100 g./sq. cm. Although the frequency of contact-points in pulp mats is probably greater and the force per contact less than for glass fiber mats, these effects are probably overshadowed by the fact that swollen cellulose fibers are more deformable than glass fibers.

CONCLUSIONS

1. As the length-to-diameter ratio of the fibers decreases, the mean z-orientation increases. Even with fibers of moderately high length-to-diameter ratio, a significant number of the fibers are deposited in the bed at an appreciable angle to the x-y plane.

2. Translation or rotation in the x-y plane of entire fibers during compression is not a significant mechanism contributing to the compaction of glass fiber beds.

3. The hysteresis in the compression response of fibrous structures is due to axial slippage of the fibers.

4. The surface characteristics and coefficient of friction of the fibers become increasingly important to the compression response of fibrous structures as the fiber length increases.

5. As the fiber diameter increases, the bending of the fibers decreases at any compacting pressure.

6. The number of fiber contacts per unit weight of fiber in newly formed beds increases as the fiber length decreases. Under high compacting stresses, the number of contact points tends to become independent of fiber length.

7. A useful method has been developed which allows one to study visually the interior of thick fibrous structures.

ACKNOWLEDGMENTS

It would be impossible to acknowledge all the people who assisted materially in the successful completion of this thesis. To these many people the author wishes to express his sincere appreciation.

There are several people whose assistance should be particularly noted. The author wishes to acknowledge the encouragement and advice of Dr. W. L. Ingmanson, acting chairman, and Dr. J. A. Van den Akker of the thesis advisory committee and especially Dr. H. D. Wilder, chairman, who guided the experimental portion of this study.

The assistance of the following people is also gratefully acknowledged:

Mr. H. Marks whose skillful construction of most of the equipment used in this study greatly contributed to the success of this investigation.

Mr. F. R. Sweeney and the other members of the photography department of The Institute of Paper Chemistry who processed the many photographs required for this study.

Miss O. Smith and Mr. D. J. MacLaurin, Jr. for taking the required electron micrographs.

Dr. R. A. A. Hentschel of E. I. du Pont de Nemours & Co. for furnishing the special 0.1-denier dacron filament.

Mr. K. Hardacker for preparing the glass filaments which were silvered *in vacuo*.

Special appreciation goes to my wife, Darlene, for her encouragement and especially for her typing of the original manuscript of this dissertation.

NOMENCLATURE

A = constant in Equation (3)

A = cross-sectional area of fibers

a = constant in Equation (6)

a = semiaxis of contact area between fibers

B = constant in Equation (6)

B' = constant in Equation (11)

C = mat solids concentration, g./cc.

C_o = mat solid concentration at zero applied stress

d = fiber diameter, microns

D_c = degree of compression of bed

E = modulus of elasticity of fibers

F = relative frequency of fibers having any z-orientation

G = constant in Equation (6)

H = height of bed

I = moment of inertia (second moment of the area of cross section)

K = constant in beam equations

L = fiber length, cm.

L_T = total fiber length in bed

ℓ = span length, distance between junctions, cm.

ℓ', m', n' = three components of direction cosines of normal to two segments

$\bar{\ell}'$, $\bar{m}'$, $\bar{n}'$ = mean values of ℓ', m', n'

M = constant in Equation (1)

N = total number of fibers in bed

N = constant in Equation (1)

N_J = number of fibers in contact with a single fiber

N_x, N_y, N_z = number of segments in x, y, and z-directions

o = subscript referring to conditions in unloaded bed

$\underline{P}$ = apparent applied stress, g./sq. cm.

$\underline{p}$ = axial force in fiber, g.

$\underline{R}$ = length-to-diameter ratio of fibers

$\underline{r}$ = fiber radius, microns

$\underline{r_c}$ = radius of curvature of neutral axis of beam

$\underline{S_r}$ = relative stiffness of fibers

$\underline{t}$ = time

$\underline{u}$ = coefficient of friction

$\underline{W}$ = normal force at contact-points

$\underline{W_b}$ = stored potential energy in beam due to bending

$\underline{Z}$ = vertical distance between any point and bottom of bed

α = constant in Equation (32)

β = coefficient which determines the effect of thickness of segments

γ = Poisson's ratio

Δ = deflection of cantilever beam

$\underline{\Delta_b}$ = deflection of beam caused by bending

$\underline{\Delta_c}$ = change in distance between fiber centers caused by deformation of fibers at points of contact

ϵ = porosity, fractional void volume of bed

θ = angle between segment and z-axis

θ_o = θ for unloaded bed

$\underline{\bar{\theta}'_w}$ = weighted mean z-orientation, measured from horizontal

μ = microns

ρ = density of fibers, g./cc.

σ = solid fraction of bed, volume of fibers per unit volume of bed

ϕ = angle between projection of segment and x-axis

$\lambda(\underline{\ell})$, $\Theta(\theta)$, $\Gamma(\phi)$, $\psi(\underline{A})$, $\chi(\underline{r})$ = frequency probabilities, probability density functions

LITERATURE CITED

1. Jones, R. L. An investigation of the effect of fiber structural properties on the compression response of fibrous beds. Doctor's Dissertation. Appleton, Wis., The Institute of Paper Chemistry, 1962. 150 p.

2. Wilder, H. D. The compression creep properties of wet pulp mats. Doctor's Dissertation. Appleton, Wis., The Institute of Paper Chemistry, 1959. 184 p.

3. Qviller, O., Papir-Journalen 26:312(Dec., 1938).

4. Ingmanson, W. L., and Whitney, R. P., Tappi 37, no. 11:523-33(1954).

5. Page, D. H., and Tydeman, P. A., Paper Technol. 1, no. 5:519-30(1960).

6. Van den Akker, J. A., Lathrop, A. L., Voelker, M. H., and Dearth, L. R., Tappi 41, no. 8:416-25(1958).

7. Helle, T. Svensk Papperstid. 66, no. 24:1015-30(1963).

8. Corte, H. Unpublished work, 1964.

9. Manby, J., J. Textile Inst., Trans. 23:T5-13(1932).

10. Hillend, W. J. The importance of fiber compression to the mechanism of fibrous mat compression. Course A-300, Problem C-1. Appleton, Wis., The Institute of Paper Chemistry, 1960. 38 p.

11. Morrell, W. F., and Hildebrand, J. H., J. Chem. Phys. 4, no. 3:224-7(1936).

12. Prindle, W. R., J. Soc. Cos. Chem. 8:86-92(1957).

13. Textile fiber materials for industry. Owens-Corning Fiberglas Corp. (Publ. No. 1-GT-1375-A), 1961.

14. Samuelsson, L.-G. Svensk Papperstid. 66, no. 15:541-6(1963).

15. Gyorgy, K., Mérés is Automatika 4, no. 9:258-63(1956); Appl. Mech. Rev. 10:2145(1957).

16. Weyl, W. A., Glass Ind. 28, no. 5:231-54(1947).

17. Sinclair, D. J., Appl. Phys. 21:380-6(1950).

18. Bikerman, J. J. Surface chemistry. p. 181, 403. New York, Academic Press Inc., 1958.

19. Aslanova, M. S., and Rebinder, P. A., Dokl. Akad. Nauk Beloruss. SSSR (N.S.) 96, no. 2:299-302(1954); Appl. Mech. Rev. 8:1984(1955).

20. Otsuki, S., J. Soc. Mech. Eng. 1, no. 3:244-50(1958).

21. Kinosita, K., J. Phys. Soc. Japan 8, no. 6:782-90(1953).

22. Harris, M. Handbook of textile fibers. Washington, Harris Research Laboratories, 1954. 356 p.

23. Hearle, J. W. S., and Peters, R. H. Fibre structure. p. 570. Manchester and London, England, Butterworth and Co., Ltd., and The Textile Institute, 1963. 667 p.

24. Estridge, R. Initial retention of fibers by wire grids. Doctor's Dissertation, Appleton, Wis., The Institute of Paper Chemistry, 1961. 129 p.

25. Myers, W. T. The rheology of synthetic fiber suspensions. Doctor's Dissertation. Appleton, Wis., The Institute of Paper Chemistry, 1962. 189 p.

26. Gardner, I. C., and Case, F. A. The making of mirrors by the deposition of metal on glass. U. S. Government Printing Office, 1931. 17 p.

27. Kimberly-Clark Corp. Electrically conductive paper, and method of making it. Brit. pat. 927,115(May 29, 1963).

28. Nethercut, P. E. Softening mechanism of paper plasticizers. Doctor's Dissertation. Appleton, Wis., The Institute of Paper Chemistry, 1949. 106 p.

29. Arnold, E. W. Light scattering in fibrous sheets. Doctor's Dissertation. Appleton, Wis., The Institute of Paper Chemistry, 1962. 139 p.

30. Cargille, J. J. Personal communication, 1964.

31. Onogi, S., and Sasaguri, K., Tappi 44, no. 12:874-80(Dec., 1961).

32. Wilder, H. D. Unpublished work, 1963.

33. The Institute of Paper Chemistry. Unpublished work.

34. Ingmanson, W. L., Andrews, B. D., and Johnson, R. C., Tappi 42, no. 10: 840-8(1959).

35. Ezekiel, M. Methods of correlation analysis. 2nd ed. p. 138. New York, John Wiley & Sons Inc., 1950. 531 p.

36. Lathrop, A. L., Phot. Sci. Eng. 6, no. 5:303-7(Sept.-Oct., 1962).

37. Bliesner, W. C. A study of the porous structure of fibrous sheets using permeability techniques. Doctor's Dissertation. Appleton, Wis., The Institute of Paper Chemistry, 1963. 200 p.

38. McMaster, D. G. The thermal conductivity of dry and partially saturated fiber beds. Doctor's Dissertation. Appleton, Wis., The Institute of Paper Chemistry, 1963. 131 p.

39. Fuller, C. E., and Johnston, W. A. Applied mechanics. Vol. II. p. 234. New York, John Wiley & Sons Inc., 1919. 556 p.

40. Pellett, G. L. Longitudinal dispersion, intrafiber diffusion, and liquid-phase mass transfer during flow through fiber beds. Doctor's Dissertation. Appleton, Wis., The Institute of Paper Chemistry, 1964. 269 p.

41. Kallmes, O., and Corte, H., Tappi 43, no. 9:737-52(1960).

42. Kallmes, O., Corte, H., and Bernier, G., Tappi 44, no. 7:519-28(1961).

43. Nimura, T., and Kido, K., Sci. Rep. RITU, B-(Elect. Comm.) 6:45-62(1954).

44. Van den Akker, J. A. In Bolam's The formation and structure of paper. Vol. I. p. 208. London, Tech. Assoc. of the Brit. Paper and Board Makers' Assoc., Inc., 1962.

45. Van Wyck, C. M., J. Textile Inst., Trans. 37:T285-92(1946).

46. Morley, A., Phil. Mag., June, 1908:711-20.

47. Howell, H. G., Mieszkis, K. W., and Tabor, D. Friction in textiles. New York, Interscience Publishers Inc., 1959. 263 p.

48. Jones, R. L. Personal communication, 1965.

49. Singer, F. L. Strength of materials. New York, Harper & Bros., 1951.

50. Van den Akker, J. A. Class Notes, Course A-257. Appleton, Wis., The Institute of Paper Chemistry, 1964.

51. Ingmanson, W. L. Unpublished work, 1965.

52. Jentzen, C. A. The effect of stress applied during drying on some of the properties of individual pulp fibers. Doctor's Dissertation. Appleton, Wis., The Institute of Paper Chemistry, 1964. 129 p.

53. Walker, E. F. Effects of the uronic acid carboxyls on the sorption of 4-O-methylglucuronoarabinoxylans and their influence on papermaking properties of cellulose fibers. Doctor's Dissertation. Appleton, Wis., The Institute of Paper Chemistry, 1964. 74 p.

54. Seely, F. B. Resistance of materials. p. 155. New York, John Wiley & Sons Inc., 1925. 442 p.

55. Finch, R. B., Textile Res. J. 21, no. 6:383-92(1951).

APPENDIX I

DERIVATION: EFFECT OF COMPRESSION UPON z-ORIENTATION

Let the degree of compression, D_c, of a bed be defined by

$$D_c = \frac{H}{H_o} = \frac{\sigma_o}{\sigma}$$

where H is the height of the bed, σ is the solid fraction and the subscripts o refer to the unloaded bed. If the bed were a perfectly homogeneous material, the vertical distance between any two points in a bed, ΔZ, at any degree of compression would be given by

$$\Delta Z = D_c \Delta Z_o \qquad (33).$$

This relation (33) does not hold exactly for fibrous structures, because as the fibers bend some portions of each fiber move up and others down with respect to the center of mass of the fiber. It was found experimentally, though, that the beds could be compressed to a degree of compression of 0.5 or lower before the bending of each fiber becomes readily noticeable. To the extent that the fibers obey Equation (33) and also keep their end-to-end length constant, the effect of compression on the z-orientation of a fiber can be calculated.

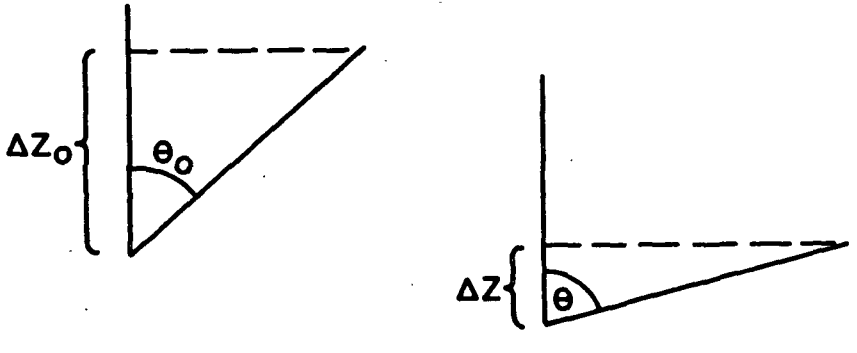

Figure 41. Effect of Compression on z-Orientation

It can be seen from Fig. 41 that if a fiber makes an angle θ_o with the z-axis in an unloaded bed, at some degree of compression, D_c, it will be oriented at an angle θ given by

$$\theta = \cos^{-1}(D_c \cos \theta_o) \qquad (34),$$

if the fiber obeys the stated conditions. For machine computation, θ was calculated from the equivalent form

$$\theta = \tan^{-1}[(\sqrt{1-D_c^2\cos^2\theta_o})/(D_c\cos\theta_o)].$$

In the extreme case, when $\theta_o = 0°$ the fiber cannot obey Equation (33) and still have its end-to-end length remain constant, so Equation (34) then does not really apply. For this case, though, the fibers tend to buckle and the mean orientation of the fibers as calculated by Equation (34) may not be in error by as much as it may at first appear. In any event, the frequency of fibers having θ near zero was small and the error in calculating their orientation would have only a small effect on the over-all angular distribution.

APPENDIX II

EXAMPLE: DEFLECTION OF A CONTINUOUS BEAM

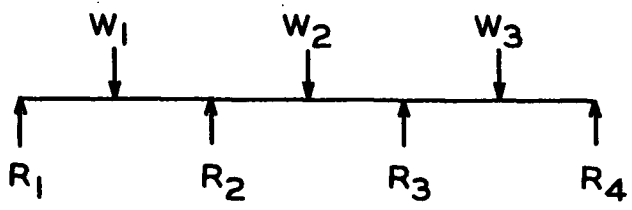

Figure 42. Continuous Beam With Three Spans

For the beam illustrated in Fig. 42 the three-moment equation is (54)

$$M_1\ell_1 + 2M_2(\ell_1 + \ell_2) + M_3\ell_3 = -W_1\ell_1^2(3/8) - W_2\ell_2^2(3/8) \qquad (35).$$

In this equation, M_1, M_2, M_3, are the bending moments at any three consecutive supports and ℓ_1 and ℓ_2 are the lengths of the two consecutive spans. By means of Equation (35) and the symmetry of the beam, when the spans are of equal length, the bending moments over the supports are calculated to be

$$M_1 = M_4 = 0$$

$$M_2 = M_3 = -3\ell/40(W_1 + W_2)$$

and the loads at the supports are

$$R_1 = R_4 = 17W_1/40 - 3W_2/40$$

$$R_2 = R_3 = 23W_1/40 + 23W_2/40.$$

This treatment assumes that only one point of support is fixed and the others are frictionless. Calculating the deflections of the spans, Δ, from the second area-moment theorem (49), one finds that

$$\Delta_1 = \Delta_3 = \frac{\ell^3}{EI}\left(\frac{31W_1}{1920} - \frac{9W_2}{1920}\right)$$

and

$$\Delta_2 = \frac{\ell^3}{EI}\left(-\frac{9W_1}{960} + \frac{11W_2}{960}\right).$$

If the loads on all spans are equal to W, then

$$\Delta_1 = \Delta_3 = \frac{\ell^3 W}{EI87.3},$$

and

$$\Delta_2 = \frac{\ell^3 W}{EI480}.$$

However, if the deflections of all spans are treated as equal to Δ, the total load W_T becomes

$$W_T = 2W_1 + W_2,$$

and

$$\Delta = \frac{\ell^3 W_T}{EI295.4}.$$

Two things should be particularly noted from this example: First, as with simple beams, the deflection of the spans of this continuous beam increases as the third power of their length, other factors remaining constant. Also note that the proportionality constant $(1/K)$ is considerably lower for this continuous beam than for a simple beam with free ends $(1/48)$. It is probable that not only does the mean span length of a fiber decrease, in a structure being loaded, but the resistance to bending at a given span length increases as the loading on the fiber becomes more complex.

APPENDIX III

CALCULATIONS

AXIAL SLIPPAGE VS. STRETCHING

It was determined experimentally that the projected length of the 2.26 mm. by 7.22 μ fibers was about 4.5 μ less than their actual length when the bed was supporting an applied stress of 107 g./sq. cm. Approximate calculations show that this difference in length caused some axial slippage of the fibers and was not due to stretching of these fibers.

The axial force, p, required to produce a change in length, ΔL, of 4.5 μ by stretching the fibers is given by

$$p = AE(\Delta L/L)$$

where A is the cross-sectional area of the fibers having a length L and a modulus of elasticity E. For these fibers we find

$$p = 4.46 \times 10^{-7} \text{ sq.cm.} \times 7.39 \times 10^{8} \text{ g./sq.cm.} \times (4.5 \times 10^{-4} \text{ cm.}/2.26 \times 10^{-1} \text{ cm.})$$
$$= 0.66 \text{ g.}$$

The maximum axial tension in these fibers will occur in the center span and will have a maximum value equal to the total frictional force on either half of the fiber. For these conditions it was determined experimentally that each fiber is in contact with 12.6 other fibers, and in the following section the mean normal force per contact is estimated to be 0.050 g. Thus, the maximum frictional force, p_F, is given by

$$p_F = 0.050 \text{ g.} \times 6.3 = 0.315 \text{ g.}$$

if the maximum value of 1.0 is used for the coefficient of friction. This value is less than the mean axial force required to extend the fibers. Since the actual coefficient of friction is probably nearer 0.3 than 1.0, it can be concluded that stretching of the fibers between their points of support was only a small effect and that slippage of the fibers over their points of support must have occurred.

EFFECT OF AXIAL SLIPPAGE UPON HYSTERESIS

It has been demonstrated that there is very little repositioning of entire fibers during compression, but that there is a small amount of axial slippage of one fiber against another. Approximate calculations indicate that the work lost during a compression-recovery cycle, which is represented by the area of the hysteresis loop, is largely due to the small amount of axial slippage.

It will be assumed at the onset that the work lost is due entirely to slippage of one fiber surface against another. That is, frictional drag due to movement of the oil with respect to the fibers is assumed to be negligible because of the slow rate of loading. Therefore, the total work lost is the sum of the work lost at all contact points. At a given contact point, the work lost equals the product of the mean frictional force and the distance over which the slippage occurred. The frictional force in turn is the product of the normal force and the coefficient of friction between the fibers. As the number of contacts, mean normal force between contacts, and probably the coefficient of friction are some function of the stress applied to the bed, we are not presently in a position to calculate with a high degree of accuracy the work lost per contact.

Nevertheless, it is informative to calculate approximately the effect of axial slippage upon the hysteresis. The following example is for the 2.26 mm. by 7.22 μ fibers. Actual measurement showed that the end-to-end length of these fibers was decreased by approximately 4.5 μ when the beds were subjected to maximum loading. As was discussed, the mean slippage per contact of one fiber over another would be about one-fourth the change in end-to-end length or 1.1 μ. As both fibers slip at a contact point, the mean total slippage at a contact point is probably near 2.2 μ. As the calculated initial number of contact points per fiber, $\underline{N}_J/2$, was approximately 3.3 and the final number was determined to be 6.3, we can use 4.8 for the approximate mean number of contact points during compression. At maximum applied stress, the mean normal force per contact was estimated to be 0.050 g., as discussed in the following section. If we use 0.025 g. for the mean normal force during compression and select a reasonable value for the coefficient of friction (0.3) we find the following:

Work lost per contact during compression = $0.025 \text{ g.} \times 0.3 \times 2.2 \times 10^{-4}$ cm.

$= 1.65 \times 10^{-6}$ g. cm.

Total work lost/g. = No. fibers/g. x mean no. contact points per fiber x work lost per contact point

$= 4.27 \times 10^{6} \times 4.8 \times 1.65 \times 10^{-6} = 33.8$ g. cm.

The total work lost during the cycle equals the sum of the work lost during compression and recovery or 67.6 g. cm. As can be seen from Table V, this value is quite close to the work loss of 72 g. cm. which was determined experimentally for the first cycle of a bed of these fibers. In view of the very approximate nature of these calculations, this agreement between the actual and predicted values is probably fortuitous. It appears, though, that it may be safely concluded that the hysteresis in the compression-recovery response of these beds was due primarily to axial slippage of the fibers.

From the above discussion it is not entirely obvious how a reduction in the frictional force between the fibers (such as produced by replacing the o-dichlorobenzene saturant with immersion oil) can cause an increase in the work lost. If one were to plot work lost versus the coefficient of friction between the fibers, the result would be similar to the hypothetical curve shown in Fig. 43. Obviously, if the coefficient of friction were zero, the work lost would be zero. If the friction were great enough to prevent slippage of the fibers, they would have to stretch between the points of contact and again the work lost would be zero. Although the shape of the curve is not known, there must be a maximum between the two extremes where the work lost equals zero. As can be seen from Fig. 43, in the region to the right of the maximum the work lost increases with decreasing coefficient of friction.

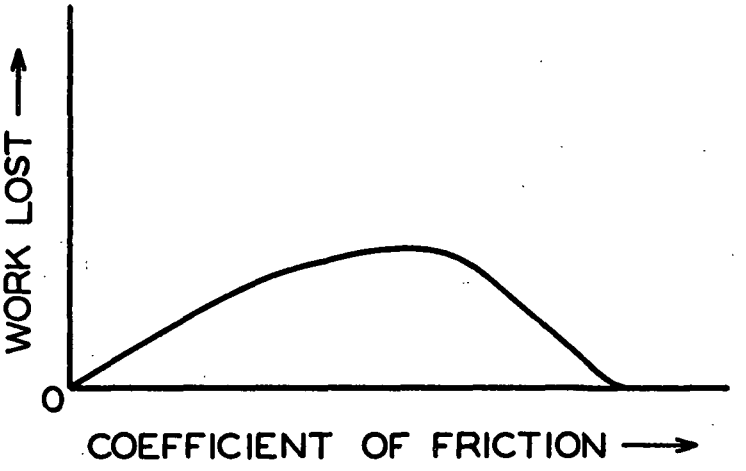

Figure 43. Hypothetical Data Showing Effect of Friction Upon Hysteresis

DEFORMATION AT CONTACT POINTS

To calculate the deformation of fibers at their points of contact, it is necessary to know the thickness of the layer in addition to the number of contacts per fiber. From the definition of a layer, the mean force between

two fibers at their points of contact is given by the ratio of the total force on the bed and the number of contact points per layer. If we express the thickness of a layer by $K_L d$, it can be shown that the mean force per contact-point, W, is given by:

$$W = \frac{\pi P d L}{2 N_J \sigma K_L} \qquad (36),$$

where N_J equals the number of contacts per fiber. For a bed of the 2.26 mm. by 7.22 μ fibers at P equal to 107 g./sq. cm. (σ = 0.0545 and N_J = 12.6), the mean force at the points of contact, W, equals 0.050 g. if K_L is assumed to be unity. If each span of these fibers is regarded as a simple beam with fixed ends, the central deflection of the span is calculated to be 12 μ. As observable from Fig. 17, this value approximates the actual deflection per span observed for these fibers. Under identical loads, the deflection of a span of a continuous beam is less than that of a similar beam with fixed ends. Even if the mean span length and loads at the points of contact were known, it is not presently possible to calculate precisely the deflection of the spans if they are treated as portions of continuous beams. The problem is further complicated when one attempts to account for the effect of axial forces within the fibers. It appears that, at P equal to 107 g./sq. cm. the thickness of a layer in beds of the 2.26 mm. by 7.22 μ fibers was somewhat less than one fiber diameter.

If the normal force between two cylinders in contact is known, the area of contact can be calculated. According to Finch (55), the contact area, A_c, between two identical cylinders crossing at right angles is given by:

$$A_c = \pi a^2,$$

where

$$a = (3Wr(1-\gamma^2)/2E)^{1/3} \qquad (37).$$

In Equation (37), $\underline{W}$ is the normal force between the cylinders, γ is their Poisson's ratio, and $\underline{E}$ their Young's modulus. For two of the 2.26 mm. by 7.22 μ glass fibers crossing at right angles, the area of the surface of contact is 0.33 μ^2 if the force between the fibers is 0.050 g.

Due to the deformation of the fibers at their points of contact, the distance between the centers of the fibers will be slightly less than the diameter of a fiber. The change in the distance between fiber centers, Δ_c, is given very nearly by

$$\Delta_c = 2r-2(r^2-a^2)^{1/2} \qquad (38).$$

For the conditions just mentioned, the distance between the centers of the two fibers would be decreased by only 0.029 μ. Obviously deformation of the glass fibers at their points of contact is a small effect compared to fiber bending. For beds composed of fibers having a low modulus of elasticity, however, at high compacting pressures deformation of the fibers at their points of contact probably makes a significant contribution to the compression response. To estimate the importance of this effect, a reliable method for determining the thickness of the layers is needed.